# Proteomic Analyses of Plant-Bacterial Interactions

by

Zhenyu Cheng

A thesis
presented to the University of Waterloo
in fulfillment of the
thesis requirement for the degree of
Doctor of Philosophy
in
Biology

Waterloo, Ontario, Canada, 2010

## AUTHOR'S DECLARATION

I hereby declare that I am the sole author of this thesis. This is a true copy of the thesis, including any required final revisions, as accepted by my examiners.

I understand that my thesis may be made electronically available to the public.

## Abstract

Proteome-level changes of both the plant growth-promoting bacterium (PGPB) *Pseudomonas putida* UW4 and its plant host *Brassica napus* (canola) were profiled using two-dimensional (2-D) difference in-gel electrophoresis (DIGE) and mass spectrometry, to elucidate the proteins' prospective of plant-bacterial interactions. This study was undertaken in an effort to elaborate how a plant growth-promoting bacterium and its plant host biochemically and physiologically influence one another. More specifically, the effects of the PGPB *P. putida* UW4 on the proteome of canola and vice versa were examined. In addition, environmental stresses including heavy metal and salt were incorporated into the system. Moreover, how the presence of a functional bacterial 1-aminocyclopropane-1-carboxylate (ACC) deaminase (AcdS), which can lower plant ethylene levels and hence promote plant growth under a variety of stresses, would affect protein expression in both the bacterium and the plant was investigated. First, 2-D DIGE was used to detect significantly up- or down- regulated proteins in *P. putida* UW4 and its AcdS minus mutant in response to the presence of 2 mM nickel. Thirty-five proteins whose expression was altered were successfully identified by mass spectrometry and sequence comparisons with related species. Nineteen of the identified proteins were detected as differentially expressed in both wild-type and AcdS minus mutant expression profiles. Functional assessment of proteins with significantly altered expression levels revealed several mechanisms involved in bacterial heavy metal detoxification, including general stress adaptation, anti-oxidative stress and heavy metal efflux proteins. In addition, by detection of bacterial protein expression changes in the presence of plant exudates, three unique *P. putida* UW4 proteins that mediate interactions between the bacterium and its plant

host were identified. However many of the observed changes of protein expression elicited by nickel and plant exudates were similar for wild-type *P. putida* UW4 and the AcdS minus mutant, with the majority of identified significant protein expression changes occurring in both strains. This is not unexpected because the *P. putida* UW4 ACC deaminase is unlikely to be involved in bacterial perception and response to plant host signals and environmental stimuli, and it causes a noticeable difference only in plant growth. A comprehensive proteome 2-D reference map of the PGPB *P. putida* UW4 containing 326 2-D gel spots representing 275 different proteins was also constructed. A 2-D database containing all the mass spectrometric information of *P. putida* UW4 proteins has been constructed. The data set has been deposited into the World-2DPAGE database and is accessible at http://world-2dpage.expasy.org/repository/. On the plant side, ninety proteins with significantly altered expression levels in the presence of salt and/or bacteria were identified by mass spectrometry. Many of these proteins are involved in photosynthesis, anti-oxidative processes, salt transportation/accumulation and pathogenesis-related responses. Importantly, the presence of the bacterial ACC deaminase was observed to alter the plant's protein expression in response to salt stress. The effects included enhanced photosynthesis and salt accumulation contributed by wild-type *P. putida* UW4. The work described in this thesis furthers our understanding of plant-bacterial interactions, and is also likely to be of importance to both organic agriculture and environmental remediation efforts.

## Acknowledgements

Many people have given me their generous support and advice throughout the completion of my thesis in many different ways. Without their help, it would not have been possible for me to finish my project.

First of all, I would like to thank my supervisors, Drs. Bernard Glick and Brendan McConkey, for giving me an opportunity to study and work in their laboratories, and providing me with tireless guidance, dedicated assistance as well as financial support. Your enormous knowledge and expertise were the most valuable resources for me.

I wish to thank members of my Ph.D. committee, Dr. Barbara Butler and Dr. Trevor Charles, for all their valuable suggestions, time, and effort towards this thesis.

I also would like to acknowledge my external examiner, Dr. Yvan Moënne-Loccoz, and internal-external examiner, Dr. John Honek, for taking time from their busy schedules to read this manuscript and to make valuable suggestions.

I would also like to express my gratitude to my present and past lab members including Jin Duan, Owen Woody, Dr. DongRyoung Kim, Dr. Jennifer Czarny, Dr. Youai Hao, Merav Kamensky, Wei Jiang, Andria Spires, Catherine Wei, Rohan Gidvani, Dr. Andrew Doxey, Carl White, Shimaila Rashid, Jing Li. Working with them has been a truly wonderful experience, and I have learned a lot from everyone. Thank you all for your encouragement, and for making our lab an excellent and supportive working environment.

I would like to thank Dr. Richard Smith and Elden Rowland for their invaluable technical support with mass spectrometry.

Last but not least, I would like to thank my dear wife, Zhong, for her unconditional love and constant affection as well as academic and emotional support.

## Table of Contents

# List of Figures

# List of Tables

# List of Abbreviations

| | |
|---|---|
| 2-DE | two dimensional gel electrophoresis |
| ACC | 1-aminocyclopropane-1-carboxylate |
| ACN | acetonitrile |
| AQUA | absolute quantification |
| CDPK | calcium-dependent protein kinase |
| DIGE | difference gel electrophoresis |
| ETI | effector-triggered immunity |
| ESI | electrospray ionization |
| FDR | false discovery rate |
| FTICR | fourier transformation ion cyclotron resonance |
| HPLC | high-pressure liquid chromatography |
| HR | hypersensitive response |
| ICAT | isotope-coded affinity tag |
| IEF | isoelectric focusing |
| IPG | immobilized pH gradients |
| IPTG | isopropyl-β-D-thiogalactoside |
| iTRAQ | isobaric tag for relative and absolute quantitation |
| MALDI | matrix-assisted laser desorption ionization |
| MAPK | mitogen-activated protein kinase |
| MIAPE | minimal information about a proteomic experiment |
| MRM | multiple-reaction monitoring |
| MS | mass spectrometry |
| MudPIT | multidimensional protein identification technology |
| NEPHGE | nonequilibrium pH gradient electrophoresis |
| PAI | protein abundance index |
| PAMP | pathogen-associated molecular pattern |
| PGPB | plant growth-promoting bacteria |

| | |
|---|---|
| PMF | peptide mass fingerprinting |
| PSAQ | protein standard absolute quantification |
| PTI | PAMP-triggered immunity |
| PTM | post-translational modifications |
| QconCAT | quantification concatamer |
| RPLC | reverse phase LC |
| SCX | strong cation exchange |
| SDS-PAGE | sodium dodecyl sulfate polyacrylamide gel electrophoresis |
| SILAC | stable isotope labeling by amino acids in cell culture |
| TOF | time-of-flight |
| XIC | extracted ion chromatogram |

# 1. Introduction

## 1.1 Plant-bacterial interactions

### 1.1.1 Plant defense

In order to survive the constant microbial pathogen challenges that they are faced with, plants depend on their multiple layers of immune responses in a delicately balanced spatial and temporal fashion. The highly effective plant defense system involves the slow-evolving PAMP (pathogen-associated molecular pattern)-triggered immunity (PTI) and the dynamic effector-triggered immunity (ETI), also known as the hypersensitive response (HR). PTI relies on the ability of plant's multiple membrane pattern recognition receptor proteins to sensitively detect highly conserved and common-featured PAMP molecules including flagellin, elongation factor Tu, peptidoglycan, chitin and ergosterol. Furthermore, plants evolve resistance (R) proteins which either directly or indirectly monitor pathogen effector proteins, initiating ETI. Both PTI and ETI lead to the activation of mitogen-activated protein kinases (MAPKs) and various hormone signaling pathways, which then starts a cascade initiating a variety of defense responses such as callose deposition, programmed cell death, production and accumulation of antimicrobial reactive oxygen species, and induction of phytoalexins and other secondary metabolites (Jones and Dangl, 2006).

### 1.1.2 Beneficial and pathogenic bacteria

The promotion of plant growth by plant growth-promoting bacteria (PGPB) generally entails (i) preventing some of the deleterious effects of a phytopathogenic organism (usually a

fungus) by either production of antibiotics or synthesis of fungal cell wall lysing enzymes, or (ii) aiding in the acquisition of nutritional resources such as nitrogen, phosphorus or iron or (iii) providing plant hormones such as auxin or cytokinin, or lowering plant ethylene levels through the action of the enzyme 1-aminocyclopropane-1-carboxylate (ACC) deaminase (Glick, 1995). A particular bacterium may affect plant growth and development using any one, or more, of the above mentioned mechanisms at various times during the life cycle of the plant. In contrast, to cause diseases, bacterial pathogens employ various strategies including secreting plant cell wall degrading enzymes and delivering a large spectrum of effector proteins into plant cells mimicking host protein functions (Jones and Dangl, 2006).

### 1.1.3 ACC-deaminase containing plant growth-promoting bacteria

One of the major mechanisms that some plant growth-promoting bacteria (PGPB) use to facilitate plant growth involves the enzyme ACC deaminase [EC 4.1.99.4], which cleaves ACC to produce α–ketobutyrate and ammonia. ACC is the immediate precursor of the phytohormone ethylene, an important mediator of stress responses, plant growth, and development (Abeles et al., 1992; Mattoo and Suttle, 1991). Stress ethylene levels become elevated as a consequence of various environmental stresses (Glick et al., 1997; Stearns and Glick, 2003). Upon the advent of stresses, there is an initial small peak of beneficial ethylene that is thought to trigger plant protective responses. Then, there is a second much larger peak of stress ethylene that is thought to initiate processes such as senescence, chlorosis and abscission, thereby causing overall inhibitory effects to plant growth (Stearns and Glick, 2003). The ACC deaminase-containing plant growth-promoting bacteria (PGPB) attach to plant host

surfaces and can act as sinks for ACC, therefore limiting the inhibitory ethylene synthesized in plant tissues (Glick et al., 1998). By alleviating some of the deleterious effects of stress ethylene, the action of ACC deaminase helps plants tolerate a wide variety of abiotic and biotic stresses that might otherwise significantly limit plant growth (Glick, 2005; Glick et al., 2007a; Glick et al., 2007b), including excess salt (Cheng et al., 2007; Mayak et al., 2004a; Nadeem et al., 2007; Saravanakumar and Samiyappan, 2007; Sergeeva et al., 2006), drought (Mayak et al., 2004b), flooding (Grichko and Glick, 2001), presence of metals (Belimov et al., 2001; Burd et al., 2000; Farwell et al., 2007; Rodriguez et al., 2008), organic contaminants (Gurska et al., 2009; Huang et al., 2004; Reed and Glick, 2005) and pathogens (Hao et al., 2007; Wang et al., 2000). The AcdS minus mutant strain, lacking a functional *acdS* gene (encoding ACC deaminase) responsible for modulating stress ethylene levels, does not prevent ethylene inhibition of plant growth (Li et al., 2000). The tremendous agricultural and environmental importance of ACC-containing PGPB has been summarized in previous reviews (Glick, 2010; Reed and Glick, 2004).

## 1.2 Proteomic tools

### 1.2.1 Two dimensional gel electrophoresis (2-DE)

2-DE, a central tool in proteomic research, is a technique that was first developed in the 1970s for large-scale protein separation (Klose, 1975; O'Farrell, 1975). This technique begins with the separation of proteins based on their isoelectric points (in the first dimension) by isoelectric focusing (IEF), and then (in the second dimension) according to their subunit molecular masses by sodium dodecyl sulfate polyacrylamide gel electrophoresis (SDS-PAGE).

The sequential combination of these methods in two orthogonal directions enables separation of thousands of proteins in a single gel. Separated protein spots may be subject to a variety of subsequent analyses, including western blotting; visualization by pre-electrophoresis fluorescence labeling; post-electrophoresis staining with coomassie blue, silver staining or SYPRO dyes; differential expression analysis; and identification by Edman degradation or mass spectrometry (MS). Protein spots of interest are excised from a gel and then digested with proteases (e.g. trypsin or GluC) before being analyzed by MS to determine their identities (Mann et al., 2001). High-resolution 2-DE remains the preferred method for protein separation because of its ability to simultaneously separate a large number of proteins and their isoforms, even though there are several technical problems inherent with this approach, including inadequate consistency of protein separation and poor resolution of proteins that are not highly abundant, basic (e.g. ribosomal and nuclear proteins) or hydrophobic (e.g. membrane proteins). The reproducibility of 2-D gels is no longer a problem since the equipment and reagents that are commercially available include the use of immobilized pH gradients (IPG) (Görg et al., 1988, 1995, 2000, 2009). In addition, the establishment of more or less standardized proteomic methodology has decreased the variability of protein separations and increased the reliability of this technique (Görg et al., 1988, 1995, 2000, 2009).

The above mentioned improvements notwithstanding, the quality of 2-D gels is still heavily dependent on the expertise of the individual experimenter. Another technical limitation with 2-D gels is the difficulty in detecting low abundance proteins, including regulatory proteins, signal transduction proteins and receptor proteins. For example, the predicted dynamic range of protein concentrations in plasma is ~12 orders of magnitude (Corthals et al.,

2000), making it extremely difficult to analyze relatively low abundance proteins. However, many more proteins can be displayed and analyzed if samples are pre-fractionated or enriched (Corthals et al., 2000; Görg et al., 2009; Stasyk and Huber, 2004), or separated on narrow-range or ultra-narrow-range immobilized pH gradient strips (Corthals et al., 2000; Görg et al., 2009). Membrane and alkaline proteins, both of which are particularly difficult to resolve, have also been sucessfully analyzed by targeted 2-D gel studies. Even though the hydrophobicity of the membrane proteins is problematic for every step in 2-DE, from protein sample extraction to entering the second dimension polyacrylamide gel, they have been successfully analyzed by 2-DE by incorporating thiourea, acetonitrile or detergents such as tetradecanoylamide-propyl-dimethyl ammonio-propane-sulfonate in the 2-D sample buffer (Görg et al., 2009; Nouwens et al., 2000). Effective 2-D separation of alkaline proteins has also been made possible by the combination of various strategies such as the addition of isopropanol to the 2-D rehydration buffer and the utilization of pH gradients up to pH 12 (Görg et al., 1997, 1998, 1999, 2009; Hoving et al., 2002). Low abundance and basic proteins may be well resolved in 2-D gels (e.g. Klose, 1975; Klose and Kobalz, 1995; O'Farrell et al., 1977) by the application of an alternative IEF method, nonequilibrium pH gradient electrophoresis (NEPHGE), in which proteins do not accumulate at their isoelectric points and are therefore less likely to precipitate. To conclude, the evolving 2-DE technology is a very powerful tool for protein separation in spite of some limitations that can mostly be overcome by a variety of strategies.

### 1.2.2 Mass spectrometry (MS)

High sensitivity and fast speed are two of the advantages of mass spectrometric (MS) analyses. The innovation that made MS a very robust tool in large-scale proteomics was the

introduction of techniques for ionization, such as electrospray ionization (ESI) (Whitehouse et al., 1985) and matrix-assisted laser desorption ionization (MALDI) (Karas and Hillenkamp, 1988; Tanaka et al., 1988), which can transform macromolecules to ions in the gas phase for mass spectrometric analyses without losing their structure or form.

A mass spectrometer consists of three main parts: an ion source for sample ionization and generation of gas-phase ions; a mass analyzer for separation of ions based on their mass:charge ($m/z$) ratios; and an ion detection system (Mann et al., 2001). Analytes are usually separated by gel-based and/or gel-free approaches prior to mass spectrometric analyses in order to simplify the analysis of complex protein samples. Sufficient pre-MS separations are required for both unambiguous protein identification and detection of low abundance protein species. In the gel-based methods, the protein mixtures are often separated by 2-DE for whole crude cell extracts or 1-DE for relatively simple protein mixtures originating from previous separation steps, e.g. affinity chromatography or immunoprecipitation. Subsequently, the separated protein spots or bands are excised and subjected to protease (generally trypsin) digestion. The resulting peptide mixtures of the target proteins are then separated and enriched by liquid chromatography (LC) or directly analyzed by MS. A high-pressure liquid chromatography (HPLC) system utilizing ion-exchange and/or reverse phase chromatography that is directly coupled to a MS instrument (LC-MS) has become a standard set-up for these protein characterization experiments (Yates, 2004). To improve the resolution and allow for the analysis of extremely complex digested protein mixtures, a combination of strong cation exchange (SCX) chromatography coupled with reverse phase LC (RPLC) is included in the

approach known as multidimensional protein identification technology (MudPIT) (Wolters et al., 2001).

Even though the basis of ion separation in all mass analyzers is identical (i.e. according to the *m*/*z* ratio), each instrument utilizes different strategies: quadrupoles (Q) use *m*/*z* stability; time-of-flight (TOF) analyze flight time; and ion trap, Orbitrap and Fourier transformation ion cyclotron resonance (FTICR) use *m*/*z* resonance frequency (Mann et al., 2001; Yates et al., 2009). Various MS instruments are created by combining different mass analyzers in tandem, thereby increasing their individual separating strengths (e.g. Hunt et al., 1987). These instruments are then interfaced with MALDI and ESI to provide a large variety of mass spectrometers with a range of different features including resolution, mass accuracy, sensitivity, dynamic range and scan rate (Domon and Aebersold, 2006; Mann and Pandey, 2001; Yates et al., 2009).

For protein identification, the MS analysis of peptide mixtures resulting from proteolytic digestion generates peptide mass fingerprinting (PMF) and/or tandem mass spectrometric (MS/MS) data, which can be searched against protein databases [e.g. Swiss-Prot, NCBI nr, and MSDB (Bairoch and Apweiler, 1997; Boechmann et al., 2003; Perkins et al., 1999; Wheeler et al., 2007)] by different algorithms [e.g. Mascot (Perkins et al., 1999), ProFound (Zhang and Chait, 2000), and PEAKS (Ma et al., 2003a)], enabling identification of target proteins (Mann et al., 2001; Steen and Mann, 2004). In the PMF method, a list of experimentally measured peptide masses, which is referred to as a protein's "peptide mass fingerprint" and is unique for each protein, is produced and compared to the theoretically derived PMFs calculated for each entry in the database. Identification is achieved when there is

a match between the PMF of the target protein and a specific protein candidate in the database (Perkins et al., 1999). In the tandem MS (MS/MS) approach, in addition to the PMF data, analysis of the MS/MS spectra reveals structural information that is related to the sequence of the peptide, contributing to the specificity of the identification of the target protein (Gygi and Aebersold, 2000; Mann et al., 2001). The peptide mixture is first analyzed by operation in the normal MS mode so that typical PMF data are acquired. Then, in the MS/MS mode, the selected peptide ion (parent ion) is fragmented via bombardment with an inert gas in a collision cell, with the resulting fragments (daughter ions) being separated in the second part of the tandem mass analyzer, generating an MS/MS spectrum. The daughter ions are sometimes further degraded so that extended sequence information can be collected ($MS/MS^n$). The MS/MS spectra obtained for peptides from different parts of the target protein are matched against a calculated spectrum for all peptides in the database to achieve identification (Eng et al., 1994).

With other methods, sequence information retrieved from *de novo* analysis (Dancik et al., 1999) is used in combination with database searching for protein identification (Ma et al., 2003a). In some cases, the DNA sequences associated with the proteins being studied are not known; however, the potential identities of these proteins can still be assigned based on their shared sequence similarities with homologues in the databases (e.g. Cheng et al., 2009a, 2009b, 2009c). Fortunately, the number of proteins without associated nucleotide sequences is rapidly decreasing thanks to the phenomenal growth in sequence information generated by next-generation DNA sequencing technologies (Metzker, 2010), reducing the impact of this issue.

Recent advances in mass spectrometry-based proteomics have contributed significantly to various areas in biology (Aebersold and Mann, 2003; de Hoog and Mann, 2004; Guerrera and Kleiner, 2005; Han et al., 2008; Pandey and Mann, 2000, Yates et al., 2009), including the identification of protein post-translational modifications (PTM) and the discovery of novel biomarker proteins for various diseases. There are many types of post-translational modifications leading to a huge heterogeneity of protein populations. These differently modified forms of proteins contribute to the tightly controlled processes of proteins executing vital cellular functions, including a plant's perception and defense against pathogens during plant-bacterial interactions (Xing et al., 2004). PTM of a protein often results in a mass change of the modified amino acid residues relative to the unmodified protein. This mass difference, which also determines the form of the modification, can be detected by accurate mass determination by MS analysis of either the intact protein or the peptide containing the modified region of the protein. Ultimately, the positions of the modifications within the protein amino acid sequence are determined by the MS/MS spectra peak shifts (Jensen, 2004; Mann and Jensen, 2003). MS-based comparative proteomics has been widely utilized to identify biomarkers or putative marker proteins indicative of a large number of diseases including various cancers, cardiovascular, infectious, neurodegenerative, and hematological disorders (Pan et al., 2009). MS-based proteomics has also been applied in an attempt to detect the presence of phytopathogens in plant-bacterial interaction studies (Padliya and Cooper, 2006).

### 1.2.3 Quantitative proteomics

#### 1.2.3.1 Gel-based quantitative proteomics

Difference gel electrophoresis (DIGE) is an important technique for comparative proteomic studies; it is exceptionally reproducible, accurate and sensitive. Conventional 2-D gel-based differential analysis involves separating each test sample on a single gel, which causes dramatic variability as a result of gel-to-gel variation; however, DIGE was developed (Ünlü et al., 1997) to improve reproducibility when comparing samples. DIGE separates two or more samples on the same gel so that real and meaningful biological changes can be readily identified.

A typical DIGE workflow may be summarized in Figure 1-1. Briefly, test and control samples are labelled with two charge- and size-matched, yet spectrally distinct, fluorescent dyes (Cy3 and Cy5) by either minimal or saturating methods (Marouga et al., 2005). These dyes exhibit both high sensitivity and a wide dynamic range in detection. Equal amounts of the differently labelled protein samples are then mixed and subjected to 2-DE separation on the same gel, ensuring that identical proteins from separate samples co-migrate and that their fluorescence images are super-imposed, thereby enabling more accurate differential expression analysis. The protein expression ratios between the samples are defined in the subsequent image analysis by comparison of the normalized intensities of each protein spot from the Cy3 and Cy5 channels. Finally, the proteins of interest (usually those with significantly changed levels of expressions) may be excised from the gel, either robotically or manually, and identified by MS (Marouga et al., 2005; Minden et al., 2009; Timms and Cramer, 2008; van

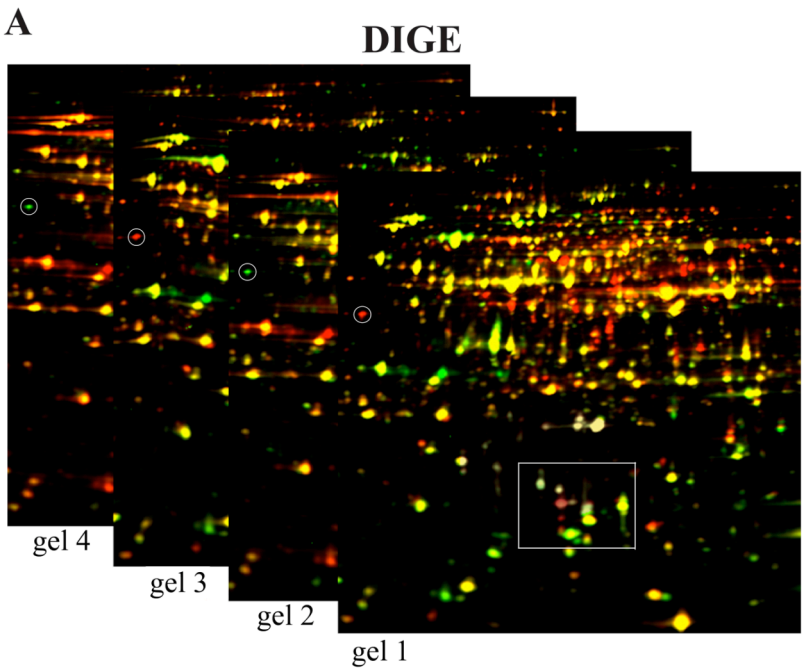
A
DIGE
gel 4
gel 3
gel 2
gel 1

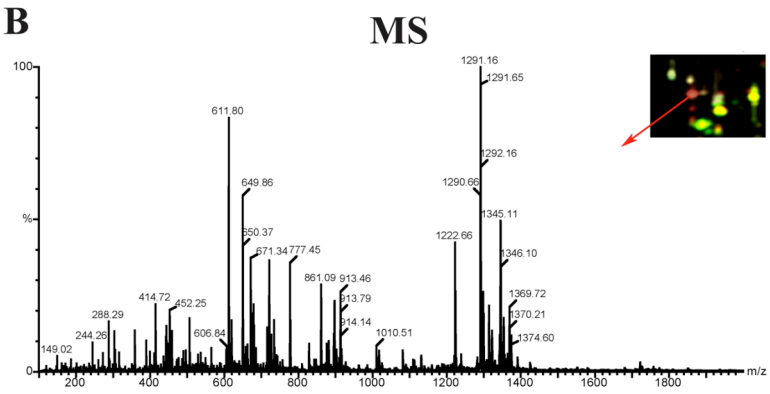
B
MS
100
%
0
1291.16
1291.65
611.80
1292.16
649.86
1290.66
1345.11
650.37
1222.66
671.34
777.45
1346.10
861.09
913.46
1369.72
913.79
414.72
452.25
1370.21
288.29
914.14
244.26
606.84
1010.51
1374.60
149.02
200
400
600
800
1000
1200
1400
1600
1800
m/z

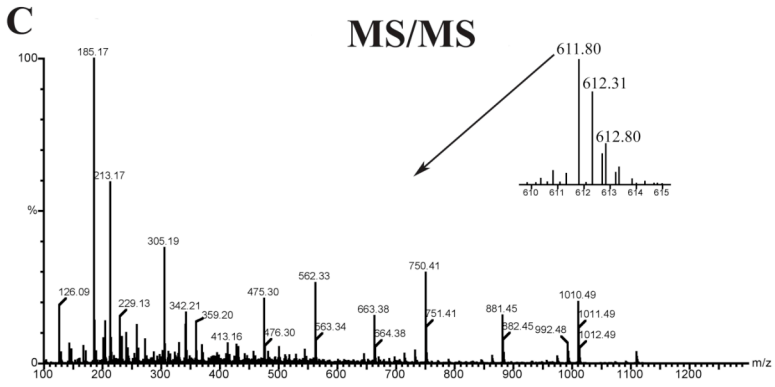
C
MS/MS
100
%
0
185.17
611.80
612.31
612.80
213.17
305.19
126.09
229.13
342.21
359.20
475.30
562.33
750.41
413.16
476.30
563.34
663.38
664.38
751.41
881.45
882.45
992.48
1010.49
1011.49
1012.49
100
200
300
400
500
600
700
800
900
1000
1100
1200
m/z

Figure 1-1. The workflow of the difference gel electrophoresis (DIGE) analysis. A. four replicates of analytical 2D-DIGE gels are shown. On gel 1 and gel 3, the test sample is labeled with Cy5 (red) and the control labeled with Cy3 (green), and up-regulated and down-regulated proteins appear as red and green spots respectively. These two dyes are switched in gels 2 and 4. So the circled spot representing the same protein in all four gels appears as red in gels 1 and 3, while as green in gels 2 and 4. Expressional (i.e., average ratios) and statistical analyses of separated proteins can be carried out using these four replicates. B. the mass spectrometric (MS) spectrum separates the tryptic peptides of a protein sample based on their mass:charge ($m/z$) ratios. Following the generation of the expressional profile, the proteins that have changed expression levels in the test samples (i.e., a red spot cut from the rectangular area of the DIGE gel 1 in Panel A) can be excised from 2-D gel and subject to MS identification. The peptide mass fingerprint (PMF) of the protein of interest can be generated from this MS spectrum and used to determine the protein's identity. C. the tandem MS (MS/MS) spectrum reveals structural information that is related to the sequence of the peptide, contributing to the specificity of the identification of the target protein. Individual selected peptide ion (parent ion) (i.e., the peptide that has a $m/z$ of 611.80 in the enlarged rectangular area of the MS spectrum in panel B) is fragmented via bombardment with an inert gas in a collision cell, with the resulting fragments (daughter ions) being separated in the second part of the tandem mass analyzer, generating an MS/MS spectrum.

den Bergh and Arckens, 2004). The entire DIGE process can be carried out with the commercially available Ettan DIGE system, which consists of CyDyes™ DIGE fluors, a Typhoon variable mode imager, and DeCyder differential analysis software (GE Healthcare).

An essential component of the DIGE experimental design is the inclusion of an internal standard, which typically consists of equal mixture of all test samples (Alban et al., 2003). The use of internal standards has led to an enormous increase in the accuracy of this techniqueattributable to its crucial role in protein spot matching and quantification (Karp et al., 2007; Timms and Cramer, 2008; van den Bergh and Arckens, 2004). Currently, there is still some debate amongst practitioners of the DIGE technique regarding how to best perform statistical analysis for different comparisons in order to reduce the number of false positives due to the simultaneous testing of expression changes across thousands of protein spots (Corzett et al., 2006; Karp et al, 2004, 2005, 2007; Urfer et al., 2006). One of the most popular statistical analyses approaches is false discovery rate (FDR) methodology (Karp et al., 2005).

Overall, 2-DE (including DIGE) coupled with protein identification by MS is by far the most frequently used platform for differential expression analysis (Jorrín-Novoa et al., 2009). However, as the developer of DIGE, Dr. Jonathan Minden concluded recently "It is important to appreciate that no proteomic method is able to sample the entire proteome – we are sampling the most prominent changes associated with the states being compared. The observed proteome changes will always need to be validated and examined for their molecular role in the process of interest." (Minden et al., 2009).

#### 1.2.3.2 MS-based quantitative proteomics

MS-based proteomics has had a substantial impact on the biological sciences

(Aebersold and Mann, 2003; Cravatt et al., 2007; Domon and Aebersold, 2006; Gingras et al., 2007; Gstaiger and Aebersold, 2009; Pan et al., 2009; Yates et al., 2009). Originally limited to qualitative analysis like protein identification (Steen and Mann, 2004), the tremendous quantitative potential of MS-based proteomics has now been realized; see Ong and Mann (2005) for a review of publications employing quantitative MS-based proteomics. There are two main categories of MS-based quantitative technologies: stable isotope label-based quantitative proteomics and label-free comparative liquid chromatography (LC)-MS. Depending on the choice of incorporating strategy, the quantification methods involve stable isotope labels that can be divided into four major sub-categories: (i) metabolic incorporation in living cells, (ii) covalent modification of proteins or peptides by isotopically labeled chemical tags, (iii) incorporation during proteolysis performed in $H_2{}^{18}O$, and (iv) spiking in known amounts of isotopically labeled synthetic internal standards. Label-free quantification usually employs two protein abundance indices (PAIs) for measurements: ion intensities and spectral counts. Moreover, to address various specific problems in different systems, numerous derivatives of both label-based and label-free methods have been developed. However, only the representative and most commonly used ones are included in the following section.

The concept for most stable isotope label-based comparative proteomics is that protein quantification can be performed in the MS mode by comparing signal intensities (peak height or peak area) of the stable isotope-labeled peptides to their native analogues in the sample. Ideally, these share identical chromatographic characteristics, but are distinguishable by mass spectrometry.

One of the first developed MS-based quantitative methods was the pioneering isotope-

coded affinity tag (ICAT) technology (Gygi et al., 1999). The conventional ICAT reagents are composed of three main elements: a cysteine-targeted reactive group for chemical tagging, a polyether linker region containing eight deuteriums, and a biotin group for affinity purification of labeled peptides. In a standard ICAT procedure, proteins from different samples are denatured and covalently modified with isotopically heavy or light ICAT reagents and digested by endoproteinases. The differently tagged peptides are then recovered by avidin affinity chromatograph, further fractionated by multidimensional protein identification technology (MudPIT) (Washburn et al., 2001), and subject to MS-based identification and quantification. The major advantage of the ICAT chemical incorporation of stable isotopes is that the approach can significantly reduce the complexity of the peptide analysis due to its exclusive focus on cysteine-containing peptides (Fenyo et al., 1998). The main caveats of this method are its incompatibility with proteins containing no or few cysteines, the impact of the large ICAT tag on tandem MS fragmentation, and separation of isotopically different analogues in reversed-phase chromatography (Zhang et al., 2001b) during MudPIT fractionation (Ong and Mann, 2005). Following the success of the original ICAT technology, countless subtle variations of the strategy, such as reactive groups targeting to different parts on protein, distinct isotope signatures, or other affinity purification tags, have been published in the literature. See Bantscheff et al. (2007) and Ong and Mann (2005) for a summary of these derivative tags.

Another widely used strategy for chemical incorporation of stable isotopes is using the isobaric Tag for Relative and Absolute Quantitation (iTRAQ) method (Ross et al., 2004). The reactive group in this method is targeted to primary amines, resulting in efficient and ubiquitous labeling of all peptides in a sample. The conventional quantification strategy

employed by most other stable isotope-based approaches compares the relative abundances of the isotopically different peptides. In contrast, differently labeled peptides in iTRAQ are uniquely isobaric, meaning they not only share identical chromatographic characteristics but also are indistinguishable in MS spectra. The release of diagnostic fragment ions in MS/MS mode allows simultaneous protein identification and quantification (Ross et al., 2004). Even though the concomitant determination of identity and relative quantity of paired peptides requires thorough tandem MS fragmentation on all peptides, which necessitates sample prefractionation, iTRAQ eliminates the intensive searching for isotopically paired peptides in MS survey for quantification. In the meanwhile, iTRAQ also has the advantage of being readily multiplexed, enabling sophisticated analyses like time-course directed comparisons.

The simplest strategy to introduce stable isotope-labeled elements in MS-based comparative proteomics relies on the isotope dilution principle, that is "spiking" known amounts of isotope-labeled synthetic analogues of predicted signature peptides (Mallick et al., 2007) or proteins into the sample as internal standards (Brun et al., 2009). Quantification of target protein can be derived by comparing the extracted ion chromatograms (XICs) of the internal peptide standard and its native analogue (Brun et al., 2009). Internal standards are usually incorporated into the sample at a late stage of the quantification procedure (close to protein digestion) (Kirkpatrick et al., 2005); therefore the dramatically increased probability of introducing quantitative variations during steps prior to internal peptide standard incorporation make this approach incompatible with sample prefractionation (Arsene et al., 2008; Havlis and Shevchenko, 2004). This absolute quantification (AQUA) strategy (Gerber et al., 2003) has been further refined by integrating biologically synthesized QconCAT (*q*uantification

*concat*amer) peptide (Beynon et al., 2005) or full-length PSAQ (protein standard absolute quantification) protein (Dupuis et al., 2008) standards. The QconCAT standards allow higher coverage of the same protein sequence and/or simultaneous quantification of multiple protein species by releasing multiple peptides upon trypsin digestion (Beynon et al., 2005). The PSAQ protein standards completely eliminate system variability and enable sample prefractionation, a step necessary for the enrichment of important low abundant proteins because they are usually "spiked" into the sample at the very beginning of the sample preparations (Dupuis et al., 2008). Instrumentally, mass spectrometers performing highly sensitive and specific selected- or multiple-reaction monitoring (SRM or MRM) analysis on pre-selected peptides partly alleviate interference from background ions (Hopfgartner et al., 2004; Kirkpatrick et al., 2005). Even though absolute quantification approaches usually focus on small-scale quantification of disease biomarkers (Kuhn et al., 2004; Pan et al., 2009), elaborate projects that are targeted to quantifying whole proteomes have also been proposed (Aebersold, 2003; Anderson et al., 2009).

The earliest stage at which stable isotope elements can be introduced into the sample is during cell growth by metabolic incorporation through cell doublings and protein turnover (Bantscheff et al., 2007; Ong and Mann, 2005). The principle advantage of metabolic labeling is that this approach eliminates the quantitative errors that would be introduced in each step of sample preparation since the differently labeled live cells are mixed ahead of all these steps, thereby potentially providing more accurate results than any other MS-based quantitative methods (Bantscheff et al., 2007; Ong and Mann, 2005). This superior accuracy is especially appreciated when measuring subtle protein expression changes or post-translational

modifications whose quantitative information is derived from limited observations (Bantscheff et al., 2007). Metabolic incorporation of stable isotopes was originally demonstrated by $^{15}N$-labeling of simple organisms, such as yeast or bacteria (Oda et al., 1999), which in turn can be fed to label small organisms like *Caenorhabditis elegans* and *Drosophila melanogaster* (Krijgsveld et al., 2003). Even higher eukaryotes, like rats (Wu et al., 2004) and plants (Palmblad et al., 2007), could potentially be labeled with $^{15}N$ metabolic proteins. Nonetheless, there are some drawbacks in using $^{15}N$ metabolic labeling. The mass increment in "heavy" peptides, whose fragmentation spectra could be used for protein identification, is sequence-dependent, thereby obstructing MS identification (Ong and Mann, 2005). Also, the necessity of using extremely enriched $^{15}N$ (to avoid complications in isotopic patterns caused by incomplete labeling) can be costly when labeling large samples (Bantscheff et al., 2007; Ong and Mann, 2005). In contrast, these obstacles are removed by the simple yet powerful alternative metabolic labeling strategy known as "stable isotope labeling by amino acids in cell culture" (SILAC) (Ong et al., 2002). In this procedure, different cell cultures in question are grown in media supplemented with isotopically heavy or light amino acids. The proteins being differently labeled *in vivo* are then combined and subject to quantification and identification.

The $^{16}O/^{18}O$ exchange during either proteolysis or postdigestion incubation in light ($H_2{}^{16}O$) or heavy ($H_2{}^{18}O$) water is another way to incorporate the stable isotopes that are necessary for quantification (Miyagi and Rao, 2007; Rose et al., 1983; Yao et al., 2001). Theoretically, one or two $^{18}O$ molecules can be incorporated by endoproteinases Lys-N or trypsin and Glu-C, introducing a 2-Da or 4-Da mass offset (Rao et al., 2005; Reynolds et al., 2002; Yao et al., 2001). However, the small mass difference or often incomplete labeling

(Johnson and Muddiman, 2004; Ramos-Fernandez et al., 2007) can cause complications in MS quantification. Consequently, this enzymatic labeling approach has not been as widely applied, in spite of its advantageous specificity.

Label-free comparative LC-MS is a relatively recent technique for relative quantification that can be implemented using either of two fundamentally distinct strategies: the peak intensity method and the spectral counting method. The peak intensity quantification method measures a set of mass spectrometric peak areas, also known as extracted ion chromatograms (XICs), of the same peptide from multiple independent MS runs. The basis of comparison is that the XIC (area under a peak curve) of a peptide is linearly related to its abundance (Silva et al., 2005). The foundation for the spectral counting method, on the other hand, is the observed logarithmic relation between the number of identified peptide fragment spectra for a given protein and the actual abundance of that protein (Ishihama et al., 2005). It is worth noting that quantification profiles and peptide identification are obtained in MS mode and MS/MS mode, respectively. Various strategies, such as rapid switching back and forth between MS and MS/MS modes, performing separate runs for quantification and identification purposes, or parallel acquisition of MS and MS/MS spectra in a MS system like Fourier transformation ion cyclotron resonance-OrbiTrap (Bateman et al., 2002; Nakamura et al., 2004; Niggeweg et al., 2006; Silva et al., 2006a; Silva et al., 2005; Silva et al., 2006b; Strittmatter et al., 2003; Vissers et al., 2007; Zimmer et al., 2006), have been used to find the right balance when operating under these two modes.

Spectral counting, on the other hand, has the advantage of exclusive MS/MS spectra acquisition across the chromatographic time scale for both protein identification and

quantification. The spectral counting method is based on the hypothesis that a peptide's abundance is positively correlated to its occurrence for fragmentation. For relative quantitative comparison, the MS/MS spectral counts of peptide ions originated from the target protein are then taken into account as a protein abundance index (PAI).

Following the incorporation of an upfront MudPIT setup, which has become a standard system for separating complex peptide mixtures (Washburn et al., 2001), comprehensive comparisons of the peak intensity versus spectral counting procedures have shown that they produced measurements that were strongly correlated (Old et al., 2005; Zybailov et al., 2005). In one study, peak intensity-based quantification was found to be more accurate in protein ratio calculation, while its sensitivity of peak detection was limited in some cases (Old et al., 2005). On the other hand, spectral counting-derived quantification was shown to possess superior reproducibility and a larger dynamic range (Zybailov et al., 2005). However, the numbers of spectra required to detect smaller protein expression changes was quite large (Old et al., 2005). In spite of their dissimilar quantification mechanisms, the peak intensity and spectral counting methods share a common workflow, consisting of: protein sample preparation, MS separation of peptide samples, and data analysis. Moreover, unlike analyzing the pooled post-labeling mixtures in stable isotope-based approaches, label-free quantification methods compare multiple LC-MS runs of samples that are separately processed, which can potentially lead to inflated quantification measurement error during the LC-MS step. Therefore, a reliable comparison depends on the reproducibility of nearly identical experimental conditions. In addition, normalization between individual runs using the spiked-in calibrants or endogenous abundant nonchanging peptides can also correct for system variability (Chelius and

Bondarenko, 2002; Dong et al., 2007; Gillette et al., 2005; Silva et al., 2006a; Silva et al., 2006b; Vissers et al., 2007). Furthermore, the use of appropriate software for peak detection, peak matching, quantitative calculation, and statistical analysis is critical to minimize false positives (America and Cordewener, 2008; Wang et al., 2003; Wiener et al., 2004; Zhang et al., 2006b; Zhu et al., 2010).

### 1.2.4 Post-translational modifications

Protein post-translational modifications (PTMs) are crucial in controlling protein function. PTMs can change protein function by toggling various protein activities, intrinsic biological behavior, subcellular localization, degradation, and interaction with other molecules (Jensen, 2006). PTM of a protein typically leads to a modification type-dependent shift on the modified amino acid residues, which can be detected by accurate mass determination by MS analysis of either the intact protein or the peptide containing the modified region of the protein. Ultimately, the exact position of PTM on the modified protein can also be determined by the shifts of peaks in MS/MS spectra (Mann and Jensen, 2003).

## 1.3 Applications of proteomics in plant-bacterial interactions

There have been a large number of studies featuring gel-based proteomic characterization of plant-bacterial interactions. A set of examples is shown in Table 1-1, addressing the following question: what are the impacts of plants on the bacterial proteome, and vice versa? Among all of the proteomic studies of plant-bacterial interactions, it is no surprise that the plant-pathogen interaction and the symbiotic relationship between nitrogen-

Table 1-1. The application of gel-based quantitative proteomics in plant-bacterial interactions

| Organisms Interactions | Main findings | References |
|---|---|---|
| | Plant Proteomics | |
| *Arabidopsis thaliana* Pathogenic | Induction of peroxiredoxins and the antioxidants glutathione S-transferases, characteristic of the establishment of basal resistance and *R*-gene mediated resistance, metabolic enzymes, photosystem II, and mitochondrial permeability transition | Jones et al., 2004, 2006 |
| *Lycopersicon hirsutum* (tomato) Pathogenic | Differential expression of proteins involved defense, stress responses, protein regulation, synthesis & processing, energy production, and metabolism; revealing distinct mechanisms conferred by two loci: Rcm 2.0 and Rcm 5.1 | Coaker et al., 2004 |
| *Nicotiana tabacum* (tobacco) Pathogenic | Induction of metabolic reprogramming and changes in cellular activities supporting protein synthesis, folding & degradation, vesicle trafficking & secretion, and cytoskeleton function | Gerber et al., 2008 |
| *Oryza sativa* (rice) Pathogenic | Differential expression of proteins related to energy, metabolism, and defense<br>Induction of pathogenesis proteins and receptor-like kinases | Mahmood et al., 2006<br>Miché et al., 2006 |
| *Glycine max* (soybean) Symbiotic | Identification of nodule-specific proteins, 17 peribacteroid membrane specific proteins including protein-processing proteins and nodulins, and proteins known to respond to rhizobial inoculation | Hoa et al., 2004<br>Panter et al., 2000<br>Wan et al., 2005<br>Winzer et al., 1999 |

| | | |
|---|---|---|
| *Melilotus alba*<br>Symbiotic | Identification of nodule-specific late nodulin, leghemoglobin | Natera et al., 2000 |
| *Medicago truncatula*<br>Symbiotic | Eukaryotes have an extensive range of functional responses to AHLs<br>Down-regulation of stress-related proteins<br>Inductions of primary antioxidant defense reaction proteins, symbiosis-related and pathogen-associated proteins<br>Overlap of proteome changes in *Medicago truncatula* in response to auxin and *Sinorhizobium meliloti* | Mathesius et al., 2003<br>Prayitno et al., 2006<br>Schenkluhn et al., 2010<br>van Noorden et al., 2007 |
| *Trifolium* subterranean clover<br>Symbiotic | Identification of 10 differentially expressed proteins and 8 constitutively expressed ones including pathogenesis and stress-related proteins; specific induction of α–fucosidase by ANU794 may cause nodulation failure | Morris and Djordjevic, 2001 |
| | Bacterial Proteomics | |
| *Agrobacterium tumefaciens*<br>Pathogenic | Induction of proteins involved in biosynthesis, metabolism, transportation, and virulence | Rosen et al., 2003 |
| *Bradyrhizobium japonicum*<br>Symbiotic | Construction of a partial bacteroids proteome map containing more than 100 identified protein spots, proteins, ABC transporters and nitrogenase<br>Up-regulation of nitrogen metabolism proteins; down-regulation of proteins related to fatty acid, nucleic acid and cell surface synthesis; similar levels of proteins involved in carbon metabolism, protein synthesis, maturation & degradation and membrane transporters | Hoa et al., 2004a<br>Sarma and Emerich, 2005<br>Sarma and Emerich, 2006 |

| | | |
|---|---|---|
| *Erwinia chrysanthemi* Pathogenic | Highly up-regulation of OmpA protein that is potentially involved in binding to host; up-regulation of type II and type III secretion pathways and oligogalacturonate-specific porins<br>Induction of secreted plant cell wall degrading enzymes: endopectate lyases, polyalacturonase, pectin acetylesterases, and pectin methlesterase | Babujee et al., 2007<br>Kazemi-Pour et al., 2004 |
| *Frankia* strains: Symbiotic | Up-regulation of proteins involved in N assimilation, oxidative defense, cellular signaling, and nitric oxide detoxification, stress response, and nodulation regulation<br>Strong down-regulation of succinate dehydrogenase<br>Strain-dependent changes in nitrogen fixation proteins | Alloisio et al., 2007<br>Hammad et al., 2001<br>Bagnarol et al., 2007 |
| *Methylobacterium extorquens* Epiphytic | Induction of methanol utilization enzymes, prominent stress proteins, and a key regulator PhyR, for adaptation to plant colonization and epiphytic life | Gourion et al., 2006 |
| *Nostoc* sp. Symbiotic | Differential expression in proteins associated with cell envelope and response to darkness<br>Up-regulation of nitrogenase and oxidative pentose phosphate pathway<br>Down-regulation of Calvin cycle enzymes | Ekman et al., 2006 |
| *Pectobacterium atrosepticum* Pathogenic | Induction of virulence determinants, such as pectic enzymes, metalloprotease, virulence protein Svx, and flagella proteins | Mattinen et al., 2007 |
| *Pseudomonas putida* Associative | Increase in proteins involved in nutrient utilization, root colonization<br>Decrease in bacterial communication (chemotaxis, quorum sensing) proteins | Cheng et al., 2009a |
| *Sinorhizobium meliloti* | Identification of putative nodule-specific proteins | Djordjevic, 2004 |

| | | |
|---|---|---|
| Symbiotic | Up-regulation of ABC-type transporters for amino acids and inorganic ions, vitamin synthesis and stress-related proteins | Djordjevic et al., 2003 |
| | Down-regulation of proteins involved in nitrogen acquisition, polyhydroxybutyrate synthesis, and cell division | Natera et al., 2000 |
| | Disruption effect of algal mimic on bacterial quorum sensing-regulated functions | Teplitski et al., 2004 |
| *Streptomyces scabies* Pathogenic | Up-regulation of proteins involved in bacterial stress response, glycolysis, nucleotide, amino acid, and secondary metabolisms | Lauzier et al., 2008 |

fixing bacteria and legumes have been studied in the greatest detail, whereas there is a dearth of proteomic studies of free-living plant growth-promoting bacteria (PGPB). Selected previous reports in this area are listed in Table 1-1, and encompass a range of different plants, bacteria, and interactions (pathogenic, symbiotic, or associative). Plants and bacteria accommodate inter-species interaction through complex shifts in their respective metabolisms. An example is the induction of a large spectrum of virulence proteins, including plant cell-wall degrading pectic enzymes, virulence protein Svx, flagellar proteins, host surface binding protein OmpA, proteins in type II and type III secretion pathways, and transportation porins, in pathogenic bacterial strains *Erwinia chrysanthemi* and *Pectobacterium atrosepticum* by plant signals (Table 1-1). Another prototypical example would be the extensive analysis of both plant and bacterial proteins in root nodules (or a mimicked symbiotic environment within a lab study). These studies investigate various events, such as nodule development and nitrogen fixation that take place in a symbiotic interaction (Table 1-1).

It is interesting to note that relatively few of the MS-based quantification tools have been applied in the analysis of plant-bacterial interactions. Some examples utilizing SILAC or iTRAQ are described in this section. Surprisingly, no examples applying ICAT could be found despite the fact that it was developed first.

The filamentous cyanobacteria *Nostoc* sp. PCC 7120 and *Nostoc punctiforme* ATCC 29133 are capable of fixing atmospheric nitrogen in heterocysts that are differentiated from vegetative cells. Heterocysts and vegetative cells co-exist symbiotically in filaments; heterocysts are dependent on vegetative cells for carbon fixation and provide nitrogen supply in return. Wright and colleagues performed comparative proteomic surveys using iTRAQ, whose multiplexing capability allowed simultaneous comparison between different cell types,

such as enriched heterocysts and vegetative cells, or mixed cells in nitrogen-fixing and non-nitrogen-fixing filaments (Ow et al., 2008; Ow et al., 2009; Stensjo et al., 2007). These studies were undertaken to facilitate future development of cyanobacterial biohydrogen production (Tamagnini et al., 2002).

Some mass spectrometry-based quantitative proteomics experiments have focused on the analysis of phosphorylation events crucial for *Arabidopsis thaliana*'s defense against pathogens. In one of the earliest applications of the iTRAQ technology to the problem of elucidating plant-bacterial interactions, Jones et al. (2006a) identified four known and one novel phosphorylation sites in *Arabidopsis* upon challenge by the bacterial pathogen *Pseudomonas syringae* pv. *tomato* DC3000. Two other papers, both reporting on the dynamics of *Arabidopsis* plasma membrane protein phosphorylation on exposure to the bacterial elicitor flg22, employed different quantitative strategies: $^{14}N/^{15}N$ metabolic labeling and iTRAQ (Benschop et al., 2007; Nuhse et al., 2007). Despite the fundamental differences in instrumentation and statistical analyses, both methods produced largely overlapping lists of flg22-induced phosphorylation sites on kinases and regulatory proteins potentially involved in defense.

In their pioneering label-free LC-MS quantitative proteomic investigation, González and colleagues revealed both plant (*Medicago truncatula*) and bacterial (*Sinorhizobium meliloti*) protein expression changes in root nodules in response to drought stress and recovery (Larrainzar et al., 2007; Larrainzar et al., 2009). Moreover, carbon metabolomic analysis was performed in parallel in one of these studies to explicate the regulation of nitrogen fixation along with the proteomic data (Larrainzar et al., 2009).

Comparative proteomics (both gel-based and MS-based) have greatly facilitated our understanding of plant-bacterial interactions. Overall, 2-DE coupled to protein identification by MS is still by far the most frequently used platform for expression analysis. More recently however, researchers have started to utilize the new tools-directed quantification methods, such as DIGE, iTRAQ, SILAC and label-free LC-MS (Jorrin-Novo et al., 2009). Comparisons of gel-based versus MS-based or MS-based versus other MS-based approaches have been carried out (DeSouza et al., 2005; Kolkman et al., 2005; Old et al., 2005; Patton et al., 2002; Timms and Cramer, 2008; Turck et al., 2007; Turtoi et al., 2010; Wu et al., 2006). It was concluded that each method had some unique advantages and therefore they could be exploited in a complementary manner to increase the proteome coverage. Moreover, since there is no single method that can exclusively unravel the complexity of a living cell, proteomic data are increasingly validated using complementary systems biology approaches and standard molecular and cellular techniques, a process that collectively forms a multidisciplinary integrative analysis to elucidate plant-bacterial interactions, e.g. Cheng et al. (2009a) and Larrainzar et al. (2009).

Protein phosphorylation is one of the most important and best-characterized PTMs among the various PTM categories. The critical roles of reversible phosphorylation modulated by different protein kinases [e.g., mitogen-activated protein kinases (MAPK) cascade, calcium-dependent protein kinases (CDPK), and pathogen-associated molecular pattern (PAMP) receptor kinases] and phosphatases in plant responses to pathogen attack have been established to some extent using various conventional molecular techniques like in-gel or *in vitro* kinase assay and immunodetection using anti-phosphorylation antibodies (Romeis, 2001; Xing et al.,

2002). Nevertheless, the dearth of details about kinase-substrate pairs, especially those involved in plant defense against bacterial pathogens, necessitates large-scale proteomic characterization of kinase-substrate interactions. Using a high-throughput yeast two-hybrid system and tandem affinity purification, comprehensive rice kinase-substrate interaction maps containing components of the rice MAPK cascade were constructed (Ding et al., 2009; Rohila et al., 2006; Rohila et al., 2009). Also, proteomic profiling of substrates of general kinases, or specific to MAPKs and CDPKs in *Arabidopsis* was carried out separately using protein arrays (Popescu et al., 2009; Popescu et al., 2007; Ritsema et al., 2007). These surveys can be used to derive potential phosphorylation-mediated pathways involved in plant defense.

Though recent discoveries of novel protein phosphorylation sites may shed light on plant defense responses (Lenman et al., 2008; Whiteman et al., 2008), plant phosphoproteomics is moving from being solely qualitative to more quantitative (see discussion in section 2.2.4.). In addition, more localization and timing information (besides the quantitative data) that may be crucial in elucidating plant-bacterial interactions can be extracted from the above-mentioned plant defense phosphoproteomic surveys (Benschop et al., 2007; Nuhse et al., 2007). While one study focused on the identification of phosphorylation events during early signaling (10 minutes after bacterial elicitor treatment) of plant defense (Benschop et al., 2007), the other work demonstrated the phosphorylation dynamics in plant protection against pathogen attack by quantifying phosphorylation at four different time points and revealed the importance of protein translocation and vesicle traffic (Nuhse et al., 2007). In conclusion, protein phosphorylation in plant defense can be depicted as an event occurring in a quantitatively appropriate, temporally and spatially coordinated manner.

In addition to the above-mentioned examples, more PTMs such as S-nitrosylation (Jorrin-Novo et al., 2009) and tyrosine nitration (Cecconi et al., 2009) were recently found to be involved in plant-bacterial interactions.

Lastly, a set of standards called the "Minimal Information about a Proteomic Experiment" (MIAPE) has been proposed (Taylor et al., 2007), to help improve the interpretability and reproducibility of the data generated in proteomics experiments. These standards serve as a guideline for documentation and reporting of experimental designs and statistical analyses of comparative proteomic studies. In addition, more comparative proteomic data being deposited in public proteomic repositories and shared freely will greatly facilitate understanding of other biological questions, such as cellular simulation in systems biology requiring large amounts of expressional data (Mead et al., 2009).

### 1.4 Objectives of the present study

The ACC deaminase-containing *Pseudomonas putida* UW4 has shown extensive plant growth-promoting (Cheng et al., 2007; Farwell et al., 2007; Gamalero et al., 2008; Li et al., 2000) and remediation-facilitating (Cheng et al., 2007) abilities. A major plant growth-promoting mechanism of *P. putida* UW4 is the expression of 1-aminocyclopropane-1-carboxylic acid (ACC) deaminase [EC 4.1.99.4], which has been described above. An advantage of growing crop plants with *P. putida* UW4 is that this bacterium has been shown to confer upon plants tolerance to a number of different environmental stresses simultaneously (Cheng et al., 2007; Farwell et al., 2007), a typical situation for plants in the field.

How *P. putida* UW4 and its plant host coordinate their protein expression during the plant growth-promoting and remediation processes is a topic of considerable interest. However,

approaches that examine only a single biochemical pathway will miss the widespread effects of PGPB-assisted growth, motivating broader, proteome-wide approaches. Large-scale proteomics characterization enables researchers to investigate global response of different organisms to various treatments.

In the present study, the effects of various stimuli on plant and bacterial proteomes were investigated using 2-D DIGE and MS to facilitate our understanding of plant-bacterial interactions.

# 2. Materials and Methods

## 2.1 Bacterial strains and growth

*Pseudomonas putida* UW4 was originally isolated from the rhizosphere of common reeds (Glick et al., 1995), and most recently has been classified as *Pseudomonas putida* based on 16S rDNA sequence analyses and metabolic activity (Hontzeas et al., 2005). The mutant strain *P. putida* UW4 AcdS minus was constructed by disrupting the ACC deaminase gene (*acdS*) by insertion of a tetracycline resistance gene within the coding region by homologous recombination (Li et al., 2000). The wild-type and mutant strains were cultivated aerobically in Tryptic Soy broth (TSB; Fisher Scientific Co., Ottawa, ON) or solid medium at 30˚C.

An estimate of the tolerance of the wild-type *P. putida* UW4 and AcdS minus strains to nickel was assessed by culturing them in the presence of 0, 2 or 5 mM of $NiSO_4$. Wild-type *P. putida* UW4 and AcdS minus mutant strain were grown to late-log phase in 50 mL of TSB medium and TSB medium supplemented with 2 mM nickel or 50 mL of 2×DF minimal salts medium (Penrose and Glick, 2003) supplemented with 50 mL of collected plant root exudates and 50 mL of sterile Milli-Q water to investigate the effects of nickel stress and plant root exudates signals on *P. putida* UW4 and AcdS minus proteomes.

*Escherichia coli* DH5α (Hanahan, 1983) was used as the host strain for the construction and maintenance of recombinant plasmids. *E. coli* strains were cultivated aerobically in Luria-Bertani broth or agar (Fisher Scientific Co., Ottawa, ON) at 37˚C.

If required, the medium was supplemented with antibiotics at final concentrations of 100 μg/mL ampicillin, 30 μg/mL kanamycin, or 15 μg/mL tetracycline.

## 2.2 Plant material and culture

### 2.2.1 Treatment with bacteria

The growth conditions of the bacterial cultures for treating plants were set up as described previously with minor modifications (Penrose and Glick, 2003). Briefly, seeds of *Brassica napus* var. Westar canola were surface sterilized for 1 minute in 1% bleach followed by 70% ethanol. Then, the sterile seeds were treated at room temperature for one hour with bacterial suspensions induced for ACC deaminase activity (Penrose and Glick, 2003). In some cases, genes that were cloned into pETP for overexpression in *P. putida* mutant strains were induced by 0.5 mM IPTG (Isopropyl-β-D-Thiogalactoside) at the same time. The bacterial cultures were diluted with sterile 0.03 M $MgSO_4$ to a final $OD_{600}$ of 0.15. Sterile 0.03 M $MgSO_4$ solution-treated seeds were kept and used as a negative control.

### 2.2.2 Growth pouch assay

For bacterial root elongation activity assay, the treated and control seeds (six/pouch) were planted in growth pouches (Cyg seed germination pouch, Mega International, St. Paul, MN) containing 20 mL of sterile Milli-Q water. The growth conditions (light intensity and temperature) were all performed exactly as described previously (Penrose and Glick, 2003). Plants were cultivated in a large growth chamber with a 12-hour photoperiod, a light intensity of 200 μE and a constant temperature of 20°C. Plant root length was measured five to seven

days after germination.

### 2.2.3 Hydroponic growth

The treated and control seeds were germinated on a moist sponge support for 3 days. Two days after germination, plants on the moist sponge support were transferred to 1 L beakers (1 plant per beaker) and supplied with hydroponic solution (contains the following components: 200 N; 54 P; 266 K; 42 Mg; 147 Ca; 55 S; 1.15 Fe; 0.05 Cu; 0.1 Mo; 0.345 Zn; 1 Mn; 0.3 B, unit ppm). The growth conditions (light intensity and temperature) were all performed exactly as described above. The hydroponic solutions were continuously aerated and replaced after 7 days. After 12 days growth in hydroponic solution, salt was added to the hydroponic solution for plants in the salt treatment group, to a final concentration of 250 mM NaCl. The plants were harvested 4 days after adding the salt. Three whole plants per treatment were used as replicates for the proteomic profiling and physiological measurements, respectively.

### 2.2.4 Chlorophyll measurements

Chlorophyll contents were measured from fresh leaf disks, one centimeter in diameter (approximately 0.1 gram), using the previously outlined method (Moran and Porath, 1980), where DMSO was used to extract total chlorophyll from tissues without maceration. Measurements were taken for one leaf disk from each of three plants per treatment.

Independent Student's t-test or one-way ANOVA followed by post hoc Scheffe's test were used for statistical analysis. A p value of $\leq 0.05$ was considered to be statistically significant.

### 2.2.5 Quantification of plant exudates components

For canola root exudates collection, canola plants were grown in growth pouches as described above, then the remaining water in all growth pouches was pooled, filtered through 0.2 μm nitrocellulose filters and the filtrates were stored at –20°C in the dark. The quantity of ACC in plant exudates was measured by the Waters AccQ·Tag Amino Acid Analysis Method™ (Waters Chromatography Inc., Mississauga, ON). The derivatization, separation and detection processes were done by following the Waters AccQ·Fluor™ user guide. Amino acid derivatives (including ACC) were separated by a Hewlett Packard HPLC system (1050 Series Quaternary Pump equipped with a high-efficiency 4 m Nova-Pak™ C18 column), and then detected by a Hewlett Packard 104a Programmable Fluorescence Detector at an excitation wavelength of 250 nm and an emission wavelength of 395 nm. The flow rate was 1 mL/min and the gradient used was as described previously (Penrose and Glick, 2001). The quantification of IAA was performed as described previously (Patten and Glick, 2002) with modifications. Plant exudates were analyzed using a Perkin Elmer Series 4 HPLC equipped with an Allure reverse-phase C18 column (5 μm; 4.6 by 150 mm) (Restek Inc. Rockville, ON). The elution buffer was acetonitrile-50 mM $KH_2PO_4$ (pH 3) (30/70) at a flow rate of 0.6 mL/min and the eluates were detected by a Micromeritics 788 Dual Variable detector at 220 nm.

## 2.3 DNA manipulations

### 2.3.1 Isolation of total genomic DNA

Bacterial genomic DNA was isolated using a Wizard® Genomic DNA Purification Kit (Promega Corporation, Madison, WI). A 2 mL bacterial culture was grown overnight in medium at optimal temperature with 200 rpm shaking. One mL of the culture was pelleted by centrifugation at 20,000 × *g* for 2 minutes, resuspended in 0.6 mL of nuclei lysis solution. The resuspended cells were lysed by incubation at 80˚C for 5 minutes. Three μL of RNase solution was added to the mixture and incubated at 30˚C for 30 minutes. To remove any protein present in the sample, 200 μL of protein precipitation solution was added. The sample was vortexed and incubated on ice (~4˚C) for 5 minutes. The mixture was centrifuged at 20,000 × *g* for 3 minutes, and the supernatant was transferred to a new 1.5 mL tube containing 600 μL of isopropanol. The tube was inverted 10 times before a centrifugation at 20,000 × *g* for 3 minutes. The supernatant was discarded and the pellet was washed with 600 μL of 70% ethanol. The supernatant was discarded again after a centrifugation at 20,000 × *g* for 2 minutes. The pellet was left to air-dry at room temperature for 15 minutes. The DNA pellet was rehydrated in 100 μL of rehydration solution for 1 hour at 65˚C. The genomic DNA was stored at -20˚C.

### 2.3.2 Isolation of plasmid DNA

Plasmid DNA was extracted from bacterial cells using a Wizard® *Plus* SV Minipreps DNA Purification System (Promega Corporation, Madison, WI). First, 5 mL of overnight bacterial culture was harvested by centrifugation for 5 minutes at 20,000 × *g* and the

supernatant was removed. Next, 250 μL of cell resuspension solution was added and used to completely resuspend the cell pellet. Then, 250 μL of cell lysis solution was added and mixed by inverting the tube 4 times. The mixture was incubated for 5 minutes at room temperature to lyse bacterial cells. Ten μL of alkaline protease solution was added and mixed by inverting the tube 4 times before incubating the tube for 5 minutes at room temperature. Then, 350 μL of Wizard® *Plus* SV neutralization solution was added and immediately mixed by inverting the tube 4 times. The bacterial lysate was centrifuged at 20,000 × *g* for 10 minutes at room temperature. The cleared lysate was transferred to the prepared spin column by decanting, avoiding disturbing or transferring any of the white precipitate with the supernatant. Again, the supernatant was centrifuged at 20,000 × *g* for 1 minute at room temperature. The spin column was removed from the tube and the flow-through was discarded. Columns were washed with 750 μL of wash solution. The column was centrifuged at 20,000 × *g* for 1 minute at room temperature and the flow-through was discarded. This wash procedure was repeated using 250 μL of wash solution followed by centrifugation at 20,000 × *g* for 2 minutes at room temperature. The plasmid DNA was eluted by adding 50 μL of nuclease-free water to the spin column followed by centrifugation at 20,000 × *g* for 1 minute at room temperature. The purified plasmid DNA was stored at –20˚C or below.

### 2.3.3 DNA amplification by PCR

*P. putida* UW4 genes were amplified from the genomic DNA by PCR with different sets of primers (Table 2-1). The reaction mixture was added on ice as follows: 100 ng genomic

Table 2-1. Oligodeoxyribonucleotide primers used in this work

| Name | Sequence |
|---|---|
| PO | 5’ TGCAGGCATGCAAGCTTGGCA 3’ |
| PI | 5’ ATAGCATGCTTCCGGCTCGTATGTTGTGT 3’ |
| PdfSF | 5’ TTATGGCCATTTTGAACATCCT 3’ |
| PdfSR | 5’ GCTTGCCGTAGCAAGCCTTTG 3’ |
| PdfCF | 5’ ATGGCCATTTTGAACATCCTC 3’ |
| PdfCR | 5’ TCAGGCGTTCTGGCGATGAA 3’ |
| FisSF | 5’ TCTACAGTCATGAGGAAGGCGG 3’ |
| FisSR | 5’ TCATAGATGATCGGTGCGCTTT 3’ |
| FisCF | 5’ ATGAGTGAAGAGATCCAAGTCGAAG 3’ |
| FisCR | 5’ TCAGCGGCGAACGGGGCGCTT 3’ |
| HypSF | 5’ GGGCTGAATTTCCTTTGACATG 3’ |
| HypSR | 5’ CACGGGCAGAGCGGGATTTTTT 3’ |
| HypCF | 5’ ATGTTGAATGACCCGATTCC 3’ |
| HypCR | 5' CTAAACGTTTGGGTCACGCTT 3' |
| OmpSF | 5’ CAGATGGGGATTTAACGGATG 3’ |
| OmpSR | 5’ CAGGCAAAGAAAAGCCCGG 3’ |
| OmpCF | 5’ ATGAAACTGAAAAACACCTTGGG 3’ |
| OmpCR | 5' TTACTTAGCTTGAGCTTCAACCTGC 3' |

DNA as template; 400 nM of each primer; 50 μL of GoTaq® Green Master Mix (Promega Corporation, Madison, WI); and sterile deionised water to a total volume of 100 μL. The components in the tube were mixed and centrifuged to make sure all of them were on the bottom of the tube. A few drops of mineral oil were added to cover the reaction mixture in order to prevent evaporation during the PCR process. The PCR program was set up as follows: one cycle of 95˚C for 5 minutes; 30 cycles of 95˚C for 1 minute, 5˚C below primers' melting temperatures for 1 minute, and 72˚C for 1kbp/minute; then one cycle of 72˚C for 5 minutes. The concentration of the PCR product was estimated by visualizing the DNA band after running the DNA on a 1% agarose gel and staining it with ethidium bromide.

### 2.3.4 Restriction endonuclease digestion and ligation

DNA samples were incubated with the restriction enzyme and its buffer according to instructions from the manufacturer (Fermentas Canada Inc., Burlington, ON). The digestion was carried out in a total volume of 50 μL that consisted of 0.1 to 1 μg of DNA sample, 5 μL of the appropriate 10× buffer, two units of each enzyme. After mixing, the digestion mixture was incubated at 37˚C for at least 1 hour.

Ligation of digested DNA fragments was performed using T4 DNA ligase according to the instructions from the manufacturer (Fermentas Canada Inc., Burlington, ON). The 10 μL ligation mixture contained 1 μL 10× ligation buffer (500 mM Tris-HCl, 100 mM $MgCl_2$, 100 mM dithiothreitol, 10 mM ATP, 300 mg/L BSA, pH 7.5), both insert and vector digest products (1-4 μL of each), 2 units of T4 DNA ligase and the rest of the volume was made up to 10 μL by water. The optimal molar ratio of insert to vector was 3:1. Then, the mixture was

incubated at 4˚C overnight.

### 2.3.5 DNA purification and recovery

After some DNA manipulation, such as PCR amplification, restriction endonuclease digestion, or agarose gel electrophoresis, a Wizard® SV Gel and PCR Clean-Up System (Promega Corporation, Madison, WI) was used to purify the DNA samples in order to get rid of the primers or enzymes. First, an equal volume of membrane binding solution was added to the PCR sample, digestion product or gel piece (100 mg ~ 100 μL). The mixture was incubated at 65°C for 10 minutes if it was for DNA recovery from agarose gel. Then, the SV spin column was placed in a provided 2 mL collection tube. The sample was applied to the column and centrifuged at 20,000 × *g* for 1 minute and the flow-through was discarded. Then, 0.7 mL membrane wash buffer was added and centrifuged at 20,000 × *g* for 1 minute, again discarding the flow-through. The column was centrifuged at 20,000 × *g* for an additional 1 minute and placed in a clean 1.5 mL microcentrifuge tube. To elute the DNA, 50 μL nuclease-free water was added to the center of the SV spin column and centrifuged at 20,000 × *g* for 1 minute.

### 2.3.6 DNA sequence analysis

Plasmids and the sequencing primers were sent to the York University, Biology Molecular Sequencing Facility for DNA sequence analysis.

### 2.3.7 Transformation in *E. coli*

Ten μL of ligation mixture was transferred into a cold sterile 1.5 mL microcentrifuge tube, and kept on ice. An aliquot of frozen competent cells was thawed on ice. The cells were

gently resuspended and the ligation mixture was added to the tube with competent cells and mixed carefully. After being incubated on ice for 30 minutes, the tube was transferred to a 42˚C heating block for 90 seconds. Five hundred μL of room temperature LB medium was added to the cells and the mixture was shaken at 37˚C for 90 minutes. Aliquots of the mixture were plated onto LB-agar plates containing appropriate antibiotics. The plates were incubated at 37˚C overnight.

### 2.3.8 Gene expression and disruption in *P. putida* UW4

#### 2.3.8.1 Construction of pETP

The *Pseudomonas-Escherichia* shuttle expression vector pETP was constructed (Figure 2-1) by inserting the origin of replication (ori1600) from pUCP26 (West et al. 1994) into the *Sph*I site of the expression vector pET30a(+) (Novagen, Hornby, ON). Using primers (Table 2-1) with either the original (PO) or the incorporated (PI) *Sph*I site, the 1557-bp fragment containing ori1600 was amplified from pUCP26 by PCR. Both the PCR fragment and the backbone vector, pET30a(+), were digested with *Sph*I and the fragment was inserted into pET30a(+). The resulting plasmid was designated as pETP (Figure 2-1).

#### 2.3.8.2 Expression in *P. putida* UW4

The genes encoding the four selected *P. putida* UW4 proteins were amplified by PCR using primers (Table 2-1) designed based on conserved up- and down-stream regions in other *Pseudomonas* genomes (*P. fluorescens* strains Pf-5 and PfO-1, and *P. putida* strains KT2440

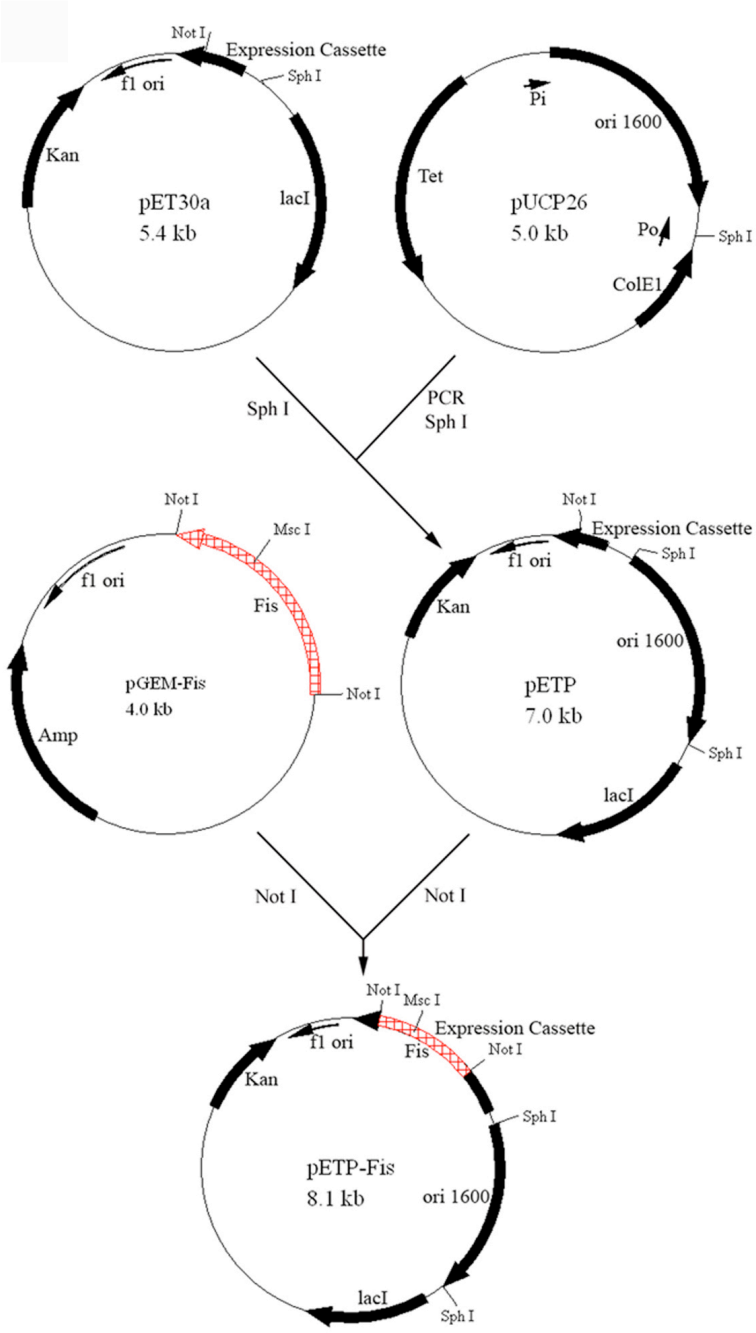


Figure 2-1. A schematic map of construction of the expression vector pETP and cloning *fis* gene in pETP.

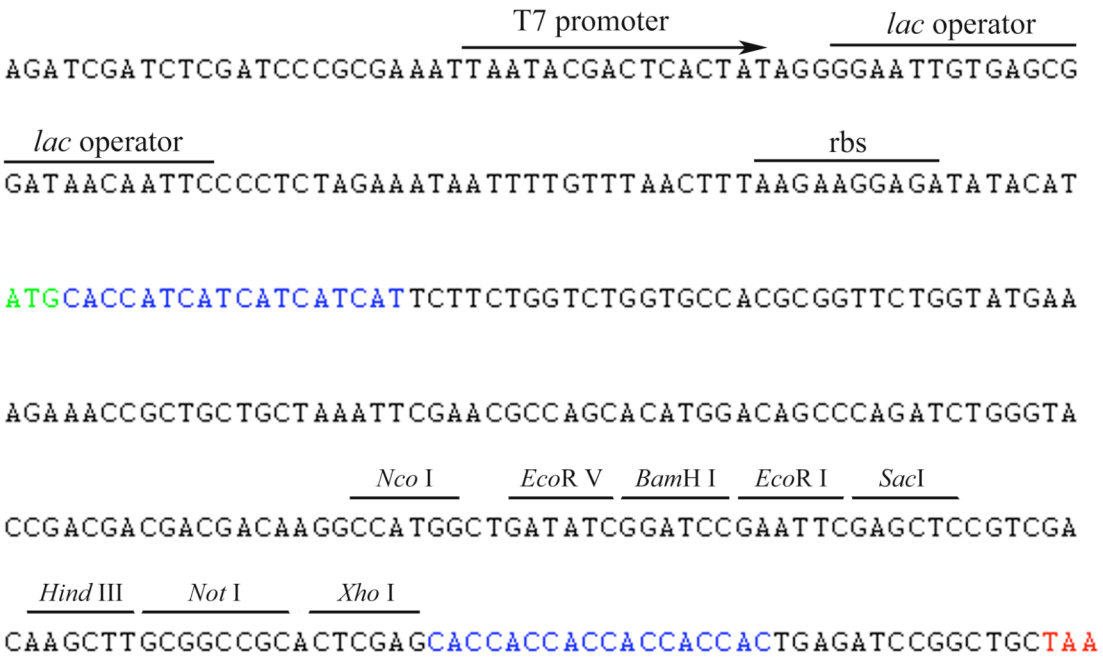


Figure 2-2. Details of the Expression Cassette on pETP. Start and stop codons are highlighted in green and red, respectively. Two 6 × His tags are highlighted in blue.

and F1). The PCR products were cloned into pGEM-T easy (Promega Corporation, Madison, WI). The DNA sequences of these four genes were determined at the Biology Molecular Sequencing Facility, York University (Toronto, ON). Four coding regions were cloned into pGEM-T easy using 4 sets of primers (Table 2-1). The inserts, released by *Not*I digestion, were sub-cloned into the *Not*I site of pETP for expression in *P. putida* UW4. Plasmid constructs were re-sequenced to ensure that genes were inserted in the right reading frame and that no alternations to the DNA sequence had taken place. Plasmids were introduced into *P. putida* UW4 by electroporation as described by Smith and Iglewski (1989).The expression of the 6×His-tagged recombinant proteins was confirmed by western blotting before these strains were used to treat canola seeds in the root elongation growth pouch assay. 2-D western blotting was performed to separate the expressed OmpF protein from a large background band with the same molecular weight in the control sample. The 6×His-tagged proteins were detected using a mouse monoclonal His tag antibody (Novagen, Hornby, ON), and an HRP-conjugated anti-mouse IgG secondary antibody (Sigma-Aldrich Canada Ltd., Oakville, ON). The immune-complexes were visualized by chemiluminescence using an ECL Plus Western blotting detection kit (GE Healthcare, Mississauga, ON).

2.3.8.3 Gene disruption in *P. putida* UW4

The mutant strains *P. putida* UW4/Fis$^{-}$, UW4/Hyp$^{-}$, and UW4/OmpF$^{-}$ were constructed by disrupting the *fis*, *hyp*, and *ompF* genes, respectively. A tetracycline resistance gene was inserted within the coding region of each of these genes by homologous

recombination as

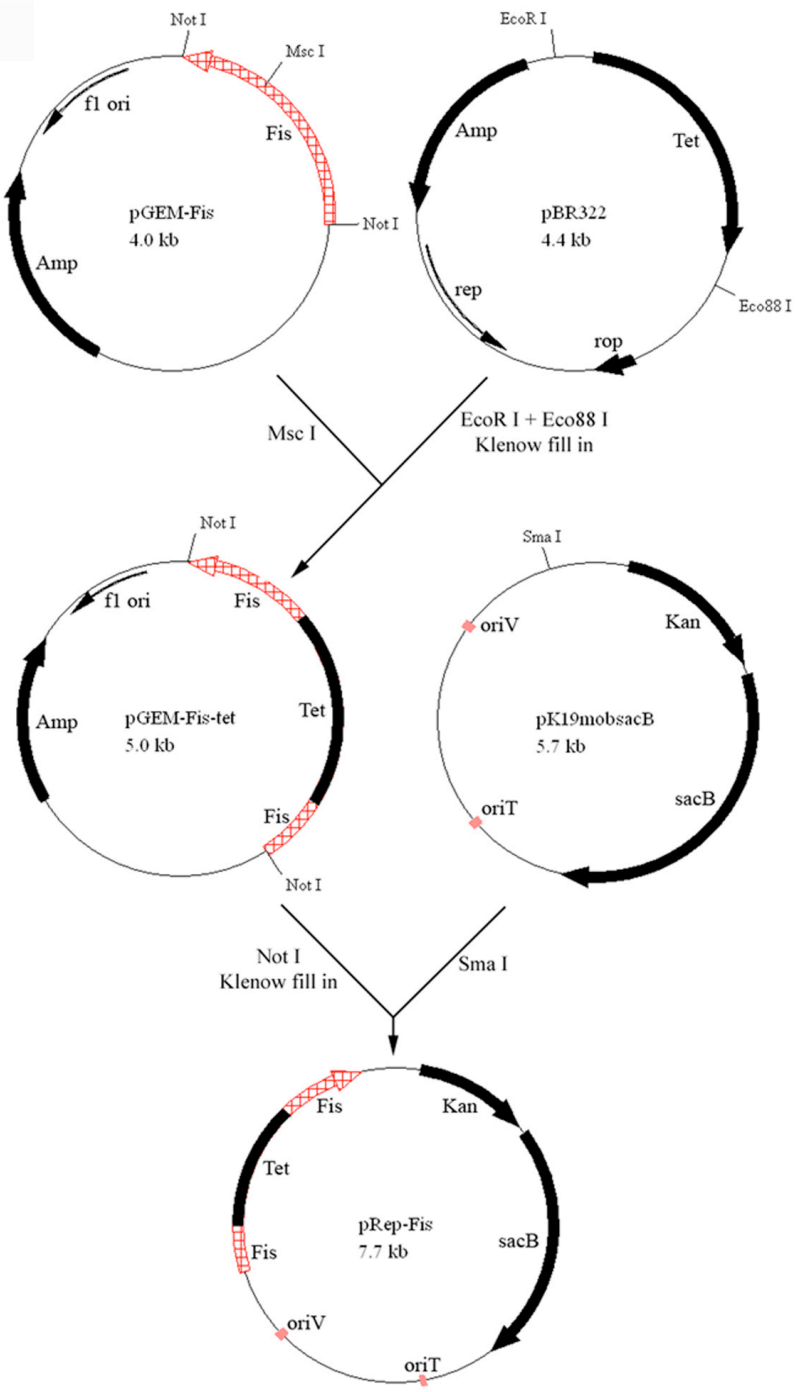


Figure 2-3. A schematic map of construction of the *fis* gene disruption in vector pRep-Fis.

Table 2-2. Restriction enzymes used for gene disruptions.

| Gene | Insertion site* | Subclone site** |
|---|---|---|
| *fis* | *Msc*I | *Not*I |
| *hyp* | *Tth*111I | *Eco*RI |
| *ompF* | *Ava*I | *Eco*RI*** |

* indicates the restriction enzyme site on target genes where the *tetA* gene was inserted.

** indicates the restriction enzyme that was used when subcloning the disrupted target gene from pGEM-T easy vector to pK19mobsacB.

*** there was a new *Eco*RI site created when the tetA gene was ligated into the *ompF* gene *Ava*I site. Partial digest was performed in order to clone the whole fragment into pK19mobsacB.

described previously (Li et al., 2000). For example, the pBR322 *Eco*RI-*Eco*88I fragment containing the tetracycline resistance gene (*tetA*) (Peden, 1983) was inserted into the *Msc*I site within the *fis* coding sequence to make pGEM-Fis-tet (Figure 2-3). Restriction enzymes that were used for disrupting other genes are listed in Table 2-2. The pGEM-Fis-tet *Not*I fragment was then subcloned into the *Sma*I site of the pK19mobsacB, which facilitates gene disruption and allelic exchange by homologous recombination (Schafer et al., 1994). The resulting plasmid pRep-Fis was transformed into *P. putida* UW4 by electroporation (Smith and Iglewski, 1989) and the transformants were selected on TSB plates containing tetracycline and sucrose. All mutant strains were tested for the disruption of the target genes by diagnostic PCR.

## 2.4 Protein extraction and quantification

### 2.4.1 Bacterial protein extraction

Wild-type *P. putida* UW4 and AcdS minus mutant strains were grown as indicated above in section 2.1. Bacterial cells were harvested by centrifugation at 8,000 *g* at 4°C for 10 minutes. The pellets were washed twice with cold water, weighed and then stored at –70°C overnight. The cell pellet was thawed on ice for 15 minutes and resuspended in ice-cold lysis buffer (2 M thiourea, 7 M urea, 4% CHAPS, 30 mM Tris pH 8.5; 5 mL/g wet cells). The cells were then stirred at 4°C for 30 minutes. The lysate was centrifuged at 10,000 *g* at 4°C for 10 minutes, followed by centrifugation at 150,000 *g* at 4°C for 90 minutes. The final supernatant was saved as the whole cell extract and stored at –80°C until use.

### 2.4.2 Plant protein extraction

Plant protein extraction was done as described previously (Zheng et al. 2007). Hydroponically grown canola shoot and root tissues from each whole plant replicate were ground in liquid nitrogen separately. For each replicate, about 0.25 gram of ground tissue was suspended in 0.5 mL of ice-cold extraction buffer (0.7 M sucrose, 0.1 M KCl, 0.5 M Tris pH 8.5, 50 mM EDTA, pH 8.5, 40 mM DTT). Protein yield from 0.25 gram of ground tissue was approximately 0.2 mg. Protein extraction was scaled up if needed) The samples were homogenized by vortexing and the resulting homogenate was mixed well with an equal volume of Tris-saturated phenol (pH 8.5) and centrifuged at 10,000 *g* for 15 minutes at 4°C. The upper phenol phase was collected and mixed well with 5 volumes of ice-cold 0.1 M ammonium acetate in 100% methanol and incubated overnight at –20°C. The samples were then centrifuged at 10,000 *g* for 15 minutes at 4°C and washed twice with ice-cold methanol and then twice with ice-cold acetone containing 20 mM DTT. The pellets were then re-dissolved in 100 μL lysis buffer (2 M thiourea, 7 M urea, 4% CHAPS, 30 mM Tris pH 8.5) and stored at –80°C until further analysis.

### 2.4.3 Protein quantification

Protein concentrations were measured according to the Protein Assay instruction from Bio-Rad Laboratories which is based on the method of Bradford (1976). The linear range of the assay for BSA is 1 to 10.0 μg/mL. Protein solutions were assayed in four replicates. Samples were incubated at room temperature for more than 5 minutes and no more than 1 hour. The absorbance at 595 nm was measured.

## 2.5 Two dimensional gel electrophoresis

### 2.5.1 Difference in gel electrophoresis (DIGE)

The DIGE analyses were performed according to the supplier's instructions (GE Healthcare, Mississauga, ON). Fifty μg of each sample was labeled with 100 pmol of Cy2, Cy3 or Cy5 CyDye DIGE fluors. After labeling, all three samples (internal standard, control sample, treated sample) were mixed together and loaded on Immobiline DryStrips (pH 3-11NL or 4-7, 24 cm). The IEF was conducted at 20ºC on an Ettan IPGphor II system (GE Healthcare, Mississauga, Ontario) using the following program: 500V for 1 hr, gradient to 1,000V for 3 hrs, gradient to 3,000V for 3 hrs, constant voltage of 3,000V for 2 hrs, gradient to 8,000V for 3 hrs, constant voltage of 8,000V for 10.5 hrs, for a total of 108,000 V·hr. Prior to the 2$^{nd}$ dimension separation, the IEF strips were incubated in equilibration buffer (6M urea, 2% w/v SDS, 50 mM Tris-HCl pH 8.8, 30% v/v Glycerol, 0.002% (w/v) bromophenol blue) containing DTT (10 mg/mL) for 20 min, then for a further 20 min with a second buffer (containing 25 mg/mL iodoacetamide instead of DTT, otherwise identical) in the dark. The strips were loaded onto 12% SDS-PAGE gels and the 2$^{nd}$ dimension separation was carried out at 10ºC. The analytical gels were scanned on a Typhoon 9400 scanner (GE Healthcare, Mississauga, ON). Each analysis was done in triplicate. Differential expression profiles were analyzed using DeCyder V 6.0 software (GE Healthcare, Mississauga, ON). The average ratios value indicated the standardized volume ratios between the treated and control bacteria. Expression ratios were calculated as R = (treated/control) for up-regulated proteins, and calculated as R = –(control/treated) for down-regulated proteins, where a 2-fold up-regulation or down-regulation

is represented by 2 and –2, respectively. Statistical significance was calculated using the DeCyder software (for bacterial proteomics), then exported and corrected for multiple hypothesis testing (for plant proteomics) using the p.adjust function (method="fdr") in the *R* statistical computing environment (R version 2.7.2, http://www.r-project.org/).

To group proteins based on their accumulation patterns under different conditions, the changes of proteins with significantly changed expressions were exported from DeCyder. For the sake of simplicity, log base 2 fold changes were used in clustering analysis, instead of the original expression ratios calculated in DeCyder, which lack the range of –1 to 1. Pearson correlation was used as a distance measure (1-correlation) along with average-link clustering (cluster to cluster distance measured as the mean distance over all pairs of objects in the two clusters). Clusters were defined by cutting the gene clustering dendrogram at a (arbitrarily selected) height of .2, producing 16 clusters. Clustering and graphical output were constructed using the heatmap.2 function of the gplots package in the *R* statistical environment (gplots version 2.6.0, R version 2.7.2).

### 2.5.2 Preparative gels

Protein components of bacterial or plant samples were separated in the first dimension using 24-cm pH 3-11NL or pH 4-7 Immobiline IPG Drystrips (GE Healthcare, Mississauga, Ontario). The IPG strips were passively rehydrated with approximately 0.5-1 mg of protein sample in 450µl of rehydration buffer (2 M thiourea, 7 M urea, 4% w/v CHAPS, 30 mM Tris pH 8.5, 60 mM DTT, 0.5% v/v IPG pH 4-7 buffer, and a trace of bromophenol blue) overnight. The IEF and 2$^{nd}$ dimension separations were carried out as described above. The resulting 2-D gels were stained overnight with Bio-Safe Coomassie or SyproRuby (Bio-Rad Laboratories,

Mississauga, ON) and de-stained with water. The de-stained preparative gel was scanned using a Typhoon Laser scanner 9400 (GE Healthcare, Mississauga, Ontario) configured to scan with an excitation wavelength of 633 nm and without an emission filter for commassie stained gels and an excitation wavelength of 457 nm and an emission filter at 610 nm for SyproRuby stained gels.

### 2.6 Mass spectrometry

Spots of interest were excised from the gel. The gel pieces were washed with water and destained with 50 mM $NH_4HCO_3$/50% acetonitrile (ACN). Proteins were reduced by incubation with 10 mM dithiothreitol in 100 mM $NH_4HCO_3$ at 50°C for 30 min, and then alkylated by incubation with 55 mM iodoacetamide in 100 mM $NH_4HCO_3$ for 30 min in the dark. After being dehydrated with 100% ACN and air-dried, the gel pieces were rehydrated for ten minutes in a trypsin solution (Promega Corporation, Madison, Wisconsin) in a ratio of approximately 1:10 (w/w) of trypsin:protein. Fifty μL of 50 mM $NH_4HCO_3$ (pH 8.0) was added to each gel piece and the proteins were digested at 37°C for 18 hours. The peptides were extracted by vortexing and then concentrated to 10 μL in a Savant SpeedVac. The samples were cleaned using a C-18 ZipTip system (Millipore) and analyzed by MS/MS using either a Waters Micromass Ultima Q-TOF mass spectrometer or LC-MS/MS performed on an Applied Biosystems Q-TRAP system. All proteins were identified by the PEAKS software 3.1 (Ma et al., 2003) (Bioinformatics Solutions Inc., Waterloo, ON), which combines auto *de novo* sequencing and database searching (MSDB and NCBI nr database were downloaded on February 28$^{th}$, 2007). The parental and fragment mass error are 0.2 Da and 0.1 Da,

respectively. Trypsin was used for the enzyme digest; with one missed cleavage allowed, and with carbamidomethylation and methionine oxidation as fixed and variable modifications, respectively. Identifications were confirmed using the MASCOT MS/MS ion search and/or peptide-fingerprinting algorithm (Perkins et al., 1999), with the same parameters used for the digestion enzyme, post-translational modifications, and missed cleavages as with the PEAKS software. Default peptide tolerances were used.

# 3. Results

## 3.1 The responses of *P. putida* UW4 to nickel stress

Small amounts of nickel are essential for the functioning of a number of nickel-containing enzymes including hydrogenase, urease, carbon monoxide dehydrogenase, and superoxide dismutase (Mulrooney and Hausinger, 2003). However, nickel is one of the most common metal contaminants in the environment and is often toxic to bacteria at high concentrations. This toxicity is generally a consequence of nickel binding to sulfhydryl groups of sensitive enzymes or displacing essential metal ions in a variety of biological processes (Valko et al., 2005). Also, cationic nickel (mostly $Ni^{2+}$) can cause a significant oxidative stress in bacteria by facilitating the production of oxidized bis-glutathione, which releases hydrogen peroxide (Valko et al., 2005). In bacterial cells, cation efflux-mediated nickel resistance is one of the best-known mechanisms of nickel detoxification (Nies, 2003; Schmidt and Schlegel, 1994). In addition, the up-regulation of genes encoding anti-oxidant enzymes is often the main response of many bacteria to various metals (Hu et al., 2005). In this regard, thiol-containing molecules were shown to be capable of detoxifying cadmium in *Rhizobium leguminosarum bv. viciae* (Figueira et al., 2005) and nickel in human cells (Lynn et al., 1999).

Recently, researchers have attempted to develop metal phytoremediation protocols including the harvesting and combusting of plants grown in metal-contaminated soil, as an alternative to the traditional remediation methods that involve excavation and removal of soil to secured landfill sites (Glick, 2010). Ideally, the plants used for metal phytoremediation grow rapidly and produce high levels of biomass. Unfortunately, plant growth, even plants that are

relatively metal tolerant, is generally inhibited in the presence of high concentrations of metals. One of the strategies that has been used to overcome this problem is the addition of ACC deaminase-containing plant growth-promoting bacteria (PGPB) that can improve plant performance under various environmentally stressful conditions (Glick, 2010).

Here, differences in expression levels in the proteome of the wild-type PGPB *P. putida* UW4 and AcdS minus mutant were examined. This work furthers understanding of the biochemical basis of bacterial resistance to nickel stress, which for *P. putida* is an important component of its ability to facilitate phytoremediation of heavy metals in soil. Although it is expected that the reduced impact of the *P. putida* UW4 AcdS minus mutant strain on plant growth is mostly likely due to higher levels of ethylene, the mutant strain was also compared to verify that the *P. putida* UW4 response to nickel stress was largely independent of the *acdS* gene.

### 3.1.1 The inhibitory effect of nickel on growth of *P. putida* strains

The growth rates of wild-type *P. putida* UW4 and AcdS minus mutant in rich medium (TSB) without nickel at their optimal growth temperature (30°C) were 0.55 and 0.63 generation/hour, respectively (Table 3-1). These rates were reduced to 44% and 40% of the control level when growth was in TSB containing 2 mM nickel, and dropped to 15% and 14% in the presence of 5 mM nickel. The inhibitory effects of different concentrations of nickel on the growth rates of the wild type and mutant strains did not notably differ from each other ($p > 0.5$).

Table 3-1. The effects of nickel on the growth rates of *P. putida* UW4 wild-type and mutant strains.

| Bacterial strains | *P. putida* UW4 | | | *P. putida* AcdS minus mutant | | |
|---|---|---|---|---|---|---|
| Added nickel | 0 mM | 2 mM | 5 mM | 0 mM | 2 mM | 5 mM |
| Growth rate ($h^{-1}$) | 0.55±0.02 | 0.24±0.03 | 0.08±0.01 | 0.63±0.05 | 0.25±0.04 | 0.09±0.01 |
| Growth rate (% of control) | 100 | 44* | 15* | 100 | 40 | 14 |

Growth rates were measured in triplicate. * Denotes values determined not to be significantly different between the wild type and the mutant growth rate values by independent t-test ($p > 0.5$).

### 3.1.2 The effects of nickel on *P. putida* proteomes

The expression profiles of wild-type *P. putida* UW4 and the AcdS minus mutant in response to 2 mM of nickel were analyzed. Of a total of 1,702 proteins detected on the analytical gels for wild-type *P. putida* UW4, the expression levels of 82 (4.82%) proteins increased significantly and 81 (4.76%) proteins decreased significantly ($p \leq 0.05$, | Ratio | $\geq$ 1.5). Results were similar for the AcdS minus mutant strain, with 1,575 proteins detected on the analytical gels. In this case, the expression levels of 74 (4.70%) proteins increased significantly and 51 (3.24%) proteins decreased significantly.

Figure 3-1 shows a representative analytical gel comparing protein expression of wild-type *P. putida* UW4 in the presence and absence of 2 mM nickel. On this gel, the 2 mM nickel treated sample is labeled with Cy5 (red) and the control labeled with Cy3 (green), and up-regulated and down-regulated proteins appear as red and green spots respectively.

All protein spots identified as having significantly changed expression levels and present in sufficient amount to be visible on a coomassie-stained preparative gel were excised for mass spectrometric analysis. From the excised protein spots, a total of 35 proteins with significantly differential expression levels were identified by mass spectrometry (Table 3-2, Figure 3-2). Although the genomic sequence of *P. putida* UW4 has not yet been characterized, proteins were able to be identified via homologous proteins from other *Pseudomonas* strains by the PEAKS software, which combines *de novo* peptide sequencing with database identifications (Table 3-2). Among these 35 proteins, the best sequence coverage (50.5%) was

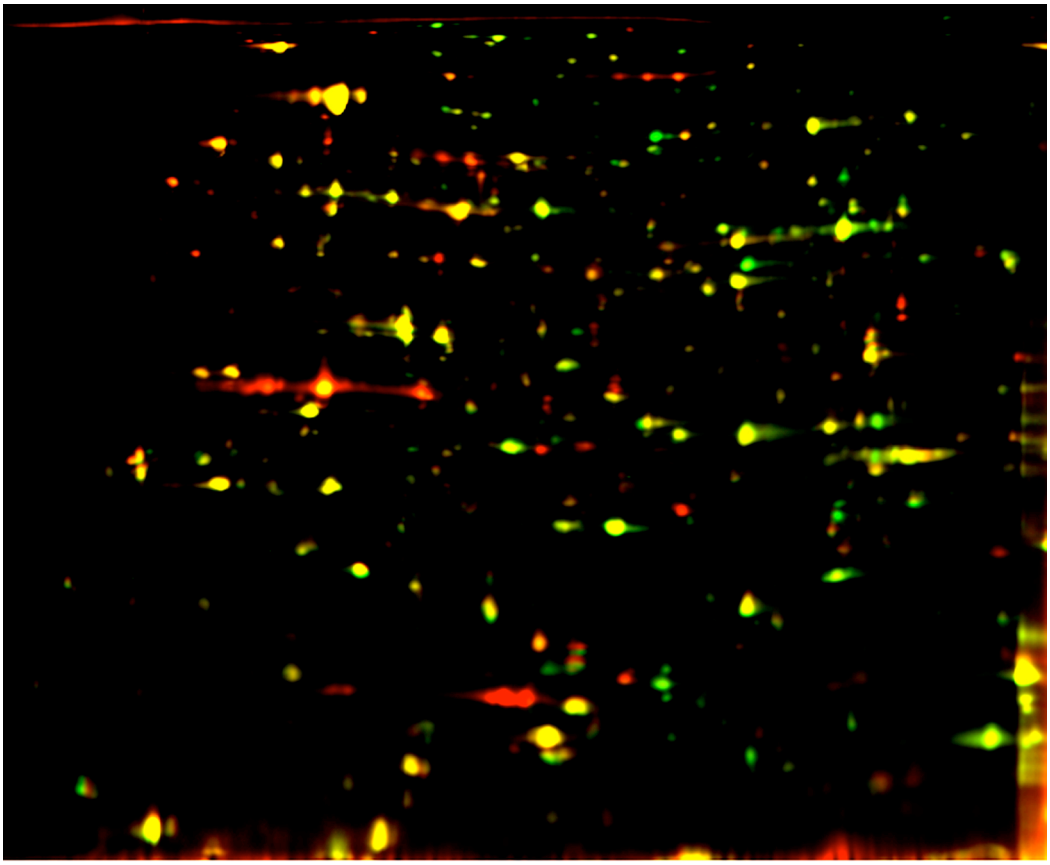

Figure 3-1. An analytical gel comparing protein expression of the bacterium *P. putida* UW4 exposed to 2 mM of nickel.

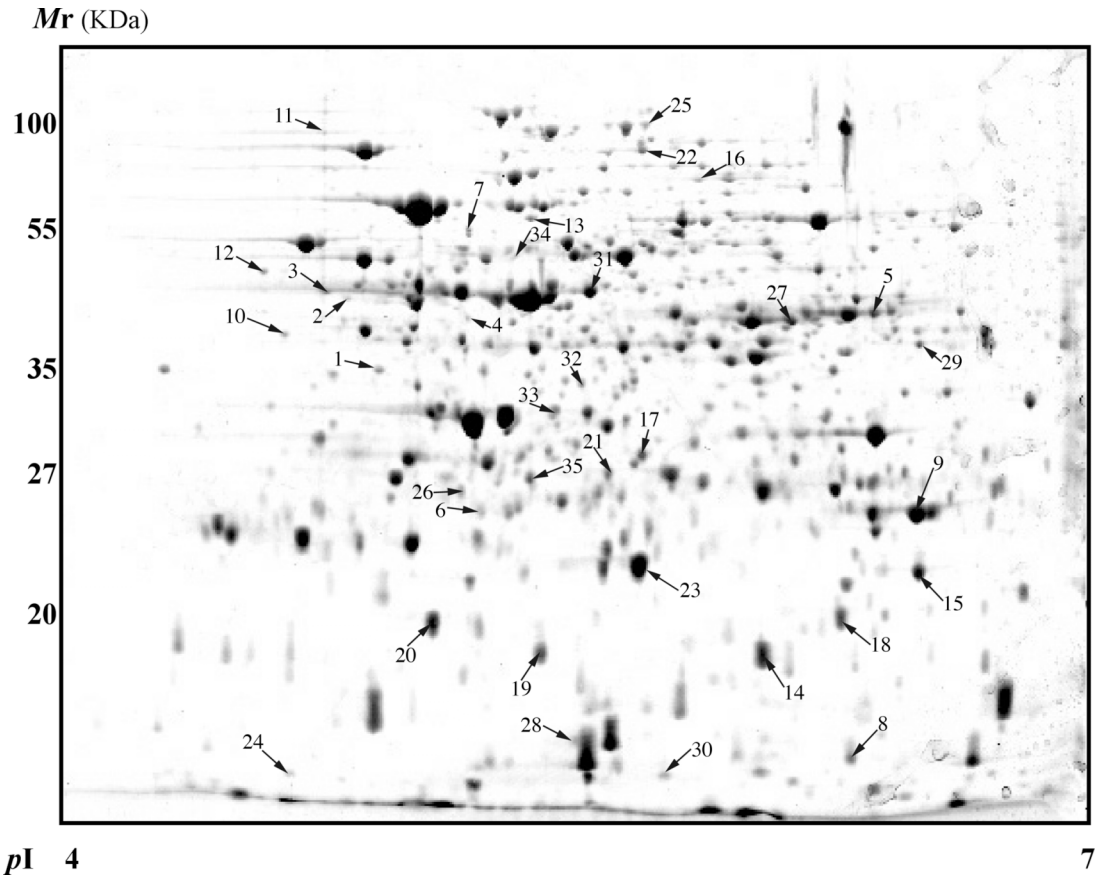


Figure 3-2. A preparative gel of *P. putida* UW4 control proteins. About 1 mg of protein samples were loaded onto IPG 4-7 strip in the first dimension, and separated using 12% SDS-PAGE gel in the second dimension. Proteins spots were visualized by Coomassie staining. The 35 identified and labeled spots are annotated by numbers according to Table 3-2.

Table 3-2. Differentially expressed proteins identified in *P. putida* UW4 wild-type and AcdS minus mutant in presence of 2 mM nickel, grouped by putative functional role.

| Protein[1] | Accession number[2] | MW(kDa) /p*I*[3] | Score/Sequence coverage %[4] | WT[5] | Mut[5] |
|---|---|---|---|---|---|
| **Amino acid metabolism** | | | | | |
| 1. ACC deaminase | Q4KK38_PSEF5 | 35.1/5.37 | 84.15/9.06 | 1.58 | N/A |
| 2. diaminopimelate decarboxylase | Q3K4R9_PSEPF | 45.1/4.97 | 93.68/10.6 | 10.3 | 2.80 |
| 3. porphyromonas-type peptidyl-arginine deiminase | Q3KJM1_PSEPF | 40.7/4.81 | 40.07/8.7 | 2.08 | 1.54 |
| 4. arginine biosynthesis protein | Q3K7U0_PSEPF | 42.6/5.16 | 96.15/8.89 | -3.05 | -2.48 |
| 5. aminotransferase | Q3KG66_PSEPF | 43.3/6.01 | 98.92/19.14 | -2.32 | -2.87 |
| 6. 3-isopropylmalate dehydratase | Q3KF23_PSEPF | 24.2/5.39 | 87.37/35.98 | -1.31 | -1.79 |
| 7. anthranilate synthase | Q4K4Z5_PSEF5 | 54.2/5.08 | 92.94/15.96 | -1.04 | -3.25 |
| **General stress** | | | | | |
| 8. universal stress protein | Q4KFC6_PSEF5 | 16.2/5.95 | 78.23/20.69 | 1.99 | 1.80 |
| 9. general stress protein CTC | Q3K6W3_PSEPF | 21.2/5.99 | 98.62/16 | 3.56 | 2.08 |
| **Transport/efflux** | | | | | |
| 10. major outer membrane protein | Q9X4L6_PSEFL | 36.5/4.68 | 90.82/13.08 | 2.00 | 2.15 |
| 11. outer membrane protein OMP85 | Q4KHG8_PSEF5 | 87.5/5.21 | 128/20 | 3.58 | 1.56 |
| 12. porin D | Q48FB5_PSE14 | 46.9/4.94 | 60.66/4.32 | 2.44 | 3.66 |
| 13. ArsA | Q89K44_BRAJA | 63.5/5.81 | 99/4 | 1.89 | 1.68 |
| **Protein synthesis and folding** | | | | | |
| 14. peptidyl-prolyl cis-trans isomerase B | Q87YQ0_PSESM | 18.2/5.86 | 71.15/6.59 | -1.62 | 1.55 |
| 15. ribosome recycling protein | Q886P0_PSESM | 20.4/6.76 | 46.7/8.65 | -2.16 | -1.51 |
| 16. glutaminyl-tRNA synthetase | Q1IBQ0_9PSED | 64.5/5.62 | 91.43/10.41 | -2.29 | -1.29 |
| **Cell cycle and communication** | | | | | |
| 17. MinD | Q3KFL9_PSEPF | 33.7/5.55 | 99.17/29.7 | -1.59 | -1.51 |
| 18. DNA-binding protein | Q889U1_PSESM | 20.9/5.88 | 46.84/16.93 | -2.27 | -1.32 |
| 19. transcription regulator TraR/DksA family | Q3K6R3_PSEPF | 16.8/5.21 | 62.4/20.41 | -1.59 | 1.05 |
| **Anti-oxidative** | | | | | |
| 20. thiol specific antioxidant | Q3KD94_PSEPF | 17.6/4.99 | 87.21/30.72 | 3.38 | 1.17 |
| 21. ferredoxin NADP-reductase | Q48FA2_PSE14 | 29.6/5.32 | 97.54/29.73 | 1.69 | 1.77 |
| 22. GTP-binding protein TypA | Q3KJG5_PSEPF | 67.0/5.40 | 95.1/9.9 | 2.32 | 1.5 |
| 23. superoxide dismutase | Q3K7N1_PSEPF | 22.0/5.56 | 99.86/50.51 | 5.62 | 4.63 |
| 24. thioredoxin | Q3K4W0_PSEPF | 11.7/5.06 | 95.81/44.04 | 19.8 | 3.41 |
| 25. 2-oxo-acid dehydrogenase | Q3KJ49_PSEPF | 99.4/5.48 | 98.77/9.31 | 1.42 | 1.73 |
| **Other** | | | | | |
| 26. ubiquinone dehydrogenase | Q3KA62_PSEPF | 25.3/5.16 | 73.16/22.77 | -1.31 | -1.93 |
| 27. thiolase | Q4ZY90_PSEU2 | 40.4/5.91 | 89.57/6.89 | -1.82 | -1.13 |
| 28. similar to immunodominant antigen B | Q4L351_STAHJ | 18.3/5.08 | 48.52/10.56 | 29.6 | 1.26 |
| 29. aldo/keto reductase | Q3K722_PSEPF | 38.9/5.88 | 69.66/12.72 | -1.61 | -1.14 |
| 30. pterin-4-alpha-carbinolamine dehydratase | Q3KG65_PSEPF | 13.3/5.83 | 99.4/78.81 | -2.91 | 2.08 |

| | | | | | |
|---|---|---|---|---|---|
| 31. isocitrate dehydrogenase | Q4K9U5_PSEF5 | 45.3/5.27 | 99.97/27.75 | -1.77 | -1.38 |
| 32. transaldolase | Q3K9H0_PSEPF | 33.7/5.66 | 96.25/15.26 | -2.8 | -1.25 |
| 33. dihydrodipicolinate synthase | Q3KGJ2_PSEPF | 31.3/5.77 | 97.86/39.04 | -1.83 | 1.01 |
| 34. hypothetical protein | Q3KFH8_PSEPF | 55.6/5.51 | 82.14/5.87 | 2.01 | 1.52 |
| 35. hypothetical protein | Q3KI45_PSEPF | 25.7/5.36 | 83.22/12.61 | -1.34 | -1.51 |

[1] The numbers next to the identified proteins refer to the numbers in Figure 3-2.

[2] Accession number of top database match from SwissProt *Expasy* database (Gasteiger et al., 2003).

[3] MW and p*I* were calculated from amino acid sequence of the top database match using the *Expasy* Compute pI/MW tool (Gasteiger et al., 2003) and compared with gel location.

[4] PEAKS Score and sequence coverage were calculated by PEAKS software, except for the underlined value which used MASCOT scores.

[5] WT and Mut represent protein expression ratios in wild-type *P. putida* UW4 and AcdS minus mutant treated with nickel respectively. Underlined numbers indicate proteins expression that was not significantly changed. N/A, not applicable.

obtained from the protein identified as iron/magnesium superoxide dismutase by database match with a homologous *P. fluorescens* protein (Figure 3-3). Figure 3-3A shows the PEAKS software identification report for the superoxide dismutase indicating overall identification score, sequence coverage, accession number, protein function, peptide-matching figure and peptides list. The peptides matching to superoxide dismutase were highlighted in red in the protein sequence. And the peptides list shows the mass/charge ratio, charge status, calculated mass, and position in the matched protein, individual identification score, and the amino acid sequence of each peptide. In Figure 3-3B and C, the MS/MS spectra of the two peptides labeled with an asterisk in Figure 3-3A are matched to the corresponding amino acid sequences, which are shown in the orientation of C-terminus to N-terminus. The protein ArsA and the immunodominant antigen B were identified via matches to proteins from *Bradyrhizobium* and *Staphylococcus*, respectively.

The functional annotation from the Swiss-Prot database of these proteins revealed a variety of cellular functions and can be divided into 7 categories (Table 3-2). Out of the 35 identified proteins, nineteen were common to both wild-type and the AcdS minus mutant expression profiles. Eleven proteins were identified as having significantly different expression only in the wild-type profile and five proteins had altered expression only in the AcdS minus mutant profile.

ACC deaminase was identified in the wild-type *P. putida* UW4 profile where its expression was increased by 1.58 fold in response to 2 mM nickel (Table 3-2). Not surprisingly, there was no data available for its expression in the AcdS minus mutant strain

A

**Q3K7N1_PSEPF** Mass: **21957.82** Score: **99.86%**
**Superoxide dismutase (EC 1.15.1.1).- Pseudomonas fluorescens (strain PfO-1).**
Sequence Coverage: **50.51%**

**Matched peptides shown in Red**

1 MAFELPPLPY AHDALQPHIS KETLEFHHDK HHNTYVVNLN NLVPGTEFEG
51 KTLEEIVKTS SGGIFNNAAQ VWNHTFYWNC LAPNAGGQPT GALAEAINAA
101 FGSFDKFKEE FSKTSIGTFG SGWGWLVKKA DGSLALASTI GAGNPLTSGD
151 TPLLTCDVWE HAYYIDYRNL RPKYVEAFWN LVNWKFVAEQ FEGKTFTA

**Peptides List**

| | Mz | Charge | Mr(calc) | Start | End | Score | Peptide |
|---|---|---|---|---|---|---|---|
| * | 416.23364 | 2 | 812.46436 | 52 | 58 | 99% | TLEEIVK |
| * | 457.72363 | 2 | 895.4439 | 107 | 113 | 99% | FKEEFSK |
| | 527.7536 | 2 | 1035.5024 | 186 | 194 | 98.23% | FVAEQFEGK |
| | 561.78546 | 4 | 2225.1633 | 2 | 21 | 96.27% | AFELPPLPYAHDALQPHISK |
| | 578.2636 | 2 | 1136.525 | 22 | 30 | 99% | ETLEFHHDK |
| | 748.70483 | 3 | 2225.1633 | 2 | 21 | 95.68% | AFELPPLPYAHDALQPHISK |
| | 784.8736 | 2 | 1549.7717 | 174 | 185 | 94.48% | YVEAFWNLVNWK |
| | 798.3836 | 2 | 1576.8038 | 114 | 128 | 99% | TSIGTFGSGWGWLVK |
| | 880.39545 | 4 | 3499.691 | 22 | 51 | 61.14% | ETLEFHHDKHHNTYVVNLNNLVPGTEFEGK |

B

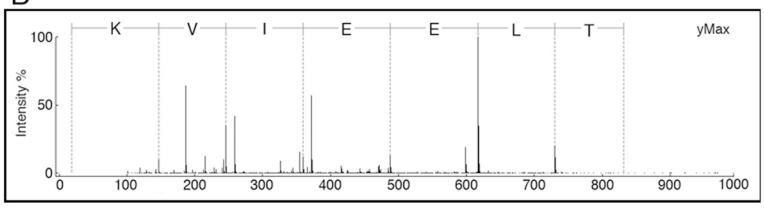


C

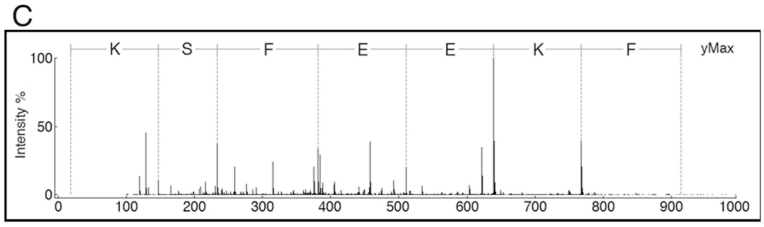


Figure 3-3. The PEAKS software identification report of superoxide dismutase. A. The peptides matched to superoxide dismutase were highlighted in red in the protein sequences and listed underneath. B and C. The yMax MS/MS spectra of the two peptides labeled with expression change in the wild-type *P. putida* UW4 profile in the protein matching an asterisk in A are matched to the corresponding amino acid sequences.

profile since the gene encoding ACC deaminase was deleted in this strain. The largest expression change was in the wild-type *P. putida* UW4 profile in the protein matching immunodominant antigen B where the increase was nearly 30-fold in response to 2 mM nickel (Table 3-2). This protein was not detected as significantly changed in the mutant expression profile.

Surprisingly, the expression of peptidyl-prolyl cis-trans isomerase B and pterin-4-alpha-carbinolamine dehydratase were altered in opposite directions between the wild-type and mutant profiles, and both had relatively small changes in expression. While it is possible these may represent real differences between the two tested strains, they may also simply be artifacts or false positives within the set false discovery rate of 5%.

The nineteen proteins that were found in both the wild-type and the mutant expression profiles, and were changed in a similar manner in both strains appear to be related to nickel stress and detoxification. Proteins involved in amino acid synthesis, such as arginine biosynthesis protein and aminotransferase were both down regulated, as was a ribosome-recycling protein, which is involved in protein synthesis. In addition, MinD, a protein essential for cell division was also down regulated. On the other hand, transport proteins (both import and export), such as major outer membrane protein, outer membrane protein OMP85, porin D and ArsA, were all up regulated. The other up regulated proteins were categorized as either general stress proteins, such as universal stress protein and general stress protein CTC, or anti-oxidative proteins such as ferredoxin NADP-reductase, GTP-binding protein TypA, superoxide dismutase, and thioredoxin. Among these stress-related proteins, superoxide dismutase expression was increased by 5.62-fold and 4.63-fold in the wild-type and the mutant

respectively, and thioredoxin was increased by 19.84-fold in the wild-type and by 3.41-fold in the mutant.

### 3.2 The responses of *P. putida* UW4 to canola root exudates

Various components in plant exudates play important roles in plant-bacterial interactions (de Weert et al., 2002; Mark et al., 2005). Most previous studies of plant exudates have focused on their ability to be utilized by surrounding bacteria and therefore facilitate plant-bacterial interactions via bacterial chemotaxis, root colonization and root growth stimulation (de Weert et al., 2002; Kamilova et al., 2006; Lugtenberg et al., 1999). For example, Mark et al. (2005) investigated global influences of plant exudates on bacterial gene expression, and identified genes involved in rhizosphere colonization using microarrays, including some genes that had not been characterized previously. Here, in order to identify bacterial proteins mediating interactions between the plant growth-promoting bacterium *P. putida* UW4 and canola, protein expression profiles of bacterial strains *P. putida* UW4 and AcdS minus mutant following exposure to canola root exudates were investigated using proteomic tools.

In addition, both ACC and IAA play important roles in the process of plant growth promotion by bacteria (Glick, 1995; Patten and Glick, 2002). It has been shown that bacteria are able to alter the levels of certain components (amino acids, sugars and organic acids) in plant exudates (Naher et al., 2008; Penrose and Glick, 2001). In this work, the IAA and ACC levels in canola root exudates from control and bacteria-treated plants were compared to assess the impacts of different bacterial strains on these levels.

### 3.2.1 Plant hormones in canola root exudates

Canola seeds were treated with either *P. putida* UW4, AcdS minus mutant, or $MgSO_4$ buffer as a control, and root exudates were collected seven days after planting. Measurement of the IAA and ACC content of these exudates pooled from 300 plants (Figure 3-4) revealed that treatment of plants with the wild-type strain dramatically increased the amount of IAA secreted by the plant while treatment the AcdS minus mutant strain only slightly increased IAA levels. In addition, treatment of plants with the wild-type but not the AcdS minus mutant bacteria lowered the amount of ACC that was exuded.

### 3.2.2 The effects of canola root exudates on *P. putida* proteomes

The protein expression profiles of *P. putida* UW4 and AcdS minus mutant in response to canola root exudates were analyzed and significant changes were observed in both samples. Out of a total number of 1,757 proteins detected on the analytical gels for *P. putida* UW4, the expression levels of 220 (12.52%) proteins were significantly increased and 172 (9.79%) proteins were significantly decreased ($p \leq 0.05$, $| \text{Ratio} | \geq 1.5$). Results were comparable for the AcdS minus mutant strain, although a smaller number of differentially expressed proteins were detected. For the mutant strain, 1,670 proteins were detected, where expression levels of 164 (9.82%) proteins were significantly increased and 115 (6.89%) proteins were significantly decreased.

A total of 72 proteins with significantly different expression levels in the presence of the added plant exudates were successfully identified by mass spectrometry via matches to

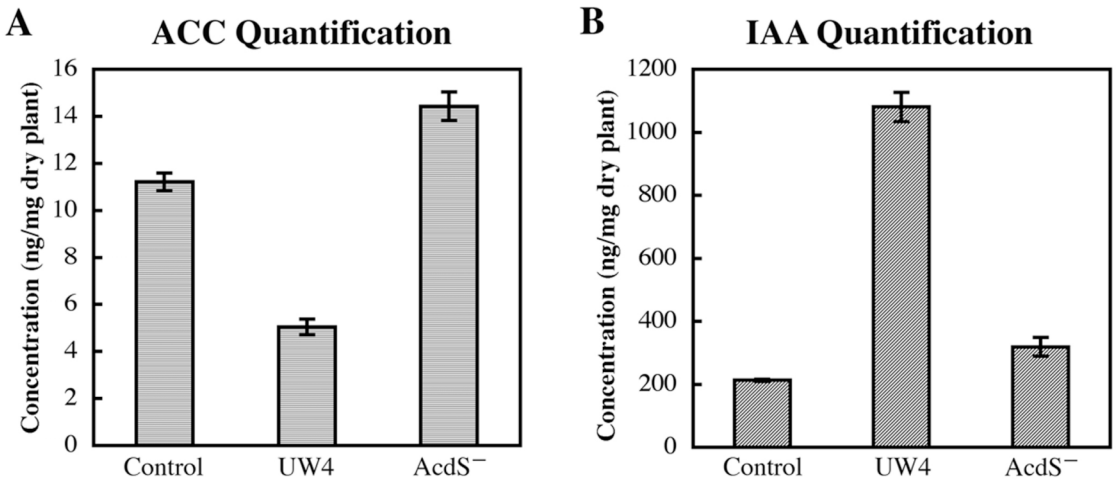


Figure 3-4. The ACC (A) and IAA (B) concentrations in the root exudates from control and treated plants. Exudates were pooled from 300 plants, and ACC and IAA concentrations measured in triplicate analytical HPLC runs.

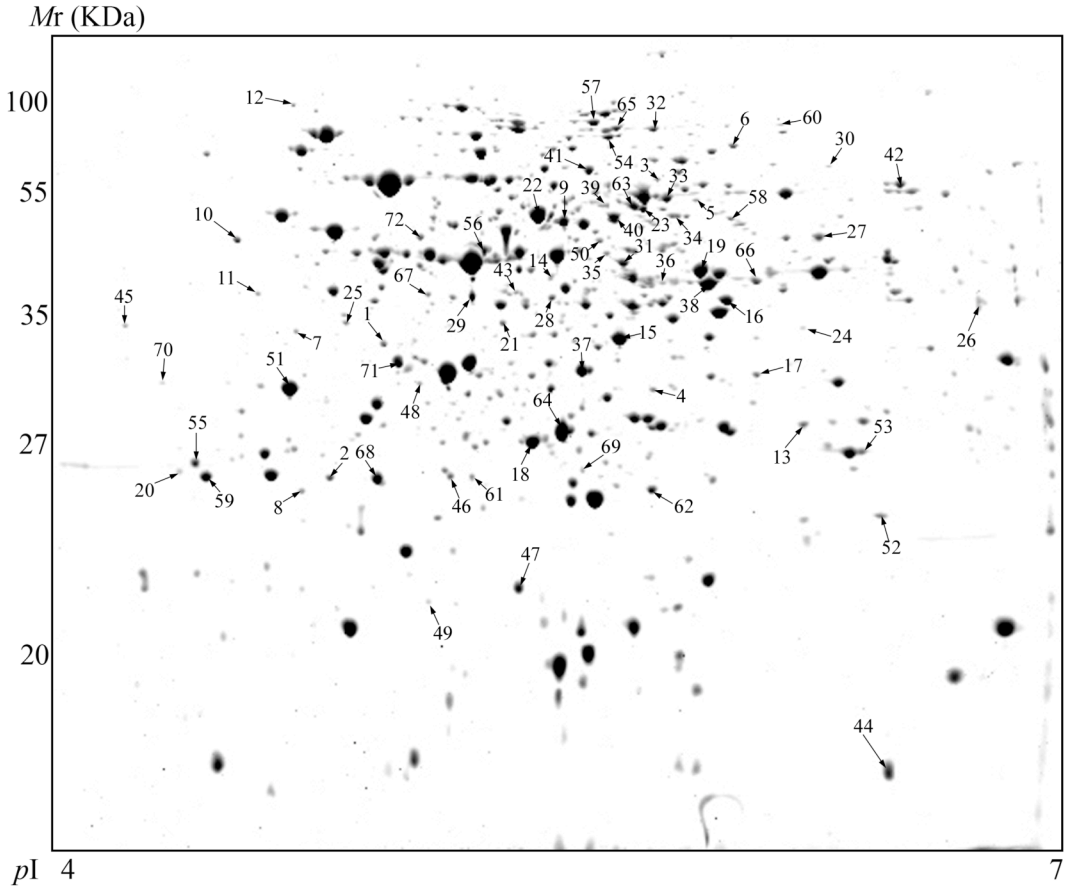


Figure 3-5. A preparative gel of *P. putida* UW4 protein. Approximately 1 mg of protein was separated using an IPG 4-7 strip in the first dimension, and a 12% SDS-PAGE gel in the second dimension. Proteins spots were visualized by Coomassie staining. The 72 identified and labeled spots are annotated according to the numbers used in Table 3-3.

homologous proteins from other *Pseudomonas* strains (Figure 3-5), and divided into nine groups based on functional annotation from the Swiss-Prot database (Figure 3-6 and Table 3-3). In Figure 3-6, differential expression is visualized on a scale with red indicating up regulation and green indicating down regulation for identified proteins in the presence of canola root exudates in wild-type and AcdS minus mutant strain, respectively. White boxes represent proteins whose expression was not significantly altered. Details of the mass spectrometric identification and differential expression are included in Table 3-3. Sixty-four of the protein expression changes were observed in the profiles of both strains. Proteins in groups I to V were significantly up-regulated in the presence of canola root exudates in both wild-type and AcdS minus mutant. These proteins are involved in bacterial envelope synthesis, membrane transportation, as well as metabolism of nucleic acids, amino acids, and carbohydrates. ACC deaminase was significantly up-regulated in the wild-type, although at only a moderate level of 1.64-fold in wild-type. On the other hand, five transcriptional regulators in group VI were down-regulated while one transcription repressor NmrA-like protein was up-regulated. NmrA is a negative transcriptional regulator involved in controlling nitrogen metabolite repression (Andrianopoulos et al., 1998). Protein expression levels within group VII (protein synthesis, folding and degradation) and group VIII (oxidoreductase) exhibited both increases and decreases. Lastly, group IX includes a previously uncharacterized protein, a hypothetical protein A and cell division protein FtsA. From the 64 proteins whose expression changed significantly in both the wild-type and AcdS minus mutant mutant, four proteins were selected for additional analyses to confirm their involvement in plant-bacterial interaction.

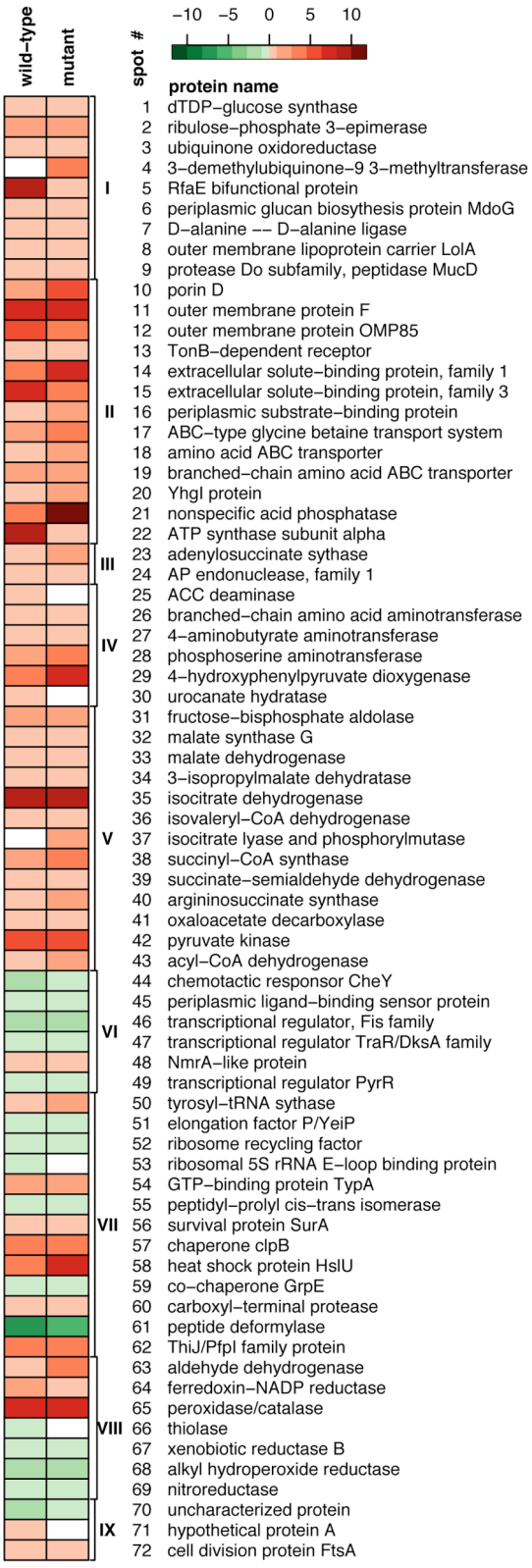
wild−type
mutant
−10 −5 0 5 10
spot #
protein name
I
II
III
IV
V
VI
VII
VIII
IX
1 dTDP−glucose synthase
2 ribulose−phosphate 3−epimerase
3 ubiquinone oxidoreductase
4 3−demethylubiquinone−9 3−methyltransferase
5 RfaE bifunctional protein
6 periplasmic glucan biosythesis protein MdoG
7 D−alanine −− D−alanine ligase
8 outer membrane lipoprotein carrier LolA
9 protease Do subfamily, peptidase MucD
10 porin D
11 outer membrane protein F
12 outer membrane protein OMP85
13 TonB−dependent receptor
14 extracellular solute−binding protein, family 1
15 extracellular solute−binding protein, family 3
16 periplasmic substrate−binding protein
17 ABC−type glycine betaine transport system
18 amino acid ABC transporter
19 branched−chain amino acid ABC transporter
20 YhgI protein
21 nonspecific acid phosphatase
22 ATP synthase subunit alpha
23 adenylosuccinate sythase
24 AP endonuclease, family 1
25 ACC deaminase
26 branched−chain amino acid aminotransferase
27 4−aminobutyrate aminotransferase
28 phosphoserine aminotransferase
29 4−hydroxyphenylpyruvate dioxygenase
30 urocanate hydratase
31 fructose−bisphosphate aldolase
32 malate synthase G
33 malate dehydrogenase
34 3−isopropylmalate dehydratase
35 isocitrate dehydrogenase
36 isovaleryl−CoA dehydrogenase
37 isocitrate lyase and phosphorylmutase
38 succinyl−CoA synthase
39 succinate−semialdehyde dehydrogenase
40 argininosuccinate synthase
41 oxaloacetate decarboxylase
42 pyruvate kinase
43 acyl−CoA dehydrogenase
44 chemotactic responsor CheY
45 periplasmic ligand−binding sensor protein
46 transcriptional regulator, Fis family
47 transcriptional regulator TraR/DksA family
48 NmrA−like protein
49 transcriptional regulator PyrR
50 tyrosyl−tRNA sythase
51 elongation factor P/YeiP
52 ribosome recycling factor
53 ribosomal 5S rRNA E−loop binding protein
54 GTP−binding protein TypA
55 peptidyl−prolyl cis−trans isomerase
56 survival protein SurA
57 chaperone clpB
58 heat shock protein HslU
59 co−chaperone GrpE
60 carboxyl−terminal protease
61 peptide deformylase
62 ThiJ/PfpI family protein
63 aldehyde dehydrogenase
64 ferredoxin−NADP reductase
65 peroxidase/catalase
66 thiolase
67 xenobiotic reductase B
68 alkyl hydroperoxide reductase
69 nitroreductase
70 uncharacterized protein
71 hypothetical protein A
72 cell division protein FtsA

Figure 3-6. Differentially expressed protein profiles of *P. putida* UW4 (left column) and AcdS minus mutant strain (right column) in response to root exudates. Fold protein expression changes are depicted according to the color scale at the top. Protein groups and names are listed to the right.

Table 3-3. Differentially expressed proteins identified in *P. putida* UW4 wild-type and AcdS minus mutant in the presence of plant exudates, grouped by putative functional role.

| Spot[1] | Accession number[2] | Protein | MW (KDa)[3] | p*I*[3] | Score[4] | SC[4] | WT[5] | Mut[5] |
|---|---|---|---|---|---|---|---|---|
| **I. Cell envelope synthesis** | | | | | | | | |
| 1 | Q4KJY3_PSEF5 | dTDP-glucose synthase | 32.6 | 5.33 | 81.9 | 16.49 | 1.5 | 2.29 |
| 2 | Q3K5U7_PSEPF | ribulose-phosphate 3-epimerase | 24.1 | 4.95 | 94.21 | 40.62 | 2.81 | 3.04 |
| 3 | Q3K8P9_PSEPF | ubiquinone oxidoreductase | 60.8 | 5.65 | 99 | 10 | 2.31 | 1.95 |
| 4 | Q4K8M4_PSEF5 | 3-demethylubiquinone-9 3-methyltransferase | 26.0 | 5.69 | 84.01 | 26.29 | 1.07 | 4.28 |
| 5 | Q48P39_PSE14 | RfaE bifunctional protein | 50.2 | 5.54 | 87.68 | 10.13 | 8.96 | 1.82 |
| 6 | Q4KJM6_PSEF5 | periplasmic glucan biosynthesis protein MdoG | 67.8 | 6.86 | 61.41 | 5.25 | 1.97 | 1.86 |
| 7 | Q3K746_PSEPF | D-alanine -- D-alanine ligase | 34.4 | 5.02 | 93.49 | 14.2 | 1.66 | 1.74 |
| 8 | Q3KA81_PSEPF | outer membrane lipoprotein carrier LolA | 20.4 | 5.11 | 90.65 | 26.21 | 1.59 | 2.05 |
| 9 | Q4KGQ4_PSEF5 | protease Do subfamily, peptidase MucD | 50.7 | 6.20 | 64.45 | 11.55 | 1.64 | 1.77 |
| **II. Membrane Transportation** | | | | | | | | |
| 10 | Q48FB5_PSE14 | porin D | 47.0 | 4.94 | 60.66 | 4.32 | 3.5 | 6.58 |
| 11 | Q9X4L6_PSEFL | outer membrane protein F | 36.6 | 4.68 | 90.82 | 13.08 | 7.57 | 7.09 |
| 12 | Q4KHG8_PSEF5 | outer membrane protein OMP85 | 87.4 | 5.21 | 78.1 | 12.69 | 5.38 | 5.21 |
| 13 | Q9HT68_PSEAE | TonB-dependent receptor | 28.1 | 5.79 | 47.86 | 10.77 | 1.52 | 2.11 |
| 14 | Q3K503_PSEPF | extracellular solute-binding protein, family 1 | 32.2 | 6.31 | 93.93 | 20.46 | 4.31 | 7.85 |
| 15 | Q3KHP0_PSEPF | extracellular solute-binding protein, family 3 | 34.1 | 5.54 | 98.37 | 22.45 | 6.79 | 4.76 |
| 16 | Q3KFH7_PSEPF | periplasmic substrate-binding protein | 35.6 | 5.72 | 94 | 10 | 1.61 | 2.76 |
| 17 | Q3K5H9_PSEPF | ABC-type glycine betaine transport system | 32.0 | 5.85 | 99.24 | 28.25 | 2.99 | 4.1 |

| | | | | | | | | |
|---|---|---|---|---|---|---|---|---|
| 18 | Q4KH87_PSEF5 | amino acid ABC transporter | 27.8 | 5.82 | 99 | 25.38 | 1.71 | 3.33 |
| 19 | Q88NR4_PSEPK | branched-chain amino acid ABC transporter | 39.4 | 6.02 | 44.09 | 3.23 | 2.78 | 3.41 |
| 20 | Q4KAH1_PSEF5 | YhgI protein | 21.0 | 4.57 | 36.66 | 6.7 | 2.36 | 3.67 |
| 21 | Q4KCT4_PSPF5 | nonspecific acid phosphatase | 38.1 | 5.80 | 43.02 | 5.87 | 5.02 | 10.91 |
| 22 | Q87TT2_PSESM | ATP synthase subunit alpha | 55.3 | 5.46 | 100 | 38.33 | 9.32 | 1.53 |
| **III. Nucleotide acid metabolism** | | | | | | | | |
| 23 | Q3KIY4_PSEPF | adenylosuccinate sythase | 46.5 | 5.57 | 99.92 | 33.1 | 1.7 | 2.87 |
| 24 | Q4ZTK7_PSEU2 | AP endonuclease, family 1 | 31.1 | 5.89 | 74.92 | 8.15 | 1.78 | 1.82 |
| **IV. Amino acid metabolism** | | | | | | | | |
| 25 | Q4KK38_PSEF5 | ACC deaminase | 35.2 | 5.37 | 84.15 | 9.06 | 1.64 | N/A |
| 26 | Q4KDP6_PSEF5 | branched-chain amino acid aminotransferase | 36.9 | 6.19 | 69.37 | 6.78 | 1.7 | 1.73 |
| 27 | Q3KJX4_PSEPF | 4-aminobutyrate aminotransferase | 44.8 | 5.91 | 99.83 | 31.76 | 1.72 | 2.41 |
| 28 | Q4K8M8_PSPF5 | phosphoserine aminotransferase | 40.0 | 5.04 | 41.82 | 2.75 | 3.21 | 5.02 |
| 29 | P80064_PSEUJ | 4-hydroxyphenylpyruvate dioxygenase | 40.1 | 5.23 | 99.65 | 31.37 | 4.44 | 7.52 |
| 30 | Q4KJN8_PSEF5 | urocanate hydratase | 61.3 | 5.79 | 74.19 | 6.61 | 1.82 | 1.13 |
| **V. Carbohydrate metabolism** | | | | | | | | |
| 31 | Q3K5F5_PSESF | fructose-bisphosphate aldolase | 38.5 | 5.48 | 94.52 | 24.86 | 3.16 | 2.9 |
| 32 | O05137_PSEFL | malate synthase G | 78.9 | 5.66 | 89.33 | 5.1 | 1.57 | 1.58 |
| 33 | Q1I6I3_9PSED | malate dehydrogenase | 60.1 | 5.89 | 73.68 | 4.22 | 1.86 | 2.3 |
| 34 | Q3KF24_PSEPF | 3-isopropylmalate dehydratase | 50.7 | 5.67 | 92.3 | 12.71 | 2.03 | 1.19 |
| 35 | Q4K9U5_PSEF5 | isocitrate dehydrogenase | 45.4 | 5.27 | 99.97 | 27.75 | 9.27 | 9.04 |
| 36 | Q4K9P7_PSEF5 | isovaleryl-CoA dehydrogenase | 42.4 | 5.74 | 60.43 | 6.46 | 1.69 | 2.47 |
| 37 | Q3KFE9_PSEPF | isocitrate lyase and phosphorylmutase | 32.0 | 5.46 | 95.24 | 20.95 | 1.28 | 3.37 |
| 38 | Q883Z4_PSESM | succinyl-CoA synthase | 41.2 | 5.70 | 98.07 | 28.35 | 3.3 | 4.06 |

| | | | | | | | | |
|---|---|---|---|---|---|---|---|---|
| 39 | Q4KKA2_PSEF5 | succinate-semialdehyde dehydrogenase | 51.6 | 5.75 | 96.18 | 14.37 | 1.77 | 2.23 |
| 40 | Q3K7K0_PSEPF | argininosuccinate synthase | 45.4 | 5.38 | 77.93 | 7.41 | 1.67 | 2.62 |
| 41 | Q3K4C9_PSEPF | oxaloacetate decarboxylase | 65.4 | 5.60 | 80 | 3 | 1.84 | 1.56 |
| 42 | Q3K7R9_PSEPF | pyruvate kinase | 52.1 | 6.04 | 97.22 | 15.53 | 6.13 | 5.82 |
| 43 | Q3KC97_PSEPF | acyl-CoA dehydrogenase | 40.9 | 5.25 | 95.43 | 20.46 | 1.78 | 3.63 |
| **VI. Transcription regulation** | | | | | | | | |
| 44 | Q51455_PSEAE | chemotactic responsor CheY | 13.9 | 6.10 | 33.02 | 19.35 | -2.88 | -2 |
| 45 | Q3K6E1_PSEPF | periplasmic ligand-binding sensor protein | 26.6 | 4.34 | 85.76 | 8.73 | -2.83 | -1.63 |
| 46 | Q3KI42_PSEPF | transcriptional regulator, Fis family | 20.5 | 5.13 | 91.3 | 30.65 | -3.31 | -4 |
| 47 | Q3K6R3_PSEPF | transcriptional regulator TraR/DksA family | 16.9 | 5.21 | 62.4 | 20.41 | -2.38 | -2.64 |
| 48 | Q3KDY8_PSEPF | NmrA-like protein | 26.8 | 5.15 | 75.2 | 13.55 | 2.34 | 2.15 |
| 49 | Q1I3U3_9PSED | transcriptional regulator PyrR | 18.7 | 5.01 | 39.15 | 9.88 | -2.5 | -1.62 |
| **VII. Protein synthesis, folding and degradation** | | | | | | | | |
| 50 | Q4K517_PSEF5 | tyrosyl-tRNA sythase | 44.2 | 5.49 | 90.7 | 10.78 | 2.36 | 2.94 |
| 51 | Q3K918_PSEPF | elongation factor P/YeiP | 21.0 | 4.72 | 99.43 | 36.51 | -1.73 | -1.56 |
| 52 | Q886P0_PSESM | ribosome recycling factor | 20.5 | 6.76 | 46.7 | 8.65 | -2.37 | -2.18 |
| 53 | Q88PX7_PSEPK | ribosomal 5S rRNA E-loop binding protein | 21.1 | 5.72 | 92.2 | 10.14 | -2.76 | -1.47 |
| 54 | Q3KJG5_PSEPF | GTP-binding protein TypA | 67.1 | 5.40 | 95.1 | 9.9 | 3.61 | 3.67 |
| 55 | Q4K5T2_PSEF5 | peptidyl-prolyl cis-trans isomerase | 21.7 | 4.69 | 93.87 | 32.68 | -1.71 | -1.9 |
| 56 | Q4K4X7_PSEF5 | survival protein SurA | 46.2 | 5.30 | 66.17 | 9.09 | 1.79 | 1.67 |
| 57 | Q3K6N3_PSEPF | chaperone clpB | 95.6 | 5.39 | 97.8 | 12.76 | 4.57 | 4.04 |
| 58 | Q3KJB6_PSEPF | heat shock protein HslU | 50.0 | 5.76 | 92.5 | 9.89 | 4.43 | 7.17 |
| 59 | Q4KIH2_PSEF5 | co-chaperone GrpE | 20.8 | 4.65 | 92.2 | 35.64 | -1.95 | -2.26 |
| 60 | A5W7L4_PSEPU | carboxyl-terminal protease | 75.0 | 6.10 | 95 | 3 | 1.87 | 2.03 |

| | | | | | | | | |
|---|---|---|---|---|---|---|---|---|
| 61 | Q3KKE5_PSEPF | peptide deformylase | 19.4 | 5.17 | 82.91 | 23.81 | -6.94 | -6.45 |
| 62 | Q4KGZ6_PSEF5 | ThiJ/PfpI family protein | 20.7 | 5.57 | 46.41 | 6.74 | 4.03 | 4.93 |
| **VIII. Oxidoreductase** | | | | | | | | |
| 63 | Q3K4N3_PSEPF | aldehyde dehydrogenase | 53.2 | 5.37 | 96.81 | 13.88 | 1.62 | 5.18 |
| 64 | Q48FA2_PSE14 | ferredoxin-NADP reductase | 29.7 | 5.32 | 97.54 | 29.73 | 3.23 | 2.2 |
| 65 | Q3KE62_PSEPF | peroxidase/catalase | 82.7 | 5.30 | 75.62 | 4.37 | 7.38 | 6.75 |
| 66 | Q4ZY90_PSEU2 | thiolase | 40.4 | 5.91 | 89.57 | 6.89 | -1.51 | -2.07 |
| 67 | Q4KH19_PSEF5 | xenobiotic reductase B | 37.4 | 5.53 | 96.43 | 16.33 | -2.53 | -1.81 |
| 68 | Q3K7J6_PSEPF | alkyl hydroperoxide reductase | 21.8 | 5.08 | 97.53 | 41 | -3.33 | -3.92 |
| 69 | Q3KGH2_PSEPF | nitroreductase | 22.0 | 5.79 | 85.9 | 20.3 | -2.32 | -2.31 |
| **IX. Others** | | | | | | | | |
| 70 | Q4KFS1_PSEF5 | uncharacterized protein | 19.4 | 4.48 | 90.24 | 32.57 | -3.02 | -2.1 |
| 71 | Q3K9Y9_PSEPF | hypothetical protein A | 25.1 | 4.94 | 77.45 | 23.93 | 1.56 | 2.29 |
| 72 | Q4ZNZ4_PSEU2 | cell division protein FtsA | 44.6 | 5.26 | 91.12 | 11.24 | 1.5 | 1.75 |

[1] The numbers next to the identified proteins refer to the numbers in Figure 3-3.

[2] Accession number of top database match from SwissProt *Expasy* database (Gasteiger et al., 2003).

[3] MW and p*I* were calculated from amino acid sequence of the top database match using the *Expasy* Compute pI/MW tool (Gasteiger et al., 2003) and compared with gel location.

[4] PEAKS Score and sequence coverage were calculated by PEAKS software.

[5] WT and Mut represent protein expression ratios in wild-type *P. putida* UW4 and AcdS minus mutant treated with plant exudates respectively. Underlined numbers indicate proteins expression that was not significantly changed. N/A, not applicable.

### 3.2.3 Root elongation activities of *P. putida* mutant strains

From the identified set of differentially expressed proteins in Table 3-3, four proteins, whose expression levels were significantly changed by canola root exudates, were over-expressed and/or disrupted in *P. putida* UW4, and the resulting mutant strains were tested for their root elongation activities. The first basis for the selection of the genes chosen for additional functional analyses is proteins that showed the greatest increase or decrease in expression (>7 for up-regulated proteins and <-2 for down-regulated proteins). Another selection criterion is confidence in the mass spectrometric identification (i.e., higher than 90% and 80% for up- and down- regulated proteins, respectively) in order to easily clone the genes from *P. putida* UW4 genome. There were four proteins that fulfilled these criteria and all of them were chosen for expression and mutagenesis studies. These proteins are: one up-regulated protein (outer membrane protein F) and three down-regulated proteins (peptide deformylase, transcription regulator Fis family, and a previously uncharacterized protein). The genes *pdf*, *fis*, *hyp*, and *ompF*, encoding peptide deformylase (Pdf) (spot 61), transcription regulator Fis family (Fis) (spot 46), uncharacterized protein (Hyp) (spot 70) and outer membrane protein F (OmpF) (spot 11), respectively were amplified by PCR using primers (Table 2-1) designed based on analogues from other closely related *Pseudomonas* strains as described in the Materials and Methods section. The coding sequences of the *pdf, fis, hyp, and ompF* genes were determined and deposited in the Genbank database under accession numbers EU514687-EU514690. These four genes were cloned into pETP constructed for protein expression in *P. putida* UW4. The expression of the 6×His-tagged recombinant proteins is shown in Figure 3-7.

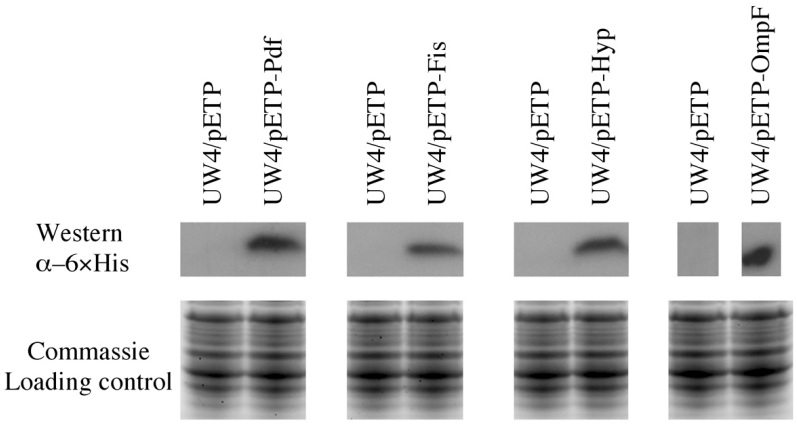


Figure 3-7. The expression of the His-tagged recombinant proteins was confirmed by western blotting. In case of OmpF protein expression, 2-D electrophoresis was performed to separate the expressed His-tagged protein from a background band with similar molecular weight.

In all instances, the expression of the cloned gene was confirmed by antibodies directed against the His-tag and from the calculated molecular mass of the proteins.

Diagnostic PCR for individual genes confirmed that the genes encoding three of these four above-mentioned proteins were disrupted in the mutant strains *P. putida* UW4/Fis$^{-}$, UW4/Hyp$^{-}$, and UW4/OmpF$^{-}$. In each case, the PCR products from the mutant strains were 1.5 kbp longer than their alleles in the wild-type, reflecting the insertion of the *tetA* gene into each of these genes (Figure 3-8). The *P. putida* UW4/Pdf$^{-}$ mutant was unable to survive, presumably because this mutation was lethal.

The plant growth promoting ability of the wild-type strain, the four over-expressing, and the three viable disruption mutant (non-expressing) strains were tested in a canola root elongation assay (Figure 3-9). This assay revealed that (i) the Fis protein over-expressing and knockout strains showed no significant difference compared to the wild-type, (ii) the strains over-expressing the Pdf and the OmpF proteins, and the Hyp protein disruption strain promoted root length more than the wild-type, and (iii) the OmpF protein disruption strain and the Hyp protein over-expresser lost their root length-promoting activity. Moreover, over-expression of Hyp inhibited root growth relative to the untreated plants, suggesting that high levels of this protein were detrimental to plant growth.

### 3.3 Construction of *P. putida* proteome reference map

Approximately 500 spots were detected on the preparative 2-D gel (Figure 3-10). Spots were manually excised from the gel and subjected to in-gel tryptic digestion. The protein spots of interest were destained, reduced, alkalized, and digested overnight with trypsin as described in the Methods. Spot identities were obtained by MS performed as described in section 2.6.

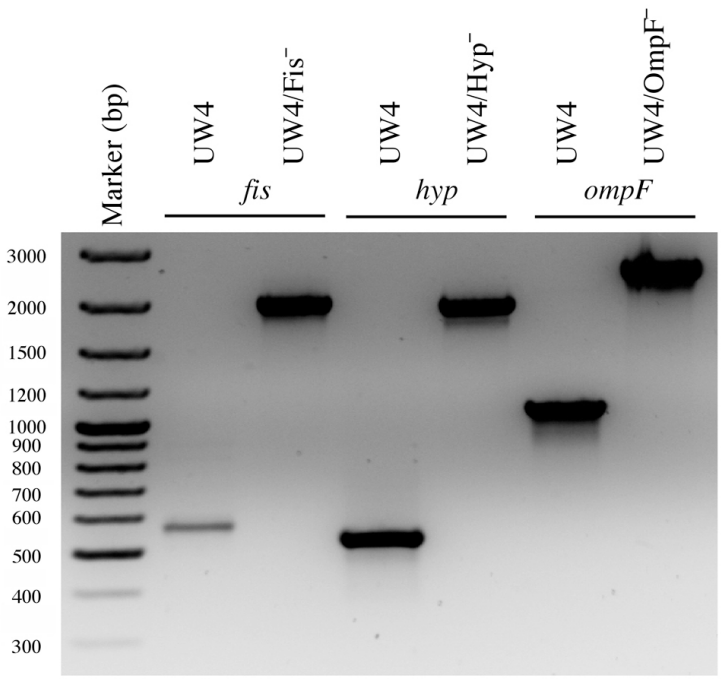


Figure 3-8. Disruptions of target genes in the *P. putida* UW4 genome were confirmed by diagnostic PCR for individual genes. In each case, the PCR products from the mutant strains were 1.5 kbp longer than their alleles in the wild-type, reflecting the insertion of the *tetA* gene into each of these genes.

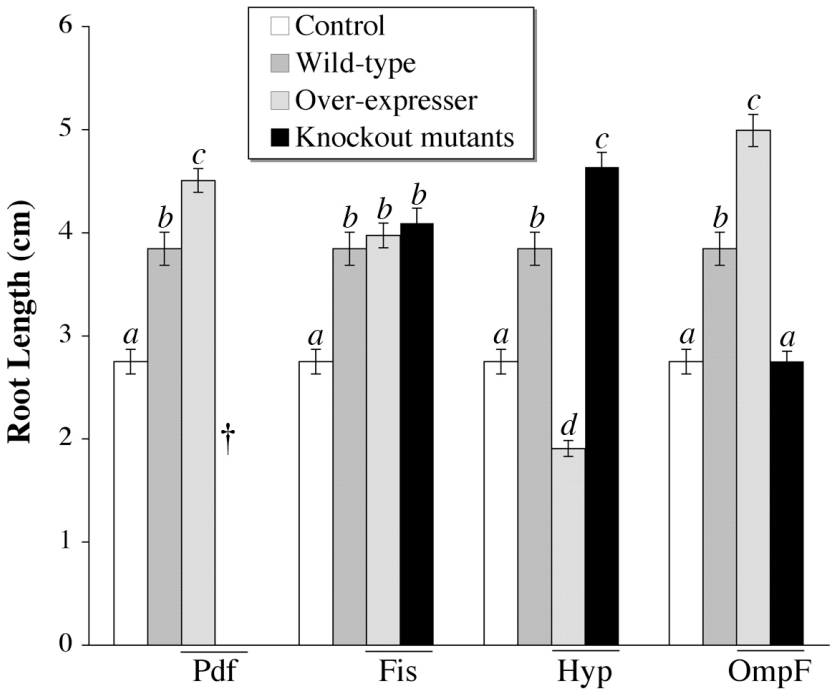


Figure 3-9. Root length of seven-day-old canola seedlings. Different letters indicate statistically significant differences between plants under different treatments. Error bars represent standard error of the mean with 67-70 plants per treatment. †There is no root length data available for the UW4/Pdf$^-$ treated plants because the Pdf protein disrupted strain was not viable.

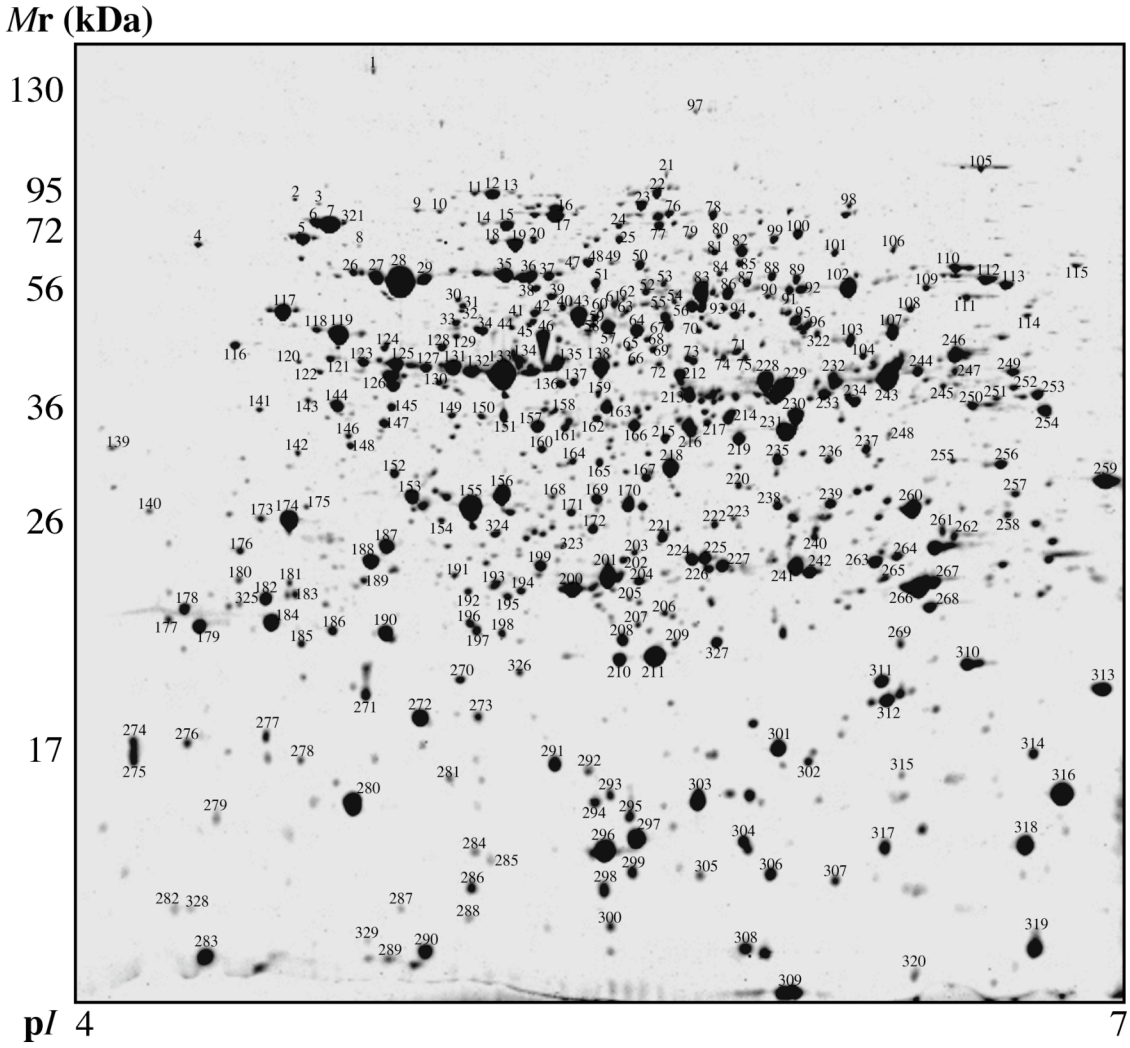


Figure 3-10. A preparative gel of *P. putida* UW4 proteins. Approximately 1 mg of protein sample was loaded onto an IPG 4-7 strip in the first dimension, and separated using a 12% SDS-PAGE gel in the second dimension. Proteins spots were visualized by Coomassie staining. The identified and labeled spots are annotated according to the numbers used in Supplementary Table 1.

A *Pseudomonas putida* UW4 proteome reference map, which contains 326 spots representing 275 different proteins (Figure 3-10), was constructed. Homology between the *P. putida* UW4 proteins and other *Pseudomonas* strains allowed all but seven identifications to be supported by MS/MS analyses (Supplementary Table 1, see Appendix A) in addition to Peptide Mass Fingerprinting (PMF) analysis (data not shown). The other seven identifications were obtained only by PMF. The identified spots are labeled in the 2-D reference map of *P. putida* UW4 (Figure 3-10). *M*r and p*I* of the identified proteins were estimated from their gel locations. Details of the mass spectrometric identification, including spot numbers, accession numbers, identification scores, sequence coverage, and calculated *M*r and p*I* have been compiled into a dataset (Supplementary Table 1).

The identified proteins were categorized based on function and cellular localization using the annotation from the Swiss-Prot database (Gasteiger et al., 2003). Identified proteins were distributed within the following categories: amino acid metabolism (14%), carbohydrate metabolism (10%), lipid metabolism (3%), nucleotide acid metabolism (5%), secondary metabolism (4%), cell envelope biosynthesis (2%), cell cycle (2%), transcription (6%), translation (8%), protein folding and degradation (6%), transportation (11%), energy generation (2%), electron transfer (3%), oxidoreductase activity (7%), response to stress (5%), other (5%), and unknown (5%) (Figure 3-11). Among the 275 identified proteins, the identification of ACC deaminase (spot 148) is noteworthy because of its substantial role in the plant growth-promoting activity of *P. putida* UW4. In addition, the existence of twelve previously hypothetical proteins (Supplementary Table 1) was confirmed by mass

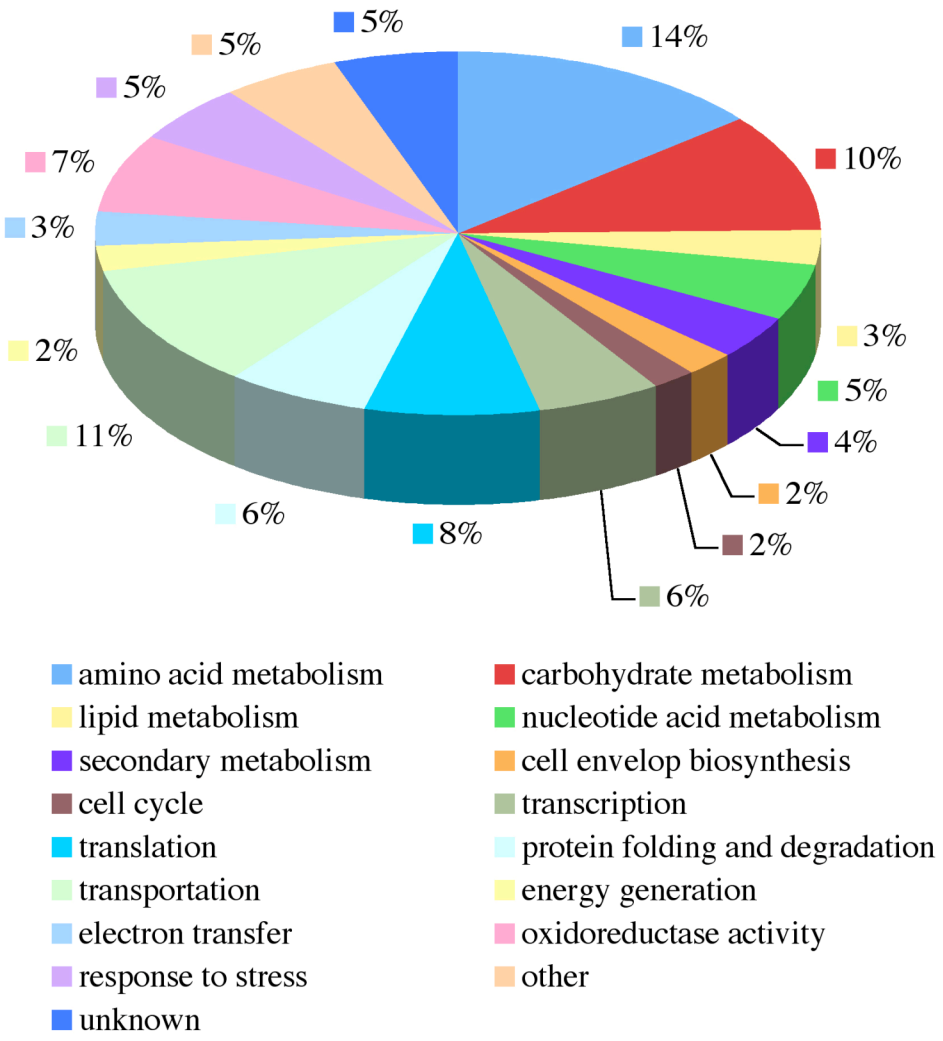


Figure 3-11. Distribution of *P. putida* UW4 proteins identified by MS into functional categories. Percentages were calculated from the total number of protein spots identified (326).

spectrometric identification. Furthermore, although the majority of the identified proteins are localized in the bacterial cytosol, the identification of periplasmic, membrane-spanning, and extracellular proteins (Supplementary Table 1) indicates that the methodology is capable of providing a degree of representation from all cellular compartments including less soluble membrane fractions. One additional protein was identified as homologous to a *Bradyrhizobium japonicum* protein (spot 40). The identification of this protein was also confirmed by several independent MS analyses. The functional diversity of the identified proteins will enable investigation of the systematic responses of *P. putida* UW4 in response to various environmental signals.

A 2-DE database containing all the MS information of *P. putida* UW4 proteins has been constructed. The dataset has been deposited into the World-2DPAGE database (accession no. 0008).

### 3.4 The combined effects of salt and *P. putida* on canola

Soil salinity is an enormous agricultural problem that limits crop growth and productivity under irrigation. High salinity affects around 20% of cultivated land, and up to 50% of all irrigated land. In fact, it had been estimated that the arable land being lost through salinity is even greater than the land gained through clearing (Frommer et al., 1999). High concentration of salt often causes ion imbalance and hyperosmotic pressure, which eventually leads to oxidative stress conditions for plants. Moreover, salt stress has been shown to elevate stress ethylene levels in some plants (Mayak et al., 2004a). Genetic engineering approaches have been effective in making plants more resistant to salt stress (Sergeeva et al., 2006; Zhang and Blumwald, 2001; Zhang et al., 2001a). Transgenic *Brassica napus* plants overexpressing

*AtNHX1,* a vacuolar $Na^+/H^+$ antiport from *Arabidopsis thaliana,* were not only able to grow, flower, and produce seeds in the presence of 200 mM NaCl, but also accumulated sodium up to 6% of their dry weight (Zhang et al., 2001a). Seed yields and the seed oil quality were not affected by the high salinity of the soil (Zhang et al., 2001a). Naturally occurring 1-aminocyclopropane-1-carboxylate (ACC) deaminase-containing plant growth promoting-bacteria have been reported to improve plant growth at high salt concentrations both at 10 °C and at 20 °C (Cheng et al., 2007; Mayak et al., 2004a). These bacteria can work together with plants for bioremediation of soil contaminated with salt (Cheng et al., 2007; Mayak et al., 2004a; Nadeem et al., 2007; Saravanakumar and Samiyappan, 2007). How plants modulate their protein expression during this remediation process is a topic of considerable interest. The impact of plant growth-promoting bacteria on plant shoot and root proteomic profiles under salinity stress was examined, while also investigating the effect of ACC deaminase on this interaction.

### 3.4.1 The effects of salt and *P. putida* strains on canola hydroponic growth

Following 18 days in hydroponic solution, the effects of salt exposure and bacterial treatment on canola shoots and roots were measured. There was no significant difference in root weights of plants treated with different conditions. The shoot fresh and dry weights are shown in Figure 3-12A and B. In the presence of 250 mM NaCl, canola shoot fresh weights (FW) and dry weights (DW) were significantly decreased, with FW of 2.72 ± 0.71 g and DW of 0.24 ± 0.02 g compared to FW of 5.94 ± 0.52 g and DW of 0.60 ± 0.05 g for plants grown in

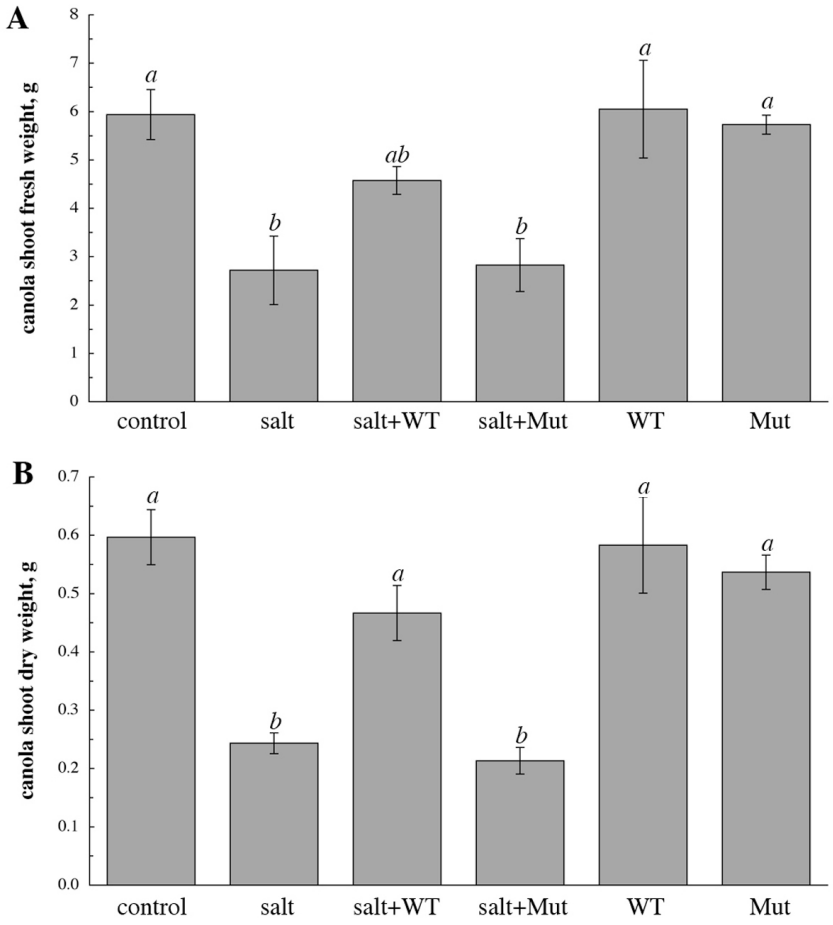


Figure 3-12. Shoot fresh weight (A), dry weight (B), of hydroponically grown canola plants. Different letters indicate statistically significant differences between plants under different treatments. Error bars represent standard error with 3 plants per treatment.

the absence of added salt. The addition of the ACC deaminase-containing bacterium *P. putida* UW4 (FW of 4.58 ± 0.29 g and DW of 0.47 ± 0.05 g), but not the AcdS minus mutant of this bacterium (FW of 2.83 ± 0.55 g and DW of 0.21 ± 0.02 g), alleviated a portion of the deleterious salt effect, supporting the relationship between ACC deaminase activity and plant stress. In the absence of salinity stress, the average shoot fresh and dry weights of the *P. putida* UW4 and AcdS minus mutant treated plants did not significantly differ from the non-treated control.

Chlorophyll content was also significantly decreased in the presence of salinity stress (39.3% of the control level), but not significantly altered by the added bacteria (Figure 3-13). Furthermore, the presence of wild-type *P. putida* UW4 (56.6% of the control level) but not the AcdS minus mutant (40.6% of the control level) partly alleviated this decrease in chlorophyll content caused by stress (Figure 3-13).

### 3.4.2 The combined effects of *P. putida* strains and salinity stress on the canola proteome

The shoot and root protein accumulation patterns of canola plants treated with salt, wild-type *P. putida* UW4, the UW4 AcdS minus mutant, salt plus wild-type *P. putida* UW4, and salt plus the UW4 AcdS minus mutant were each compared to separate sets of untreated controls.

In the three comparisons where salt was used as a treatment (canola treated with salt, salt plus wild-type *P. putida* UW4, and salt plus the UW4 AcdS minus mutant), 97 to 119 shoot proteins, representing 5.7% to 7.0% of the detected shoot proteome (1,709 proteins), were

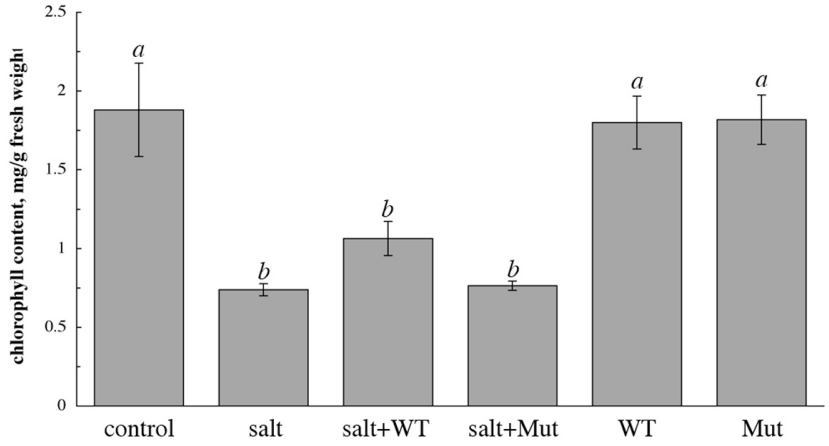


Figure 3-13. Chlorophyll content of hydroponically grown canola plants. Different letters indicate statistically significant differences between plants under different treatments. Error bars represent standard error with 3 plants per treatment.

significantly (false discovery rate corrected t-test $p < 0.05$ and | Expression Ratio | > 1.5) altered relative to the untreated control, with the largest number of changes observed in plants exposed to salt plus wild-type *P. putida* UW4 (Table 3-4). Approximately three times as many shoot proteins were down-regulated as were up-regulated in each salt treatment. Out of a total of 1,700 detected root proteins, about 70 (~4.1%) showed significant differences in expression, with the largest number of changes observed in plants exposed to salt plus wild-type *P. putida* UW4. In contrast to the shoot profiles, approximately three times as many proteins were up-regulated as were down-regulated in the roots (Table 3-4). When there was no salinity stress and the canola plants were treated only with bacterium *P. putida* UW4 or the UW4 AcdS minus mutant, far fewer proteins (representing only 0.4 – 1.1% of the total proteins detected) displayed changed expression levels compared to the non-treated control (Table 3-4).

Figure 3-14 shows representative analytical gels comparing protein expression of canola shoot (A) and root (B) in the presence and absence of salt. On these gels, up- regulated and down- regulated proteins appear as red and green spots respectively.

The identities of 53 shoot protein spots (representing 42 different proteins) and 37 root protein spots (representing 34 different proteins) with significantly altered expression levels were subsequently determined by mass spectrometry (Table 3-5). Details of the mass spectrometric identification, including accession numbers, identification score, sequence coverage, number of matched peptides, molecular weight and p*I* are presented alongside the associated protein accumulation pattern/fold change in Table 3-5. Figure 3-15A and B show preparative gels of canola shoot and root proteins, respectively, from the non-treated control

Table 3-4. Effects of salt and bacteria on protein expression in *Brassica napus* shoot and root. A total of 1,709 shoot proteins and 1,700 root proteins were detected.

| Level of protein expression relative to control | No. of *Brassica napus* proteins that are significantly altered in expression in response to salt and bacteria | | | | |
|---|---|---|---|---|---|
| | Salt | Salt + WT | Salt + Mut | WT | Mut |
| | | | shoot | | |
| Increased | 25(1.5%) | 30(1.8%) | 23(1.3%) | 8(0.5%) | 11(0.6%) |
| Decreased | 72(4.2%) | 89(5.2%) | 76(4.4%) | 6(0.4%) | 5(0.4%) |
| | | | root | | |
| Increased | 50(2.9%) | 55(3.2%) | 49(2.9%) | 15(0.9%) | 19(1.1%) |
| Decreased | 15(0.9%) | 18(1.1%) | 17(1.0%) | 7(0.4%) | 12(0.7%) |

Salt, Salt + WT, and Salt + Mut, WT, Mut represent protein expression profiles in plants treated with salt only, salt plus wild-type *P. putida* UW4, salt plus UW4 AcdS minus mutant, wild-type *P. putida* UW4 only, and UW4 AcdS minus mutant respectively.

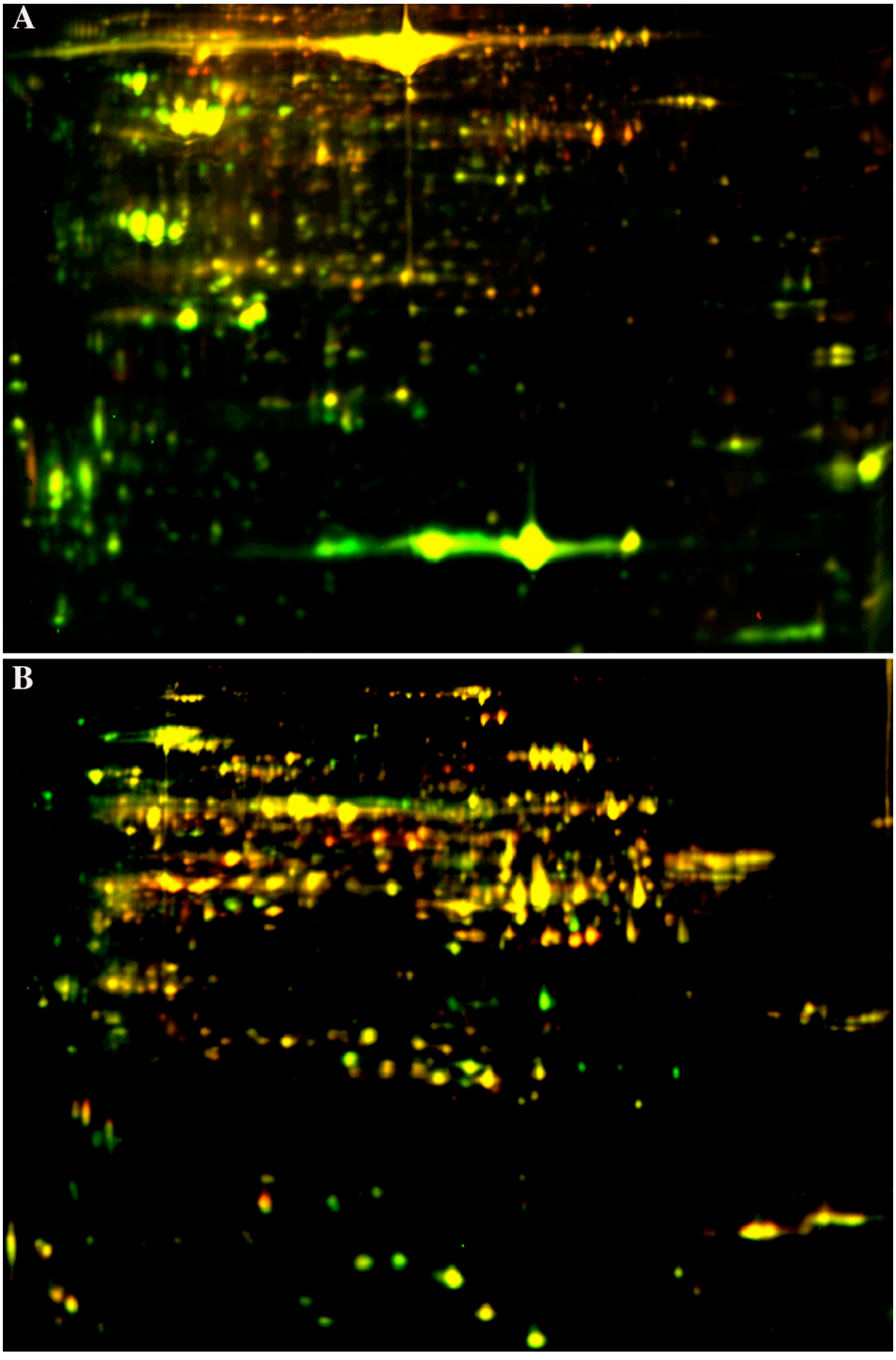


Figure 3-14. Analytical gels comparing shoot (A) and root (B) protein expression of the canola exposed to salt.

**Table 3-5. *Brassica napus* shoot and root proteins altered in response to salt and bacteria**

| Spot [1] | Accession number [2] | Protein [2] | MW (kDa) [3] | p*I* [3] | Score [4] | SC [4] | MPN [4] | Salt [5] | Salt + WT [5] | Salt + Mut [5] | WT [5] | Mut [5] | CL [6] |
|---|---|---|---|---|---|---|---|---|---|---|---|---|---|
| Part I. Shoot Proteins | | | | | | | | | | | | | |
| S1 | gil15222111 | Glyceraldehydes-3-phosphate dehydrogenase | 44.4 | 5.75 | 98 | 19 | 6 | 1.62 | 1.71 | 1.49 | 1.32 | 1.08 | 16 |
| S2 | gil15219721 | Malate dehydrogenase | 41.4 | 7.73 | 99 | 28 | 9 | 1.87 | 1.58 | 1.73 | 1.07 | 1.11 | 16 |
| S3 | gil8778996 | Ferredoxin-NADP reductase | 36.5 | 7.03 | 97 | 19 | 6 | 1.62 | 1.77 | 1.68 | 1.45 | 1.24 | 16 |
| S4 | gil33285914 | Dehydroascorbate reductase | 28.9 | 6.39 | 99 | 44 | 4 | 1.65 | 1.58 | 1.97 | 1.28 | 1.36 | 14 |
| S5 | gil119980 | Ferredoxin | 20.4 | 3.1 | 85 | 34 | 2 | 1.74 | 1.69 | 1.63 | 1.19 | 1.22 | 16 |
| S6 | gil15292893 | Peroxiredoxin | 18.5 | 4.26 | 99 | 24 | 7 | 1.69 | 1.59 | 1.88 | -1.11 | 1.05 | 14 |
| S7 | gil110742393 | Thioredoxin m4 | 19.8 | 4.1 | 67 | 12 | 2 | 1.61 | 1.78 | 1.79 | 1.33 | 1.47 | 15 |
| S8 | gil11135407 | M-type thioredoxin | 15.3 | 3.65 | 55 | 8 | 2 | 1.74 | 1.39 | 1.52 | 1.45 | 2.11 | 8 |
| S9 | gil30678634 | Thioredoxin m1; thiol-disulfide exchange intermediate | 15.4 | 4.12 | 69 | 7 | 2 | 1.53 | 1.87 | 1.73 | 1.26 | 1.05 | 16 |
| S10 | gil544437 | Phospholipids hydroperoxide glutathione peroxidase (salt-associated protein) | 25.3 | 8.76 | 92 | 13 | 3 | 1.72 | 1.69 | 1.92 | 1.09 | 1.4 | 14 |
| S11 | gil115334979 | Chloroplast ribulose-1,5-bisphosphate carboxylasse/oxygenase activase | 47.8 | 4.38 | 97 | 11 | 4 | -1.77 | -1.47 | -1.83 | -1.24 | 1.03 | 1 |
| S12 | gil30687999 | Rubisco activase | 48.5 | 4.51 | 99 | 16 | 6 | -1.92 | -1.59 | -1.87 | -1.11 | -1.27 | 1 |
| S13 | gil30687999 | Rubisco activase | 43.8 | 4.74 | 99 | 11 | 5 | -1.76 | -1.37 | -1.85 | -1.34 | -1.33 | 1 |
| S14 | gil10720247 | Ribulose bisphosphate carboxylase/oxygenase activase, chloroplast precursor | 43.1 | 4.93 | 99 | 5 | 3 | -2.18 | -1.63 | -2.07 | -1.26 | -1.29 | 1 |
| S15 | gil78100212 | Ribulose-1,5-bisphosphate carboxylase/oxygenase activase alpha 2 | 43.3 | 5.15 | 90 | 10 | 3 | -1.99 | -1.78 | -1.83 | -1.45 | -1.38 | 1 |

| | | | | | | | | | | | | | |
|---|---|---|---|---|---|---|---|---|---|---|---|---|---|
| S16 | gil15240013 | Oxygen-evolving enhancer 33 | 33 | 4.46 | 99 | 30 | 7 | -2.39 | -1.78 | 1.22 | 1.32 | 1.17 | 3 |
| S17 | gil15230324 | Photosystem II subunit O-2; oxygen evolving | 32.8 | 4.63 | 99 | 17 | 3 | -1.65 | -1.29 | -1.75 | 1.04 | -1.26 | 1 |
| S18 | gil15240013 | Oxygen-evolving enhancer 33 | 33.2 | 4.83 | 99 | 17 | 3 | -2.32 | -1.37 | -2.07 | -1.08 | -1.33 | 1 |
| S19 | gil829289 | Oxygen-evolving enhancer 2 | 26.3 | 4.9 | 99 | 26 | 5 | -1.64 | -1.51 | -1.73 | -1.2 | 1.07 | 1 |
| S20 | gil829289 | Oxygen-evolving enhancer 2 | 26.6 | 5.52 | 99 | 27 | 4 | -1.62 | -1.03 | -1.58 | -1.15 | -1.24 | 2 |
| S21 | gil130262 | plastocyanin | 16.7 | 3.55 | 84 | 23 | 2 | -1.76 | -1.26 | -1.89 | -1.07 | 1.12 | 1 |
| S22 | gil30679426 | Photosynthetic electron transfer C protein | 22.5 | 6.09 | 88 | 18 | 4 | -2.59 | -1.78 | -2.34 | 1.05 | 1.31 | 1 |
| S23 | gil30679426 | Photosynthetic electron transfer C protein | 22.5 | 6.86 | 84 | 8 | 2 | -2.39 | -1.93 | -2.36 | -1.14 | -1.42 | 1 |
| S24 | gil119720808 | Ribulose bisphosphate carboxylase | 14.7 | 6.02 | 99 | 44 | 7 | -2.56 | -1.88 | -1.93 | -1.27 | -1.36 | 3 |
| S25 | gil119720808 | Ribulose bisphosphate carboxylase | 14.7 | 6.24 | 99 | 28 | 4 | -2.87 | -1.57 | -2.56 | -1.19 | 1.14 | 1 |
| S26 | gil119720808 | Ribulose bisphosphate carboxylase | 15.1 | 6.95 | 99 | 35 | 5 | -2.3 | -1.72 | -2.22 | 1.04 | -1.08 | 1 |
| S27 | gil119720808 | Ribulose bisphosphate carboxylase | 15.3 | 7.5 | 99 | 44 | 7 | -2.09 | -1.56 | -2.13 | 1.13 | 1.22 | 1 |
| S28 | gil406727 | Ribulose-1,5-bisphosphate carboxylase/oxygenase | 14.7 | 7.91 | 99 | 42 | 6 | -1.76 | -1.27 | -1.71 | 1.08 | -1.09 | 1 |
| S29 | gil119720808 | Ribulose bisphosphate carboxylase | 14.5 | 7.21 | 99 | 22 | 3 | -1.77 | -1.32 | -1.91 | -1.05 | 1.25 | 1 |
| S30 | gil119720808 | Ribulose bisphosphate carboxylase | 14.5 | 7.38 | 99 | 29 | 4 | -1.58 | -1.73 | -1.69 | -1.42 | -1.48 | 5 |
| S31 | gil119720808 | Ribulose bisphosphate carboxylase | 14.3 | 7.62 | 99 | 22 | 3 | -2.3 | 1.09 | -1.97 | -1.04 | 1.08 | 2 |
| S32 | gil119720808 | Ribulose bisphosphate carboxylase | 13.6 | 8.63 | 99 | 47 | 7 | -2.68 | -1.47 | -3.09 | -1.22 | -1.37 | 1 |
| S33 | gil119720808 | Ribulose bisphosphate carboxylase | 14.4 | 8.76 | 99 | 41 | 7 | -2.55 | -1.5 | -2.38 | -1.23 | -1.4 | 1 |
| S34 | gil15237593 | Photosystem I reaction center subunit; calmodulin binding | 11.9 | 10.8 | 99 | 22 | 4 | -1.74 | -1.17 | -1.68 | 1.29 | 1.21 | 1 |
| S35 | gil6966930 | Glutamine synthetase | 46.3 | 4.7 | 99 | 21 | 6 | 2.01 | 5.5 | 3.02 | 1.46 | 1.33 | 15 |
| S36 | gil1934754 | Plastidic glutamine synthetase precursor | 46 | 4.86 | 99 | 19 | 5 | 2.3 | 6.7 | 2.78 | 1.25 | -1.07 | 15 |
| S37 | gil6966930 | Glutamine synthetase | 45.6 | 5.04 | 99 | 18 | 4 | 2.33 | 4.98 | 2.07 | 1.49 | 1.27 | 16 |
| S38 | gil42601787 | Voltage-dependent anion-selective channel protein | 36.3 | 9.7 | 99 | 21 | 5 | 1.78 | 2.73 | 2.08 | 1.33 | 1.41 | 15 |

| | | | | | | | | | | | | | |
|---|---|---|---|---|---|---|---|---|---|---|---|---|---|
| S39 | gil56693623 | Porin-like protein | 36.4 | 9.84 | 89 | 8 | 3 | 1.53 | 3.21 | 1.98 | 1.37 | 1.36 | 15 |
| S40 | gil79314806 | ATP synthase D chain, mitochondrial | 22.4 | 4.26 | 98 | 20 | 3 | 2.62 | 2.98 | 2.7 | 1.42 | 1.42 | 16 |
| S41 | gil30684083 | Jacalin lectin | 48.5 | 5.23 | 99 | 7 | 3 | 1.07 | 2.11 | 1.96 | 1.77 | 2.01 | 3 |
| S42 | gil30684083 | Jacalin lectin | 48.5 | 5.45 | 99 | 14 | 5 | 1.11 | 2.81 | 1.17 | 1.83 | 2.29 | 2 |
| S43 | gil15220216 | Calcium ion binding / calcium-dependent phospholipids binding | 41.6 | 5.59 | 99 | 18 | 9 | 1.78 | 3.33 | 1.23 | 2.34 | 1.07 | 11 |
| S44 | gil18420348 | Fructose-bisphosphate aldolase | 39.3 | 5.96 | 99 | 15 | 4 | 3.21 | 2.08 | 1.77 | 1.25 | 1.3 | 12 |
| S45 | gil79314806 | Serine hydroxymethyltransferase | 52.5 | 8.64 | 99 | 21 | 10 | 2.4 | 2.03 | 2.76 | -1.33 | 2.05 | 13 |
| S46 | gil15229443 | Ribosomal protein L1 | 44.3 | 9.78 | 99 | 15 | 5 | -1.8 | -1.46 | -1.77 | -2.36 | -2.09 | 16 |
| S47 | gil15230476 | Nascent polypeptide associated complex alpha chain protein | 30.7 | 3.65 | 99 | 26 | 4 | -2.11 | -1.43 | -1.98 | -1.09 | 1.05 | 1 |
| S48 | gil15232276 | Ribosomal protein L12-C | 18.7 | 3.98 | 99 | 15 | 3 | -1.74 | -1.81 | -1.36 | -1.64 | 1.24 | 7 |
| S49 | gil15235247 | Polygalacturonate 4-alpha-galacturonosyltransferase | 18.9 | 4.97 | 90 | 1 | 2 | 1.08 | -2.72 | -2.97 | -1.45 | -1.4 | 4 |
| S50 | gil1346180 | Glycine-rich RNA-binding protein 1A | 16 | 5.19 | 60 | 7 | 2 | -3.95 | -2.2 | -3.73 | -1.48 | -1.38 | 1 |
| S51 | gil21553354 | Glycine-rich RNA-binding protein 2A | 17.3 | 5.05 | 83 | 5 | 2 | -1.11 | -6.13 | -7.7 | 1.15 | -2.52 | 4 |
| S52 | gil110739384 | Translational inhibitor protein | 15.6 | 5.08 | 99 | 13 | 3 | 1.64 | 1.47 | 1.69 | 1.03 | 1.24 | 14 |
| S53 | gil15226467 | Peptidyl-prolyl cis-trans isomerase/cyclophilin/rotamase | 20.7 | 9.5 | 99 | 10 | 2 | 2.12 | 1.87 | 1.97 | 1.29 | 1.16 | 16 |

Part II. Root Proteins

| | | | | | | | | | | | | | |
|---|---|---|---|---|---|---|---|---|---|---|---|---|---|
| R1 | gil28207601 | Malate dehydrogenase | 63.4 | 4.88 | 77 | 7 | 2 | 1.63 | 1.44 | 1.75 | 1.32 | 1.19 | 14 |
| R2 | gil18414298 | Monodehydroascorbate reductase | 53 | 4.27 | 90 | 2 | 2 | 1.27 | 2.14 | 2.08 | 1.1 | 1.24 | 15 |
| R3 | gil15240075 | Succinate dehydrogenase | 67.6 | 6.2 | 98 | 6 | 5 | 1.98 | 2.35 | 2.37 | 1.43 | 1.3 | 16 |
| R4 | gil15228319 | Aldehyde dehydrogenase 2 | 54.1 | 6.87 | 99 | 12 | 7 | 2.86 | 2.71 | 2.34 | 1.48 | 1.27 | 16 |

| | | | | | | | | | | | | | |
|---|---|---|---|---|---|---|---|---|---|---|---|---|---|
| R5 | gil15221044 | Dihydrolipoamide dehydrogenase 1 | 59.8 | 7.89 | 84 | 8 | 5 | 1.86 | 1.95 | 1.94 | 1.24 | 1.14 | 16 |
| R6 | gil15231702 | Monodehydroascorbate reductase 1 | 43.2 | 6.14 | 99 | 9 | 5 | 2.39 | 2.91 | 2.66 | 1.37 | 1.07 | 16 |
| R7 | gil6684341 | Alcohol dehydrogenase | 37.3 | 7.73 | 99 | 12 | 6 | 2.19 | 1.5 | 2.63 | -1.06 | 1.36 | 14 |
| R8 | gil19310885 | NADP dependent sorbitol 6-phosphate dehydrogenase | 37.6 | 8.82 | 62 | 3 | 2 | 2.46 | 2.11 | 1.93 | 1.41 | 1.44 | 16 |
| R9 | gil18420117 | NADH-cytochrome b5 reductase | 27.9 | 10.7 | 76 | 9 | 4 | 1.56 | 1.78 | 1.59 | 1.32 | 1.39 | 16 |
| R10 | gil49609452 | Peroxidase | 35.6 | 6.7 | 79 | 7 | 2 | 2.12 | 1.41 | 1.89 | 1.25 | 1.26 | 14 |
| R11 | gil15232468 | Malate dehydrogenase | 35.9 | 6.78 | 96 | 15 | 5 | 1.99 | 2.28 | 1.63 | -1.09 | 1.17 | 16 |
| R12 | gil15239652 | Flavodoxin-like quinine reductase | 23.6 | 6.85 | 98 | 16 | 3 | 2.14 | 1.72 | 2.32 | 1.38 | 1.23 | 14 |
| R13 | gil2493122 | Vacuolar ATP synthase, catalytic subunit A | 67.6 | 4.94 | 99 | 17 | 11 | 1.78 | 4.74 | 3.24 | 1.46 | 1.3 | 15 |
| R14 | gil26986106 | Vacuolar ATPase subunit B | 56.3 | 4.24 | 99 | 8 | 3 | 1.39 | 3.22 | 2.18 | 1.42 | 1.21 | 15 |
| R15 | gil18415911 | Mitochondrial ATP synthase beta chain 2 | 58.1 | 5.33 | 99 | 17 | 7 | 1.71 | 1.59 | 1.98 | 1.23 | 1.37 | 14 |
| R16 | gil40317420 | Glutamine synthetase isoform GSe1 | 44.7 | 4.72 | 94 | 6 | 2 | 1.52 | 3.74 | 2.91 | 1.39 | 1.21 | 15 |
| R17 | gil854928 | Endochitinase CH25 precursor | 34.8 | 9.31 | 81 | 8 | 3 | 1.05 | 1.94 | 2.31 | 2.28 | 1.99 | 3 |
| R18 | gil15239271 | 20S proteasome alpha sununit D2 | 27.3 | 10.1 | 99 | 16 | 6 | -1.03 | 1.9 | 2.49 | 2.24 | 2.22 | 3 |
| R19 | gil15228197 | Jacalin lectin family protein | 30.6 | 6.34 | 43 | 2 | 2 | 1.3 | 2.12 | 1.74 | 1.4 | 1.17 | 15 |
| R20 | gil15225839 | 20S proteasome alpha subunit G1 | 29.4 | 7.23 | 99 | 14 | 4 | 1.26 | 2.11 | 2.04 | 3.2 | 2.61 | 3 |
| R21 | gil584928 | Endochitinase CH25 precursor | 34.9 | 8.01 | 75 | 6 | 2 | -1.23 | 2.18 | 1.9 | 2.33 | 1.45 | 3 |
| R22 | gil79322198 | 20S proteasome alpha subunit A2 | 27.3 | 7.33 | 99 | 20 | 4 | 1.28 | 1.88 | 2.01 | 2.66 | 2.34 | 3 |
| R23 | gil22324586 | PR-protein | 24.2 | 6.96 | 45 | 8 | 2 | 1.51 | 1.7 | 2.82 | 1.02 | -1.04 | 14 |
| R24 | gil15220961 | 20S proteasome alpha subunit E1 | 20.1 | 3.51 | 99 | 10 | 2 | -1.13 | 1.88 | 2.19 | 2.65 | 2.49 | 3 |
| R25 | gil34334177 | Osmotin-like pathogenesis-related protein 5 | 15.5 | 10.2 | 91 | 8 | 2 | 1.84 | 1.34 | 1.21 | 1.01 | 1.12 | 12 |
| R26 | gil4586021 | Cytoplasmic aconitate hydratase | 98.2 | 6.7 | 93 | 7 | 7 | -1.77 | -1.68 | -1.88 | -1.9 | -2.04 | 16 |
| R27 | gil15231939 | Phosphoglycerate mutase | 64.8 | 5.96 | 99 | 13 | 8 | -1.47 | -1.59 | -1.66 | -1.2 | -1.67 | 6 |

| | | | | | | | | | | | | | |
|---|---|---|---|---|---|---|---|---|---|---|---|---|---|
| R28 | gil1883006 | Jasmonate inducible protein | 69.6 | 6.41 | 99 | 18 | 9 | 1.37 | 2.88 | 1.41 | 1.08 | 1.37 | 15 |
| R29 | gil47600741 | Cobalamin-independent methionine synthase | 84.3 | 7.45 | 83 | 7 | 6 | 2.54 | 2.1 | 1.43 | 1.29 | 1.22 | 12 |
| R30 | gil47600741 | Cobalamin-independent methionine synthase | 84.3 | 7.63 | 99 | 11 | 10 | 2.13 | 1.89 | 2.37 | 1.21 | 1.34 | 14 |
| R31 | gil15232845 | metalloendopeptidase | 59.2 | 6.91 | 99 | 11 | 9 | 1.05 | -1.74 | 1.71 | -1.02 | 1.1 | 9 |
| R32 | gil15233272 | Cytosolic triose-phosphate isomerase | 27.4 | 5.97 | 99 | 17 | 4 | -2.61 | -1.73 | -1.86 | -1.3 | -1.48 | 3 |
| R33 | gil15233272 | Cytosolic triose-phosphate isomerase | 23.4 | 6.54 | 96 | 15 | 3 | -2.18 | -2.74 | -2.35 | -2.27 | -1.98 | 8 |
| R34 | gil2204102 | Glutathione-S-transferase | 18.3 | 7.98 | 86 | 18 | 4 | 2.17 | 2.68 | 1.87 | 1.24 | 1.26 | 16 |
| R35 | gil121483748 | Glutathione transferase | 17.8 | 7.94 | 82 | 8 | 2 | 1.5 | 1.93 | 1.36 | 1.33 | 1.08 | 16 |
| R36 | gil21553555 | Dehydration stress-induced protein | 11.1 | 3.76 | 90 | 4 | 2 | 1.56 | 1.72 | 1.74 | 1.42 | 1.37 | 16 |
| R37 | gil1928939 | Stress responsive cyclophilin | 14.2 | 10.6 | 88 | 9 | 2 | 1.61 | 1.82 | 1.64 | 1.41 | 1.95 | 10 |

[1] Protein numbering refers to numbers in Figure 3-14.

[2] Protein identities and accession numbers are from top database matches in the NCBI nr database.

[3] MW and p*I* were estimated from gel locations of protein spots and compared to expected values.

[4] Protein identification score, percentage sequence coverage (SC), and matched peptide numbers (MPN) were determined from the top NCBI nr database match using PEAKS software. All identifications were confirmed using MASCOT MS/MS ion search and significant matches ($p < 0.05$) were retained.

[5] Salt, Salt + WT, and Salt + Mut, WT, Mut represent protein expression ratios in plants treated with salt only, salt plus wild-type *P. putida* UW4, salt plus UW4 AcdS minus mutant, wild-type *P. putida* UW4 only, and UW4 AcdS minus mutant respectively. Expression ratios were determined using DeCyder V 6.0 software with triplicates. The underlined ratios indicate protein expression that was not significantly changed.

[6] CL stands for Cluster numbering referring to numbers in Figure 3-16.

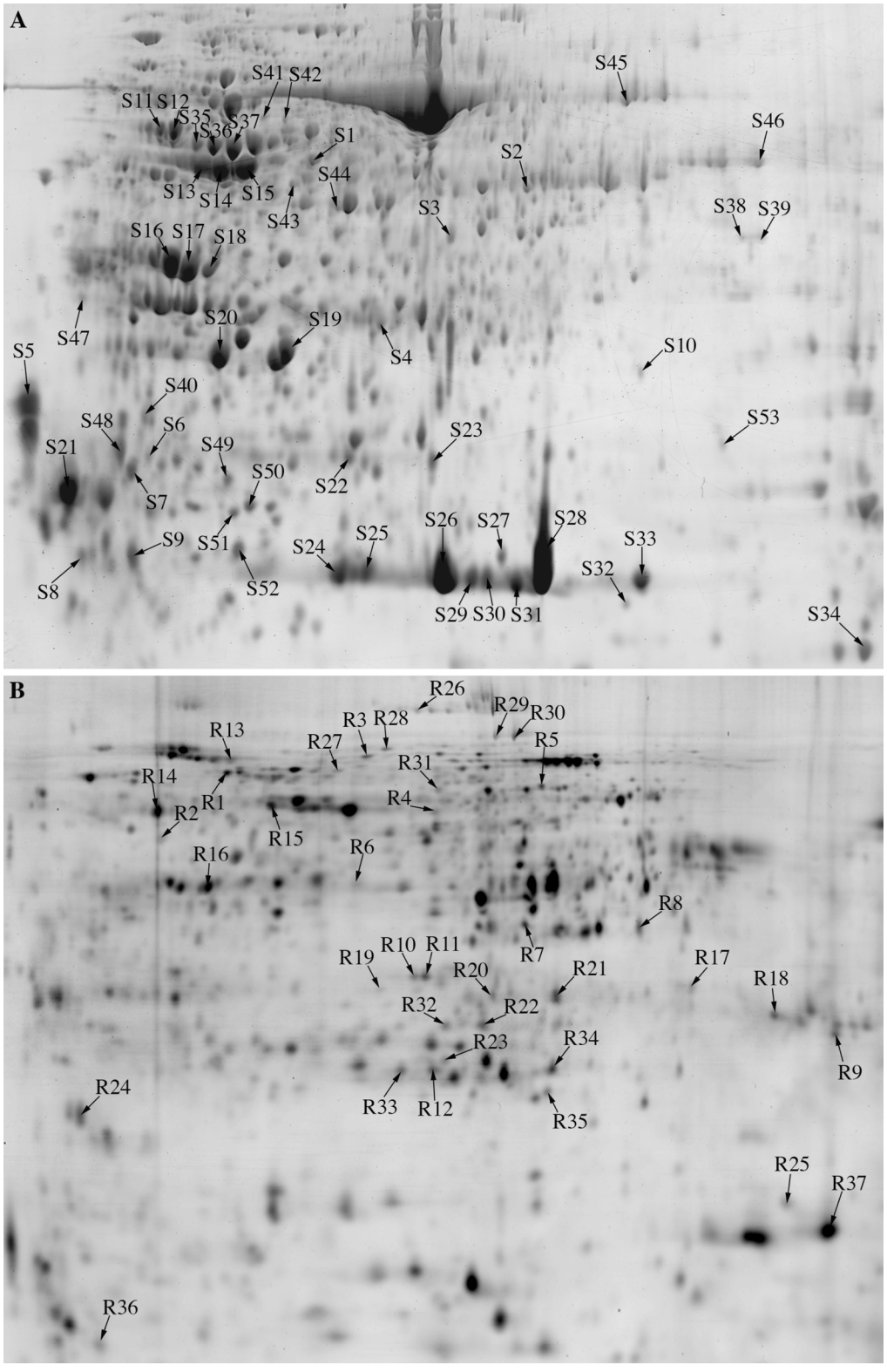
A
S41
S42
S45
S11
S12
S35
S37
S36
S1
S46
S2
S44
S13
S14
S15
S43
S3
S38
S39
S16
S17
S18
S20
S19
S47
S4
S10
S5
S40
S48
S6
S53
S23
S21
S49
S50
S22
S7
S26
S27
S28
S33
S9
S51
S24
S25
S32
S8
S52
S29
S30
S31
S34
B
R26
R29
R30
R3
R28
R13
R27
R5
R31
R14
R1
R4
R2
R15
R6
R16
R8
R10
R11
R7
R19
R17
R20
R21
R18
R32
R22
R23
R34
R9
R24
R33
R12
R35
R25
R37
R36

Figure 3-15. Preparative gels of *Brassica napus* shoot (A) and root (B) proteins. Approximately 0.5 mg of control protein samples from non-treated plants was loaded onto IPG 3-11NL strips in the first dimension, and separated using a 12% SDS-PAGE gel in the second dimension. Proteins spots were visualized by SyproRuby staining. The identified and labeled spots are annotated according to the numbers used in Table 3-5.

plants; spots were identified by mass spectrometry and labeled according to the numbers used in Table 3-5. About 80% of the identified spots had significant changes in abundance (relative to controls) in both plants treated with salt and plants treated with salt plus bacteria (both wild-type *P. putida* UW4 and the UW4 AcdS minus mutant) (Table 3-5).

In order to identify groups of proteins with similar stress-response profiles, a hierarchical clustering algorithm was applied to fold change data for identified protein spots. Pearson correlation was used as a distance measure (1-correlation) in order to capture behavioral trends ("up" and "down" in response to treatments). Eighty percent of proteins could be grouped into five clusters (clusters 1, 3, 14, 15, 16) with similar response profiles. Cluster 1 contains a set of proteins that were largely down-regulated by the presence of salt. This salt-induced down-regulation was reduced in the presence of wild-type *P. putida* UW4 but not the AcdS mutant strain. Proteins in Cluster 3 were largely up-regulated by presence of bacteria, independent of whether ACC deaminase was present. Clusters 14, 15 and 16 are comprised of proteins that were up-regulated by salt. The degrees of up-regulation were reduced, enhanced or unaltered by the presence of ACC deaminase in Cluster 14, 15 or 16, respectively. No more than 3 proteins with various functions were grouped together within each other cluster (Clusters 2, 4 to 13). Some of these proteins, such as serine hydroxymethyltransferase, glycine-rich RNA binding proteins, and cytosolic triose-phosphate isomerase, are also involved in salt responses (Kim et al., 2007; Moreno et al., 2005; Yan et al., 2005). Glycine-rich RNA binding protein 2A (S51) was previously shown to play important roles in plant responses to environmental stresses, such as high-salinity, cold and osmotic stress, by modulating the

expression of various classes of genes (Kim et al., 2007). Interestingly, this protein was strongly down-regulated, but only under salt stress in the presence of bacteria (Table 3-5).

Overall, many of the plant protein expressional changes due to the presence of salt can be associated with three functional categories. First, in Clusters 14 and 16 a set of 8 shoot and 11 root oxidoreductase protein spots (Figure 3-16, Table 3-5), many of which are involved in anti-oxidative protection, were up-regulated primarily in response to salt. A second category, largely grouped together into Cluster 1, contained nineteen down-regulated shoot protein spots involved in photosynthesis, such as ribulose bisphosphate carboxylase activases, oxygen-evolving enhancers in photosystem II, photosynthetic electron transfer proteins, ribulose bisphosphate carboxylase, and plastocyanin (Figure 3-16, Table 3-5). In addition, various shoot and root membrane transportation proteins and osmoprotectants synthesis enzymes were up-regulated, including anion-selective channel protein, porin-like protein, vacuolar ATPase, and glutamine synthase (Cluster 15).

Cluster 3 showed that a primary effect of bacterial treatment on the plant proteome was the up-regulation of both shoot and root proteins involved in plant pathogen defense. These proteins included jacalin lectin, 20S proteasome subunits, and endochitinase CH25; the latter protein was only observed when the bacterial strains were present (Figure 3-16).

Interestingly, in Clusters 1 and 15, the presence of ACC deaminase modulated the plant's stress response to salt in many cases. For example, the expression of photosynthesis proteins was down-regulated to a lesser extent in plants treated with the wild-type bacterium compared to plants that were treated with only salt or salt plus the UW4 AcdS minus mutant. Moreover, in plants treated with the wild-type bacterium, there was an increase (relative to

plants that were treated with only salt and salt plus the UW4 AcdS minus mutant) in the expression of some proteins involved in ion transport, and salt accumulation (Figure 3-16, Table 3-5).

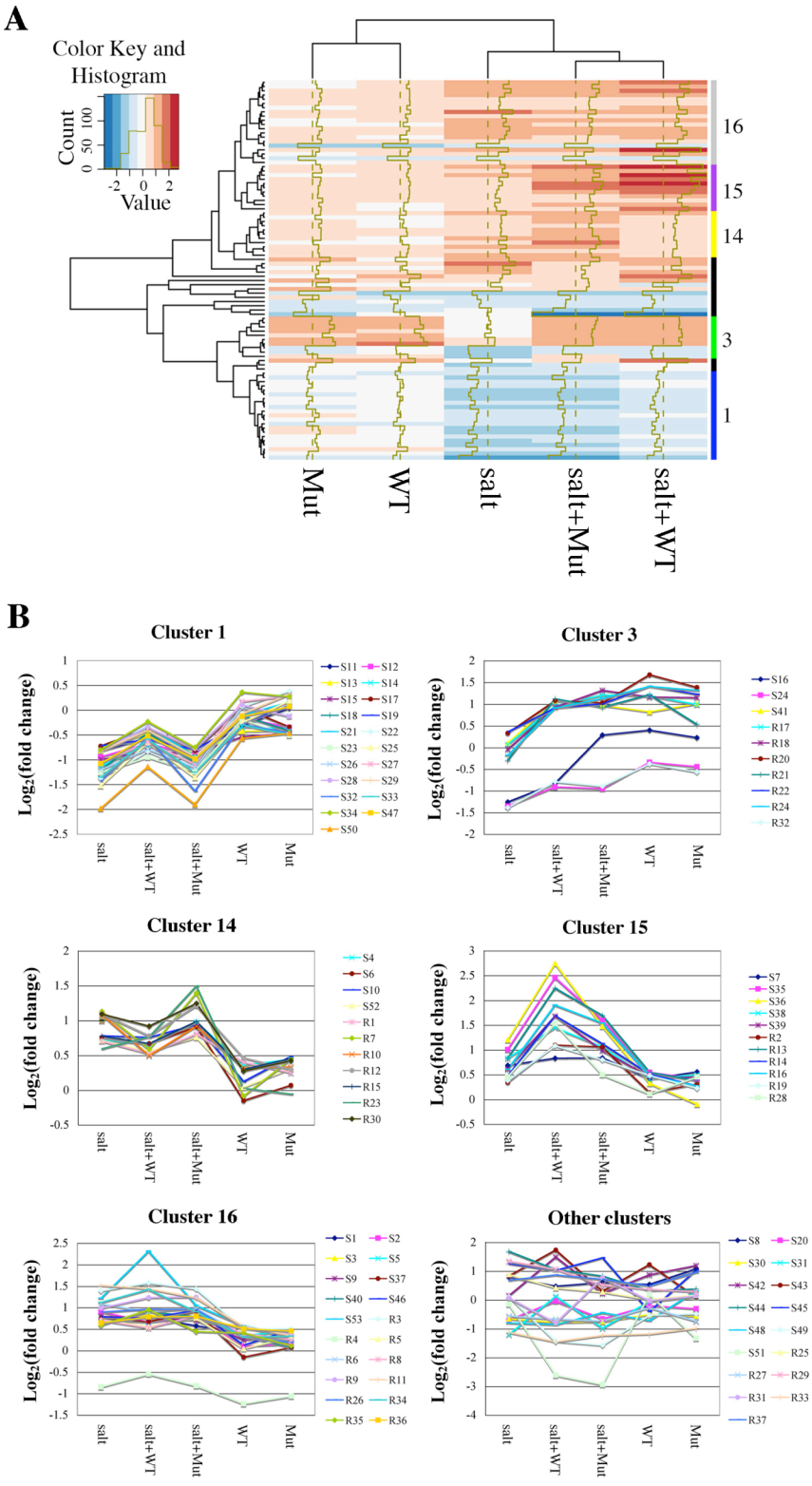
A
Color Key and Histogram
Count
0 50 100
-2 0 2
Value
16
15
14
3
1
Mut
WT
salt
salt+Mut
salt+WT
B
Cluster 1
Log2(fold change)
Cluster 3
Log2(fold change)
Cluster 14
Log2(fold change)
Cluster 15
Log2(fold change)
Cluster 16
Log2(fold change)
Other clusters
Log2(fold change)
salt
salt+WT
salt+Mut
WT
Mut

Figure 3-16. *Brassica napus* protein expressional profiles in response to salt and bacteria. Proteins were annotated with numbers from Table 3-5. A. Log base 2 fold changes for the identified spots (blue, down-regulated; red, up-regulated) were clustered using correlation as a distance metric (1-correlation). The brown line through the color key shows a histogram of the distribution of fold change values, whereas the lines running down the center of each column track the specific fold change value for each spot in the corresponding condition. The color bar and numbers to the right of the heatmap indicate which rows correspond to the major clusters (containing more than 3 protein spots). Black entries in the color bar correspond to non-major (mostly singleton) clusters. B. Protein responses to salt and bacteria for proteins in cluster groups. Log base 2 fold changes for the identified spots are on the y-axis, and the x-axis separates the five experimental conditions.

# 4. Discussion

## 4.1 The effects of *P. putida* UW4 and AcdS minus mutant on canola physiology

### 4.1.1 The effects on ACC and IAA levels in canola root exudates

Both ACC and IAA play important roles in the process of plant growth promotion by bacteria (Glick, 1995; Patten and Glick, 2002). In agreement with a previously proposed model (Glick et al., 1998) and published data showing a decrease in endogenous ACC levels when ACC deaminase is present (Penrose and Glick, 2001), treatment of plants with *P. putida* UW4 decreased the exogenous ACC content to about half of the control level, while the AcdS minus mutant, which doesn't have ACC deaminase, slightly increased the ACC concentration. On the other hand, there was a dramatic increase (4.5-fold) in the IAA level when plants were treated with *P. putida* UW4, and only a small increase (~50%) following the treatment with the AcdS minus mutant. Although plant endogenous IAA and ACC levels were not measured directly, the levels found in root exudates are expected to be highly correlated to the levels in root tissues. As ACC deaminase decreases the negative feedback of ethylene on IAA signal transduction and synthesis (Glick et al., 2007a), it is not surprising that the wild-type *P. putida* UW4 can decrease the amount of ACC and at the same time increase the IAA level. In fact, some plant auxin-regulated genes were up-regulated following treatment with an endophytic plant growth-promoting *Pseudomonas fluorescens* strain that contains ACC deaminase (Wang et al., 2005). With the AcdS minus mutant strain, the small observed increase in the IAA level may reflect exogenous IAA supplied by the bacterium without any change to the feed back

inhibition of ethylene on IAA signal transduction and synthesis (Glick et al., 2007a; Li et al., 2000). The increased level of ACC following treatment of plants with the mutant is most likely a consequence of the IAA-activation of ACC synthase. This data is consistent with the model describing how an ACC deaminase-containing bacterium modulates levels of both ethylene and IAA (Glick et al., 1998; Glick et al., 2007a). In this model, ethylene inhibition of IAA signal transduction limits the amount of ethylene that is produced by a plant as a consequence of the addition of exogenous IAA. IAA plays a dual role in promoting cell proliferation and root elongation while at the same time stimulating the transcription of ACC synthase, one of the key steps in ethylene synthesis. In this way, ethylene may limit the amount of its own synthesis. By lowering the amount of ethylene, ACC deaminase relieves the ethylene repression of auxin response factor synthesis. This results in an increase in the IAA stimulation of growth without causing an increase in ethylene production.

### 4.1.2 The effects on canola grown in hydroponic solution

The shoot fresh and dry weights of canola plant treated with salt plus *P. putida* UW4 were 1.7-fold and nearly 2-fold, respectively, greater than those of plants treated with salt only ($p < 0.05$), even though they were still significantly less than the weights of non-treated controls ($p < 0.05$). By contrast, the plants treated with salt plus the ACC deaminase minus mutant didn't show any statistically significant ($p > 0.25$) differences from the ones treated with salt only, indicating that plant growth enhancement by bacteria was dependent on having a functional ACC deaminase and supporting the notion that growth promotion of stressed plants is largely attributable to reducing inhibitory ethylene levels by bacterial ACC deaminase (Glick et al., 1998).

In the absence of salinity stress, no statistically significant differences in shoot weights were observed between the non-treated controls and bacterially treated (both wild-type UW4 and the AcdS minus mutant) plants. This is probably due to the fact that the effects of bacterial treatments in relatively mature plants were minor in the absence of stress ethylene. This is also consistent with the findings that fewer changes (only a small number of defense-related proteins) in protein accumulation patterns were identified in plants treated with only bacteria (both wild-type UW4 and the AcdS minus mutant) than in plants treated with salt (Table 3-5).

Irrespective of the presence of salt and/or bacteria, no significant differences in average root weights of differently treated plants were observed, consistent with the fact that the major differences in root protein accumulation patterns across all conditions was the up-regulation of various defense proteins, unlike the large decrease in a wide range of proteins in shoots (Table 3-5).

## 4.2 The effects of environmental signals on *P. putida* proteomes

In spite of the lack of genomic information regarding *P. putida* UW4, proteins were identified by mass spectrometric analyses with high confidence. The quantitative proteomic analysis of differential protein expression profiles utilized in this work was effective in identifying both comprehensive and biologically significant bacterial responses to environmental factors.

### 4.2.1 The effects of nickel on *P. putida* proteomes

The effects of nickel on protein expression were very similar for wild-type *P. putida* UW4 and AcdS minus mutant. More than half of the identified protein expression changes in

the presence of nickel occurred in both wild-type and mutant strains. As expected, ACC deaminase was only present in the wild-type expression profile; it was slightly up regulated in the presence of 2 mM nickel. No other notable changes were observed, suggesting that interactions between nickel response and ACC deaminase activity are minimal.

Interestingly, the expression of the protein spot corresponding to Q4L351_STAHJ was increased almost 30-fold in the wild-type *P. putida* UW4 in response to 2 mM nickel (Table 3-2). The top match for this protein was a *Staphylococcus haemolyticus* protein annotated as 'similar to immunodominant antigen B' with a relatively low score (48.52%). *S. haemolyticus* is not closely related to *P. putida* UW4 since *S. haemolyticus* is Gram-positive and *P. putida* UW4 is Gram-negative. However, three peptides were matched with approximately 10% sequence coverage to Q4L351_STAHJ. And the observed molecular weight (18.3 KDa) and p*I* (5.08) of this protein on the gel matched well with the calculated values of Q4L351_STAHJ protein (18.4 KDa, p*I* 5.01). In addition, the possibility of *S. haemolyticus* contamination in the original culture is unlikely since 33 out of 35 proteins in this work were identified as *Pseudomonas* proteins. The *P. putida* AcdS minus mutant was constructed by specifically disrupting the ACC deaminase gene using homologous recombination (Li et al., 2000), so that is possible that regulation of this protein may be affected by ACC deaminase, a protein whose expression is regulated by a variety of factors in a complex manner (Cheng et al., 2008; Grichko and Glick, 2000; Li and Glick, 2001). Very little is known about the function of this *S. haemolyticus* protein. An NCBI Blast analysis of this protein found no known homologous proteins in *Pseudomonas* species, and relatively few related proteins in other *Staphylococcus* species. Previous results showed that an immunodominant antigen in *Burkholderia cepacia*

functioned as an efflux pump (Wigfield et al., 2002). It is likely that the identified protein in *P. putida* UW4 is a cell surface protein, and may possibly be involved in import/export functions, but this is conjecture at this point. It is possible that the gene coding for this protein was acquired by *P. putida* UW4 by lateral gene transfer, a common mechanism for the acquisition of *acdS* and other genes by pseudomonads (Hontzeas et al., 2005). The ArsA protein that was identified via a match to a *Bradyrhizobium* protein was also likely to have been obtained by *P. putida* UW4 via a similar mechanism.

As expected, bacterial cells responded to nickel stress by decreasing expression of proteins involved in cellular activities, such as amino acid synthesis, protein synthesis and folding, DNA replication, cell division and cell communication. Proteins involved in these processes were all down regulated when cells were exposed to nickel stress. Proteins involved in general non-specific importation of metabolites into the cell was up regulated, although this could possibly result in the intensification of the toxic effects of the nickel.

In addition, bacterial universal stress protein and general stress protein CTC, which were previously reported to be induced by and responsible for the resistance to various stresses (Duche et al., 2002; Gardan et al., 2003; Kvint et al., 2003), were also up regulated in both strains and presumably participate in the nickel resistance response. An efflux protein ArsA, which is involved in arsenate exportation (Nies, 2003), was also up regulated in both strains. Although it was only one protein of many that are responsible for efflux-mediated detoxification of arsenate, the up regulation of this protein suggests that a similar efflux-mediated mechanism may be involved in nickel detoxification in *P. putida* UW4.

In Gram-negative bacteria, heavy metal cations can bind to glutathione and the

resulting products (bisglutathione complexes) tend to react with molecular oxygen to form oxidized bisglutathione, releasing the metal cation and hydrogen peroxide (Valko et al., 2005). Since bisglutathione must be reduced in an NADPH-dependent reaction and the released metal cations immediately begin another cycle of binding and oxidation, this can cause considerable oxidative stress. Here, a variety of anti-oxidative proteins were up regulated in both strains in the presence of 2 mM nickel. In particular the expression of thioredoxin was increased almost 20-fold (Table 2). All anti-oxidative proteins that were observed to be up regulated in *P. putida* UW4 were previously shown to be responsible for anti-oxidative stress and/or up regulated in the presence of the oxidative stress (Bittel et al., 2003; Bunik, 2003a, 2003b; Culotta, 2000; Kiss et al., 2004; Lee et al., 2006; Wang et al., 2006). Both the numbers of the proteins that were up regulated and the magnitude of their changes suggested that the production of anti-oxidative stress proteins was a major response of *P. putida* UW4 to the presence of nickel. Other studies have also suggested that these proteins are involved in nickel detoxification (Bittel et al., 2003; Bunik, 2003a, 2003b; Culotta, 2000; Culotta et al., 2006; Kiss et al., 2004; Lee et al., 2006; Wang et al., 2006).

Two hypothetical proteins with altered expression levels were identified and one of them was up regulated in both the wild-type and mutant. The NCBI Blast search of the hypothetical protein with accession number Q3KFH8_PSEPF matches a number of other hypothetical proteins, but none has been functionally annotated. The other hypothetical protein, with accession number Q3KI45_PSEPF, matches a putative *Pseudomonas* signal peptide with a 72% identity and a predicted *Pseudomonas* periplasmic/secreted protein with a 60% identity. In both cases, the hypothetical proteins may be involved in environmental signal transduction.

In any event, additional studies focused on these genes may facilitate a better understanding of the mechanisms involved in bacterial heavy metal resistance.

### 4.2.2 The effects of canola root exudates on *P. putida* proteomes

The effect of canola root exudates on protein expression was similar for wild-type *P. putida* UW4 and AcdS minus, with the majority of identified significant protein expression changes occurring in both the wild-type and AcdS minus mutant.

Many of the proteins that were up-regulated in response to canola root exudates are involved in the utilization of nutrients (Figure 3-6 and Table 3-3). This observation is consistent with a transcriptomic study of bacterial responses to plant root exudates (Mark et al., 2005), and with the notion that the utilization of the major components in plant root exudates by pseudomonads is the nutritional basis for their colonization of host plant roots (Lugtenberg et al., 1999). Another group of proteins whose expression is increased participate in bacterial cell envelope synthesis, including exopolysaccharide and peptidoglycan biosynthesis and membrane lipoprotein localization, which are thought to be essential for bacterial root colonization, symbiosis, virulence, or even viability (Dekkers et al., 1998; Gao et al., 2001; Tanaka et al., 2001; Yorgey et al., 2001). In addition, a few other up-regulated proteins, such as GTP-binding protein TypA, chaperone clpB and a ThiJ/PfpI family protein, were all previously shown to be required during the interaction of bacteria with their plant hosts (Caldelari et al., 2006; Hughes et al., 2007; Kiss et al., 2004).

On the other hand, a protein involved in chemotaxis as a two-component response regulator, CheY, was down-regulated by canola root exudates (Figure 3-6 and Table 3-3). This finding is in agreement with the previous observation (Mark et al., 2005), and with the idea that

chemotaxis plays important roles in bacterial host selection and colonization (Mark et al., 2005) and response to environmental stimuli (Nixon et al., 1986). The expression of a transcriptional regulator, a TraR/DksA family protein involved in quorum sensing, was also down-regulated by canola root exudates. Previous studies have shown that the quorum sensing circuitry that is operative in *Pseudomonas aeruginosa* is essential for the expression of its virulence factors as well as for its biofilm formation when colonizing the lungs of cystic fibrosis patients (Singh et al., 2000). In addition, expression of an essential protein in bacterial protein synthesis (peptide deformylase), a Fis family protein involved in DNA repair/modification and a previously uncharacterized protein were also decreased more than 2-fold by canola root exudates.

While some *P. putida* UW4 proteins that facilitate the establishment of host-bacterial interactions were up-regulated in response to canola root exudates, some essential proteins were down-regulated, which should inhibit bacterial growth. This down-regulation could reflect the fact that in the presence of sufficient resources, the bacterium no longer needs to synthesize proteins to the same extent as in the absence of nutrients. Again, this complexity in changing protein expression level in response to root exudates would appear to reflect a major shift in the physiology of bacteria that are associated with plant roots rather than free-living.

The roles played by selected proteins that were differentially expressed in the presence of root exudates were investigated by over-expression or knock out of the corresponding genes. In the first instance, it was ascertained that the plant growth-promoting activity of *P. putida* UW4 depends on the outer membrane protein OmpF. The OmpF porin is a trimeric integral membrane protein, which forms a non-specific transport channel responsible for passive

transport of small molecules, such as nutrients and waste products, across the outer membrane of Gram-negative bacteria (Cowan et al., 1995). The OmpF protein is also thought to be involved in adhesion and invasion of the Crohn's disease-associated *Escherichia coli* strain LF82 (Rolhion et al., 2007). The fact that the OmpF protein over-expression and elimination in *P. putida* UW4 led to an increase and decrease, respectively, of its root elongation activity (Figure 3-9) can be explained by two mechanisms. The plant growth-promoting activity of *P. putida* UW4 relies on the transport of ACC from plant cells into attached bacterial cells, since ACC deaminase is localized and functions in the bacterial cytosol. Disruption or enrichment of the OmpF protein, which potentially transports ACC through the *P. putida* UW4 outer membrane, may directly affect its plant growth-promoting ability. In this regard, changes to the expression of the OmpF protein are predicted to have little or no impact on the growth-promoting activity of the ACC deaminase minus mutant of strain UW4. Alternatively, the plant growth-promoting activity of *P. putida* UW4, which is dependent on the direct physical binding of bacterial cells to plant surfaces, may also be dependent on the OmpF protein that may be involved in bacterial cell adhesion to the plant.

Second, based on the expression results, canola root exudates appears to contain a bacterial peptide deformylase inhibitory compound, which could potentially be employed as an antibacterial agent candidate. Peptide deformylase (Pdf) is involved in protein maturation after translation through its activity to remove the *N*-formyl group of *N*-formyl methionine. The Pdf protein is essential in eubacteria and absent in mammalian cells, making it an appealing target for the selection of novel antibiotics (Leeds and Dean, 2006). The fact that the Pdf protein disrupted strain was not viable suggests that this protein is essential in bacterial cells (Figure 3-

9). Down-regulation of the peptide deformylase in response to plant exudates (Figure 3-6 and Table 3-3) may reflect a plant mechanism to inhibit bacterial growth and limit colonization by bacterial pathogens. The strain over-expressing the Pdf protein promoted root length to a greater extent than the wild-type, possibly by overcoming the inhibitory effects of a putative plant compound. Previously, exudates containing plant-derived antibacterial metabolites were shown to confer tissue-specific resistance to various bacterial pathogens (Bais et al. 2005). For example, actinonin, a naturally occurring bacterially-encoded antibacterial agent, was previously identified as a Pdf protein inhibitor (Chen et al. 2000). Thus, the presence of a bacterial peptide deformylase inhibitory compound in root exudates may provide an opportunity to derive a potent and broad spectrum antibacterial agent.

The previously uncharacterized protein (Hyp) has been predicted to be a potential DNA binding protein (Marchler-Bauer et al. 2007). The observation that the Hyp protein may be involved in plant growth promotion has not been observed previously. However, whether the Hyp protein is a DNA-binding protein possibly involved in gene transcriptional regulation is still conjecture at this point. As over-expression of the Hyp protein led to a growth inhibition of canola roots greater than that in the absence of bacteria (Figure 3-9), it is possible that the Hyp protein has a role in regulation of genes related to virulence in *P. putida* UW4, causing detrimental effects on plant growth. Thus, the Hyp protein over-expressing strain not only abolished the plant growth-promoting ability of *P. putida* UW4, but also may have transformed this bacterium into a deleterious organism that caused a decrease in root length compared to control plants (Figure 3-9). Conversely, the Hyp protein knockout strain demonstrated an enhanced plant growth-promoting ability probably due to elimination of deleterious effects that

could have been attributed to the Hyp protein. Again, down-regulation of the expression of the Hyp protein in response to plant root exudates (Figure 3-6 and Table 3-3) may be another plant-self-protection strategy.

### 4.2.3 The presence of *acdS* gene does not affect *P. putida* proteomic changes

This is consistent with the *P. putida* UW4 ACC deaminase enzyme not having a direct role in the resistance of the bacterium to nickel toxicity or bacterial perception and response to plant host signals caused a noticeable difference only in plant growth. Nevertheless, we can draw the conclusion that the presence or absence of ACC deaminase has no significant impact on detected *P. putida* UW4 gene expression on the exposure to nickel or canola root exudates, in other words, the wild-type *P. putida* UW4 and AcdS minus mutant strain respond similarly to environmental signals. However, the DIGE analysis and especially the subsequent mass spectrometric analysis were both biased in that they largely examined highly abundant proteins. Thus, any less abundant proteins that did happen to be differentially regulated in the wild-type *P. putida* UW4 and the AcdS minus mutant were not readily detectable on the 2-D gels or could be below the sensitivity level of the mass spectrometer.

## 4.3 Effects of environmental stimuli on canola proteome

Proteomic profiling of *Brassica napus* under different treatments has helped identify systematic responses of the plant to multiple environmental stimuli including salinity stress and/or plant growth-promoting bacteria simultaneously. These responses include general anti-oxidative and salt transportation/accumulation mechanisms, as well as shoot-specific photosynthesis and root-dominant plant-bacterial interaction responses. The overall effects of

each condition on plant proteome are summarized in Table 4-1. Our contribution to this body of research was to identify how these responses are affected by the addition of plant growth-promoting bacteria with or without ACC deaminase activity.

### 4.3.1 Salinity stress responses of canola

Besides the primary ionic and osmotic stresses, salt induces several secondary stresses including an oxidative stress through the accumulation of reactive oxygen species (Munns and Tester, 2008). This stress can cause oxidative damage to membrane lipids, proteins, and nucleic acids (Pang and Wang, 2008). One detoxifying strategy for this type of stress is for the plant to increase the synthesis of anti-oxidative enzymes. This whole-plant anti-oxidative stress response activity was observed in the current study under all three salinity conditions tested; a total of 19 shoot and root proteins (clusters 14 & 16) involved in anti-oxidative protection were significantly up-regulated (Table 3-5). Included within this category of proteins is monodehydroascorbate reductase (EC 1.6.5.4), which is crucial for the regeneration of a major antioxidant ascorbate. Previously, tobacco plants engineered to over-express this protein have been reported to exhibit enhanced salt-stress tolerance (Eltayeb et al., 2007).

One of the most dramatic and readily measurable responses induced by the osmotic effect of salt is the decrease of stomatal aperture, which subsequently results in a diminished rate of photosynthesis per plant (Munns and Tester, 2008). The current proteome analysis is consistent with this finding, as there were 19 protein spots (cluster 1) involved in the down-regulation of photosynthesis in response to salt stress in shoots but not roots (Table 3-5). It is also consistent

Table 4-1. Summary of protein expression changes in shoots and roots of *Brassica napus* plants treated with salt and bacteria.

| Pathways | Shoot | | | | | Root | | | | |
|---|---|---|---|---|---|---|---|---|---|---|
| | Salt | Salt + WT | Salt + Mut | WT | Mut | Salt | Salt + WT | Salt + Mut | WT | Mut |
| Anti-oxidative | + + | + + | + + | NC | NC | + + | + + | + + | NC | NC |
| Photosynthesis | – – | – | – – | NC | NC | ND | ND | ND | ND | ND |
| Salt transport & accumulation | + | + + + | + + | NC | NC | + | + + + | + + | NC | NC |
| Pathogenesis-related | NC | + | + | + | + | NC | + + | + + | + + | + + |

Plus and minus signs indicate magnitude of up- and down-regulation, respectively. NC stands for “no change”. ND stands for “not detected”. Salt, Salt + WT, and Salt + Mut, WT, Mut represent protein expression profiles in plants treated with salt only, salt plus wild-type *P. putida* UW4, salt plus UW4 AcdS minus mutant, wild-type *P. putida* UW4 only, and UW4 AcdS minus mutant respectively.

with the decreased chlorophyll level observed in salt-stressed plants compared to the non-treated control (Figure 3-13).

In most plants, the leaf blade rather than the root is thought to be the main site of salt toxicity, as it's the final destination of sodium ions carried through the transpiration stream (Munns and Tester, 2008). Nevertheless, the roots are the interface through which sodium ions are accumulated and subsequently redistributed through the plant (Munns and Tester, 2008). Accordingly, sodium accumulates in both the shoots and roots of NaCl-treated canola, with approximately 2-fold higher salt concentration in shoots than in roots (Cheng et al., 2007). This ion accumulation also explains the up-regulation of various membrane transport proteins (cluster 15), such as voltage-dependent anion-selective channel protein, porin-like protein, vacuolar ATP synthase, and vacuolar ATPase, in the shoots and roots under all conditions involving salt treatment (Table 3-5). Some of these proteins like mitochondrial ATP synthase, vacuolar ATP synthase, and vacuolar ATPase may be indirectly involved in salt transport by participating as the energy generating portion of the transport apparatus. Plants have evolved a variety of mechanisms to overcome the toxicity caused by salt accumulation inside cells. One approach is to sequester sodium ions in intracellular organelles such as vacuoles. Mitochondrial ATP synthase, which was observed to be up-regulated in this study when plants were treated with salt and salt plus bacteria, has previously been shown to be induced by salt stress, and to confer enhanced salinity tolerance when it is over-expressed in plants (Zhang et al., 2006a; Zhang et al., 2008). The up-regulation of the mitochondrial ATP synthase may indicate that plants produced more ATP than could be used by proton pumping ATPase. The proton pumping ATPase in turn would be more active and thus provide a better membrane

potential to help exclude $Na^+$ from the cytoplasm by exporting it into the apoplasm or storing it in the vacuole.

### 4.3.2 Bacterial effects on canola proteome

The main response of canola (both shoots and roots) to bacterial interaction is the up-regulation of pathogenesis-related proteins (cluster 3). This defense response was active in both the presence and absence of salt stress (Table 3-5). Although some pathogenesis-related proteins have been shown to be induced by general stress (Ohshima et al., 1990), almost all of the pathogen responsive proteins identified in this work were only significantly induced when bacteria (either wild-type *P. putida* UW4 or the UW4 AcdS minus mutant) were present (Table 3-5). In the shoot protein accumulation pattern, only one protein (jacalin lectin) was determined to be significantly up-regulated both in plants that were treated with either wild-type *P. putida* UW4 or the UW4 AcdS minus mutant relative to the non-treated control (Table 3-5). This protein has previously been observed at the bacterial infection site, protecting plants against pathogenic bacteria by inhibiting bacterial growth (Etzler, 1985). Meanwhile, there were seven up-regulated proteins in the root (Table 3-5), including four different subunits of 20S proteasome and endochitinase CH25, all of which are involved in the plant defense response. It has been suggested that the name "20S proteasome" be replaced with "plant defense proteasomes" because of the important roles that these proteins play in a plant's defense (Suty et al., 2003). Previous studies on various defense models indicated an accumulation of various 20S proteasome subunits in plants developing a systemic acquired resistance response, suggesting a tight correlation between the regulation of 20S proteasome subunits and the activation of a plant's defense reactions (Suty et al., 2003). Therefore, the

simultaneous up-regulation of four 20S proteasome subunits (A2, D2, E1, and G1) is suggestive of a systemic plant defense response induced by both *P. putida* UW4 and the UW4 AcdS minus mutant. The up-regulation of anti-fungal chitinase might be due to its inclusion in a broad-spectrum, ethylene-regulated defense network. Chitinase is mainly involved in fungal pathogen resistance (Grison et al., 1996), and not in bacterial pathogen defense due to differences in cell wall content between bacteria and fungi. However, it was previously shown that ethylene regulated the plant's response to both bacterial and fungal pathogen infections in tomato (Lund et al., 1998). The predominant up-regulation of plant defense proteins in the root suggests an important role in defense against potential invaders.

### 4.3.3 ACC deaminase effects on plant salinity stress responses

Data from plants that were treated only with salt and ones treated with both salt and bacteria (either *P. putida* UW4 or the UW4 AcdS minus mutant) are consistent with ACC deaminase activity broadly reducing the impact of salt on plant proteins. A number of researchers have reported that treatment of plants with either *Azospirillum lipoferum* or *A. brasilense* can mitigate some of the inhibitory effects of salt stress on wheat, maize, beans or lettuce (Bacilio et al., 2004; Barassi et al., 2006; Hamdia et al., 2004; Rabie and Almadini, 2005). Since at least some of these strains do not possess ACC deaminase activity (Holguin and Glick, 2001), those bacteria must utilize mechanisms other than lowering ethylene with ACC deaminase to protect plants. In this regard, it is possible (but not proven) that bacterial indole acetic acid, synthesized by these *Azospirillum* spp. strains is responsible for the promotion of plant growth in the presence of salt. Here however, ACC deaminase appears to

have a significant role in modulating the plant response to salt, as changes in protein expression due to salt plus the AcdS minus strain are more similar to salt exposure alone than the response of the salt plus wild-type bacteria treatment (Figure 3-16, Table 3-5). This is consistent with modulation of the ethylene stress response in the plant being a key pathway in ameliorating the effects of salt stress.

In particular, some of the deleterious effects of decreased photosynthesis in the presence of salt were alleviated by the addition of *P. putida* UW4, but not by the UW4 AcdS minus mutant (Table 3-5). For example, proteins involved in photosynthesis (cluster 1) were down-regulated to a lesser extent in plants that were treated with salt plus wild-type UW4, compared to the salt only or the salt plus the UW4 AcdS minus mutant treatments. This alleviation of impaired photosynthesis was also reflected by the fact that the presence of bacterial ACC deaminase in wild-type UW4 diminished the decrease in chlorophyll content caused by salt stress (Figure 3-13). The overall changes of photosynthetic proteins coincide with the fluctuation in measured chlorophyll levels under all conditions (Figure 3-13). Like many other stress responses, photosynthesis reduction is also mediated by ethylene levels, via ethylene's influence on stomatal conductance (Pallas and Kays, 1982). This supports the known mechanism utilized by the ACC deaminase-containing *P. putida* UW4, i.e. decreasing stress ethylene level to promote plant growth under salinity stress (Mayak et al., 2004a). Although it is not clear whether the decreased rate of photosynthesis is a cause or a result of plant growth inhibition, it is very likely that the enhanced photosynthesis in plants treated with *P. putida* UW4 contributes to their salinity tolerance, consistent with the finding that the halophilic alga *Dunaliella* sp. obtains salinity tolerance by enhancing photosynthesis (Liska et

al., 2004). The slightly greater degree of up-regulation of salt transport and accumulation proteins (cluster 15) in plants treated with salt plus the *P. putida* UW4 compared to plants treated with salt only helps to explain the earlier finding that canola plants treated with both salt and *P. putida* UW4 could accumulate more salt than the canola plants treated with only salt (Cheng et al., 2007). This observation is consistent with the notion that ACC deaminase-containing plant growth-promoting bacteria help balance the level of ethylene, allowing it to exert its beneficial effects without accumulating to the point of being detrimental (Stearns and Glick, 2003). Moreover, canola seed oil quality was previously shown to be unaffected by the high salinity in plants (Zhang and Blumwald, 2001).

Since no proteins directly involved in ethylene synthesis and/or regulation were among those identified as differentially expressed in the presence of *P. putida* UW4, the degree to which these are affected remains an open question. It is likely that these proteins exist at relatively low levels in plants, and may not be readily visualized in 2-D gels; it is also possible that although ACC deaminase acts on the precursor to ethylene, expression levels of proteins involved in ethylene synthesis and/or regulation are not significantly changed. Nevertheless, as the plant growth promotion activity of *P. putida* UW4 is correlated with its ability to manipulate plant ethylene levels (Glick et al., 1998; Penrose and Glick, 2003; Stearns and Glick, 2003), it is reasonable to postulate that the differences in plant protein expression were partly caused by differences in ethylene abundance between plants under different treatments. Moreover, on the 2-D gels, three protein spots representing glutamine synthetase, which is involved in ammonium ion assimilation, were up-regulated to a greater extent in plants treated with salt plus wild-type *P. putida* UW4 (approximately 5-fold) compared to plants that were

treated with salt only or salt plus the UW4 AcdS minus mutant (2- to 3-fold) (Table 3-5). This may be due to the ability of the ACC deaminase-containing wild-type *P. putida* UW4 to produce more ammonium ion for assimilation through the breakdown of ACC from the salt stressed plants. The fact that the expression levels of these three spots were not significantly up-regulated without the salt stress induced increase in ACC levels (i.e., when plants were treated with bacteria only), even though the presence of ACC deaminase was still able to up-regulate these enzymes slightly (Table 3-5), is consistent with the model explaining how ACC deaminase containing bacteria manipulate plant ACC levels.

## 4.4 Conclusions

In this work, proteomic profiling of the plant growth-promoting bacterium *P. putida* UW4 and its plant host canola in response to environmental stimuli have suggested how some proteins may be involved in host-bacterial interactions in rhizosphere. These results should contribute to a better understanding of plant-bacterial interactions.

Firstly, an examination of the proteome of both the wild-type *P. putida* UW4 and the AcdS minus mutant revealed systematic nickel resistance responses of this bacterium including general stress adaptation, anti-oxidative stress and heavy metal efflux, which may be useful in the development of PGPB-mediated phytoremediation protocols.

Then, proteomic profiling of the plant growth-promoting bacterium *P. putida* UW4 in response to canola root exudates, followed by functional analyses, have suggested how some proteins may be involved in host-bacterial interactions. This approach should contribute to a better understanding of how both beneficial and pathogenic bacterial strains establish

interactions with their hosts, as many of the proteins identified in this work were previously shown to be involved in pathogenic bacterial or fungal infections of plants and animals (Caldelari et al. 2006; Dumas-Gaudot et al. 2004; Hughes et al. 2007; Yorgey et al. 2001).

Proteomic profiling of *Brassica napus* under bacterial and/or inhibitory salt treatments has helped identify systematic responses of the plant to multiple environmental stimuli including salinity stress and/or plant growth-promoting bacteria. This body of research identifies how these responses are affected by the addition of plant growth-promoting bacteria with or without ACC deaminase activity. These results should contribute to a better understanding of how plant proteins are regulated during plant-environment interactions.

Furthermore, we have constructed a comprehensive proteome 2-D reference map of the plant growth-promoting bacterium *Pseudomonas putida* UW4. Using the World-2DPAGE Constellation (Hoogland et al., 2008), a 2-DE database containing all the MS information of *P. putida* UW4 proteins has been constructed. The dataset has been deposited into the World-2DPAGE database (accession no. 0008). This dataset will facilitate investigation of plant growth-promoting mechanisms present in this and similar bacteria, and will further contribute to characterization of bacterial interactions in the environment. This dataset can be extended by incorporating additional expression information as it becomes available.

Lastly, a better understanding of the mechanism employed by both bacteria and plants to confer resistance to environmental stresses and adjust to the host-bacterial relationship can facilitate the development of strategies for plant-growth promotion, environmental clean-up, and identification of potential antibacterial agents.

## Appendix A

## MS information of *P. putida* UW4 proteins

Supplementary Table 1. MS information of identified *P. putida* UW4 spots.

| Spot # | Accesion number* | Protein* | MW (KDa)† | p*I*† | Score %* | Sequence coverage%* |
|---|---|---|---|---|---|---|
| 1 | Q4ZVY6_PSEU2 | ribonuclease E and G | 125.3 | 4.89 | 53.7 | 5.14 |
| 2 | Q4KHG8_PSEF5 | outer membrane protein 85 | 87.0 | 4.67 | 78.1 | 12.69 |
| 3 | Q4K9J7_PSEF5 | ATP-dependent Clp protease | 78.6 | 4.73 | 93.6 | 18.72 |
| 4 | Q3KI85_PSEPF | NusA antitermination factor | 68.3 | 4.40 | 62.27 | 9.74 |
| 5 | Q885T1_PSESM | ribosomal protein S1 | 69.4 | 4.69 | 97.5 | 20.43 |
| 6 | Q9HV43_PSEAE | Chaperone protein DnaK protein | 73.4 | 4.73 | 76.43 | 4.71 |
| 7 | Q9HV43_PSEAE | Chaperone protein DnaK protein | 72.9 | 4.76 | 91.52 | 8.48 |
| 8 | Q4KJR8_PSEF5 | 2,3-bisphosphoglycerate-independent phosphoglycerate mutase | 68.0 | 4.85 | 60.19 | 2.14 |
| 9 | Q3KFE3_PSEPF | phosphoenolpyruvate synthase | 76.8 | 5.01 | 85‡ | 15‡ |
| 10 | Q3KFE3_PSEPF | phosphoenolpyruvate synthase | 76.6 | 5.07 | 85‡ | 15‡ |
| 11 | Q87YP3_PSESM | aconitate hydratase 2 | 81.7 | 5.17 | 77.1 | 3.23 |
| 12 | Q87YP3_PSESM | aconitate hydratase 2 | 81.1 | 5.22 | 83.17 | 7.62 |
| 13 | Q87YP3_PSESM | aconitate hydratase 2 | 81.5 | 5.27 | 77.1 | 3.23 |
| 14 | Q3KI80_PSEPF | 3' exoribonuclease | 73.3 | 5.19 | 79.38 | 10.41 |
| 15 | Q59638_PSEAE | dihydrolipoamide acetyltransferase | 72.6 | 5.26 | 79.65 | 4.2 |
| 16 | Q59638_PSEAE | dihydrolipoamide acetyltransferase | 77.0 | 5.40 | 79.65 | 4.2 |
| 17 | Q88AG3_PSESM | signal recognition particle-docking protein FtsY | 74.8 | 5.39 | 82 | 4 |
| 18 | Q1EPQ1_9PSED | heat shock protein 90 | 69.0 | 5.22 | 96.62 | 17.19 |
| 19 | Q1EPQ1_9PSED | heat shock protein 90 | 68.1 | 5.28 | 99.09 | 15.3 |
| 20 | Q1EPQ1_9PSED | heat shock protein 90 | 69.4 | 5.33 | 95.39 | 14.83 |
| 21 | Q3K7T9_PSEPF | secA protein | 87.4 | 5.71 | 102‡ | 18‡ |
| 22 | Q3KJ49_PSEPF | 2-oxo-acid dehydrogenase | 81.5 | 5.68 | 98.77 | 9.31 |
| 23 | Q3K6N3_PSEPF | chaperone clpB | 78.2 | 5.64 | 97.8 | 12.76 |
| 24 | Q3KA72_PSEPF | isocitrate dehydrogenase | 72.6 | 5.57 | 57.47 | 7.96 |
| 25 | Q3KH16_PSEPF | prolyl-tRNA synthetase | 69.4 | 5.57 | 85.19 | 12.08 |
| 26 | Q4K764_PSEF5 | chaperonin groEL protein | 62.0 | 4.83 | 97.99 | 16.82 |
| 27 | Q4K764_PSEF5 | chaperonin groEL protein | 60.9 | 4.89 | 99.75 | 36.75 |
| 28 | Q4K764_PSEF5 | chaperonin groEL protein | 60.4 | 4.96 | 97.99 | 16.82 |
| 29 | Q4K764_PSEF5 | chaperonin groEL protein | 60.5 | 5.03 | 97.99 | 16.82 |

| | | | | | | |
|---|---|---|---|---|---|---|
| 30 | Q4K4Z5_PSEF5 | anthranilate synthase | 56.3 | 5.12 | 92.94 | 15.96 |
| 31 | Q3KI28_PSEPF | aspartyl/glutamyl-tRNA aminotransferase | 55.2 | 5.14 | 84‡ | 19‡ |
| 32 | Q4K465_PSEF5 | oxidoreductase | 54.1 | 5.13 | 63.47 | 7.33 |
| 33 | Q4K9J7_PSEF5 | ATP-dependent Clp protease | 51.7 | 5.12 | 93.6 | 18.72 |
| 34 | Q3KA84_PSEPF | tRNA synthetase, class II (G, H, P and S) | 50.7 | 5.19 | 98.81 | 22.54 |
| 35 | Q4KJQ3_PSEF5 | glutamine synthetase, type I | 61.2 | 5.25 | 97.56 | 27.35 |
| 36 | Q4KAU0_PSEF5 | dipeptidase | 60.9 | 5.31 | 80.62 | 5.66 |
| 37 | Q3KJP4_PSEPF | phosphoenolpyruvate carboxykinase | 61.0 | 5.38 | 97.63 | 19.88 |
| 38 | Q4KJQ3_PSEF5 | glutamine synthetase, type I | 58.5 | 5.34 | 98.53 | 25 |
| 39 | Q4K5E6_PSEF5 | aldehyde dehydrogenase | 56.9 | 5.39 | 60.19 | 3.36 |
| 40 | Q89K44_BRAJA | ArsA | 54.8 | 5.42 | 99 | 4 |
| 41 | Q3KA64_PSEPF | isocitrate lyase | 53.2 | 5.29 | 58.69 | 4.99 |
| 42 | Q87TT2_PSESM | ATP synthase subunit alpha | 53.9 | 5.34 | 94.57 | 14.98 |
| 43 | Q87TT2_PSESM | ATP synthase subunit alpha | 53.0 | 5.46 | 100 | 38.33 |
| 44 | Q3KFH8_PSEPF | hypothetical protein | 51.1 | 5.27 | 82.14 | 5.87 |
| 45 | Q3K885_PSEPF | aldehyde dehydrogenase | 51.9 | 5.33 | 60.19 | 2.46 |
| 46 | Q4KFX1_PSEF5 | beta-ketoacyl-ACP synthase I | 48.6 | 5.36 | 84.16 | 9.85 |
| 47 | Q3KA36_PSEPF | extracellular solute-binding protein, family1 | 62.6 | 5.44 | 92.14 | 13.97 |
| 48 | Q3K7C3_PSEPF | 2-isopropylmalate synthase | 64.0 | 5.49 | 85.5 | 22 |
| 49 | Q3K4C9_PSEPF | oxaloacetate decarboxylase | 64.1 | 5.56 | 80 | 3 |
| 50 | Q3K4C9_PSEPF | oxaloacetate decarboxylase | 63.4 | 5.63 | 80 | 3 |
| 51 | Q3KA36_PSEPF | extracellular solute-binding protein, family1 | 59.4 | 5.51 | 91.9 | 8.97 |
| 52 | Q3K4N3_PSEPF | aldehyde dehydrogenase | 58.0 | 5.65 | 75.07 | 10.26 |
| 53 | Q4K602_PSEF5 | hypothetical protein | 59.5 | 5.70 | 44.32 | 2.69 |
| 54 | Q3KA28_PSEPF | cysteinyl-tRNA synthetase | 56.0 | 5.73 | 64.2 | 10 |
| 55 | Q4KKA2_PSEF5 | succinate-semialdehyde dehydrogenase | 55.1 | 5.68 | 96.18 | 14.37 |
| 56 | Q3K4N3_PSEPF | aldehyde dehydrogenase | 55.0 | 5.78 | 96.81 | 13.88 |
| 57 | Q4KGQ4_PSEF5 | protease Do subfamilly, peptidase MucD | 51.2 | 5.54 | 64.45 | 11.55 |
| 58 | Q4KI73_PSEF5 | histidinol dehydrogenase | 51.4 | 5.50 | 60.19 | 3.26 |
| 59 | Q3KA64_PSEPF | isocitrate lyase | 52.9 | 5.51 | 73.71 | 4.99 |
| 60 | Q3KHG9_PSEPF | betaine-aldehyde dehydrogenase | 54.6 | 5.52 | 74 | 8.02 |
| 61 | Q4K4H7_PSEF5 | S-adenosyl-L-homocysteine hydrolase | 55.3 | 5.56 | 77.66 | 10.66 |
| 62 | Q3KCU4_PSEPF | alpha-D-glucose phosphate-specific phosphoglucomutase | 56.6 | 5.58 | 25.56 | 2.19 |
| 63 | Q87TT2_PSESM | ATP synthase subunit alpha | 53.9 | 5.59 | 70.8 | 10.51 |
| 64 | Q3K7Y1_PSEPF | arginine deiminase | 50.5 | 5.62 | 99.27 | 27.03 |
| 65 | Q885V0_PSESM | fumarate hydratase class II | 47.7 | 5.60 | 91.16 | 10.78 |
| 66 | Q4KJ00_PSEF5 | branched-chain amino acid ABC transporter | 45.3 | 5.61 | 62.61 | 8.79 |
| 67 | Q3K7K0_PSEPF | argininosuccinate synthase | 52.1 | 5.71 | 77.93 | 7.41 |

| | | | | | | |
|---|---|---|---|---|---|---|
| 68 | Q48ED7_PSE14 | tryptophanyl-tRNA synthetase | 49.1 | 5.65 | 84.15 | 5.79 |
| 69 | Q4K517_PSEF5 | tyrosyl-tRNA sythase | 47.5 | 5.67 | 90.7 | 10.78 |
| 70 | Q4KHP9_PSEF5 | homoserine dehydrogenase | 50.6 | 5.80 | 87.01 | 8.76 |
| 71 | Q3K8X9_PSEPF | beta-ketoacyl synthase | 47.1 | 5.90 | 36.09 | 3.03 |
| 72 | Q4K9U5_PSEF5 | isocitrate dehydrogenase | 45.0 | 5.69 | 99.97 | 27.75 |
| 73 | Q4K7T2_PSEF5 | sugar ABC transporter | 45.8 | 5.78 | 99.9 | 23.26 |
| 74 | Q3KHZ4_PSEPF | UDP-N-acetylglucosamine 1-carboxyvinyltransferase | 46.3 | 5.87 | 86.56 | 11.4 |
| 75 | Q3K8L2_PSEPF | beta-ketoacyl synthase | 46.1 | 5.93 | 41.91 | 4.71 |
| 76 | Q3KE62_PSEPF | peorxidase/catalase | 75.9 | 5.71 | 75.62 | 4.37 |
| 77 | Q3KJG5_PSEPF | GTP-binding protein TypA | 72.6 | 5.69 | 95.1 | 9.9 |
| 78 | O05137_PSEFL | malate synthase G | 75.5 | 5.84 | 89.33 | 5.1 |
| 81 | Q1IBQ0_9PSED | glytaminyl-tRNA synthetase | 66.6 | 5.84 | 91.43 | 10.41 |
| 82 | Q1IBQ0_9PSED | glytaminyl-tRNA synthetase | 66.6 | 5.92 | 91.43 | 10.41 |
| 83 | Q3KIY4_PSEPF | adenylosuccinate synthase | 57.9 | 5.80 | 99.92 | 33.1 |
| 84 | Q3K8P9_PSEPF | ubiquinone oxidoreductase | 61.6 | 5.85 | 99 | 10 |
| 85 | Q886M5_PSESM | CTP synthase | 63.9 | 5.91 | 81.52 | 9.21 |
| 86 | Q1I6I3_9PSED | malate dehydrogenase | 57.4 | 5.88 | 73.68 | 4.22 |
| 87 | Q3KIP9_PSEPF | phosphoribosylaminoimidazolecarboxamide formyltransferase | 59.6 | 5.93 | 99.46 | 18.92 |
| 88 | Q3K745_PSEPF | UDP-N-acetylmuramate--L-alanine ligase | 61.0 | 6.00 | 98.57 | 25.93 |
| 89 | Q9Z9H2_PSEAE | tetrahydrodipicolinate succinylase | 60.5 | 6.07 | 75.98 | 6.4 |
| 90 | Q48P39_PSE14 | RfaE bifunctional protein | 57.0 | 6.00 | 87.68 | 10.13 |
| 91 | Q3K745_PSEPF | UDP-N-acetylmuramate--L-alanine ligase | 58.2 | 6.05 | 73.2 | 5.35 |
| 92 | Q4KFY7_PSEF5 | 2-oxoglutarate dehydrogenase | 58.3 | 6.08 | 93.6 | 19.46 |
| 93 | Q3K740_PSEPF | UDP-N-acetylmuramoylalanyl-D-glutamyl-2,6-diaminopimelate-D-alanyl-D-alanyl ligase | 54.7 | 5.87 | 22.31 | 3.3 |
| 94 | Q3KF24_PSEPF | 3-isopropylmalate dehydratase | 53.4 | 5.90 | 92.3 | 12.71 |
| 95 | Q3KJB6_PSEPF | heat shock protein HslU | 53.9 | 6.04 | 92.5 | 9.89 |
| 96 | Q3KJB6_PSEPF | heat shock protein HslU | 51.7 | 6.08 | 92.5 | 9.89 |
| 97 | Q4K526_PSEF5 | DNA-directed RNA polymerase beta subunit (RpoB) | 108.8 | 5.79 | 117‡ | 19‡ |
| 98 | A5W7L4_PSEPU | carboxyl-terminal protease | 78.2 | 6.22 | 95 | 3 |
| 99 | Q3K5S8_PSEPF | serine protein kinase PrkA | 69.5 | 6.01 | 85.74 | 10.16 |
| 100 | Q4KJM6_PSEF5 | periplasmic glucan biosynthesis protein MdoG | 70.7 | 6.07 | 61.41 | 5.25 |
| 101 | Q3K7Z2_PSEPF | 6-phosphogluconate dehydratase | 66.4 | 6.18 | 91.62 | 5.26 |
| 102 | Q4KFY7_PSEF5 | 2-oxoglutarate dehydrogenase | 58.4 | 6.22 | 95.47 | 19.46 |
| 103 | Q88Q27_PSEPK | serine hydroxymethyltransferase 2 | 49.0 | 6.22 | 92.38 | 14.39 |
| 104 | Q3K7A5_PSEPF | cysteine desulfurase IscS | 46.5 | 6.26 | 94.4 | 27.23 |
| 105 | Q3KFU9_PSEPF | 2-oxoglutarate dehydrogenase | 88.9 | 6.59 | 83.27 | 4.56 |

| | | | | | | |
|---|---|---|---|---|---|---|
| 106 | Q4KJN8_PSEF5 | urocanate hydratase | 67.4 | 6.34 | 74.19 | 6.61 |
| 107 | Q3KJX4_PSEF5 | 4-aminobutyrate aminotransferase | 50.1 | 6.34 | 99.83 | 31.76 |
| 108 | Q4K3B1_PSEF5 | bifunctional protein glmU (include UDP-N-acetylglucosamine pyrophosphorylase and glucosamine-1-phosphate N-acetyltransferase) | 54.7 | 6.39 | 91.13 | 8.79 |
| 109 | Q4ZNS7_PSEU2 | glutamyl-tRNA aminotransferase subunit A | 58.8 | 6.43 | 68.46 | 6.63 |
| 110 | Q3K7R9_PSEPF | pyruvate kinase | 62.8 | 6.51 | 97.22 | 15.53 |
| 111 | Q4KIX0_PSEF5 | biotin carboxylase | 56.8 | 6.54 | 97.17 | 14.32 |
| 112 | Q3K7C9_PSEPF | IMP dehydrogenase | 60.4 | 6.60 | 99.87 | 35.99 |
| 113 | Q3K7C9_PSEPF | IMP dehydrogenase | 59.4 | 6.66 | 49.46 | 6.95 |
| 114 | Q3KA07_PSEPF | carbamoyl-phosphate synthase L chain | 53.2 | 6.71 | 137‡ | 18‡ |
| 115 | Q4KEK5_PSEF5 | quinoprotein ethanol dehydrogenase | 63.4 | 6.86 | 98.94 | 18.44 |
| 116 | Q48FB5_PSE14 | porin D | 47.7 | 4.50 | 60.66 | 4.32 |
| 117 | Q3K9W8_PSEPF | trigger factor | 53.8 | 4.63 | 99.76 | 27.52 |
| 118 | Q4K3A9_PSEF5 | ATP synthase F1, beta subunit | 50.9 | 4.73 | 97.33 | 16.59 |
| 119 | Q4K3A9_PSEF5 | ATP synthase F1, beta subunit | 49.7 | 4.79 | 99.19 | 28.17 |
| 120 | Q3KJM1_PSEPF | porphyromonas-type peptidyl-arginine deiminase | 45.3 | 4.68 | 40.07 | 8.7 |
| 121 | Q3KBL7_PSEPF | cobalamin synthesis protein P47K | 45.9 | 4.77 | 49.9 | 7.84 |
| 122 | Q3K4R9_PSEPF | diaminopimelate decarboxylase | 43.9 | 4.74 | 93.68 | 10.6 |
| 123 | Q3KH92_PSEPF | enolase | 45.3 | 4.86 | 93.39 | 13.75 |
| 124 | Q3K6K9_PSEPF | HSR1-like GTP-binding protein | 47.9 | 4.92 | 85.53 | 11.3 |
| 125 | Q3KH92_PSEPF | enolase | 44.9 | 4.95 | 99.83 | 36.13 |
| 126 | Q3K749_PSEPF | cell division protein FtsZ | 42.5 | 4.94 | 99.99 | 49.75 |
| 127 | Q4K4I7_PSEF5 | S-adenosylmethionine synthetase | 44.5 | 5.03 | 98.26 | 14.14 |
| 128 | Q4ZNZ4_PSEU2 | cell division protein FtsA | 47.7 | 5.08 | 91.12 | 11.24 |
| 129 | Q3KI16_PSEPF | peptidase U62, modulator of DNA gyrase | 49.6 | 5.12 | 81.75 | 19.87 |
| 130 | Q1I332_9PSED | delta-aminolevulinic acid dehydratase | 42.1 | 5.08 | 58.89 | 6.55 |
| 131 | Q4KJJ6_PSEF5 | malic enzyme family protein | 44.6 | 5.09 | 99.99 | 41.94 |
| 132 | Q1IFW8_PSEE4 | translation elongation factor Tu: small GTP-binding protein domain | 43.9 | 5.16 | 99.87 | 34.26 |
| 133 | Q1IFW8_9PSED | protein chain elongation factor (EF-Tu-A) | 43.2 | 5.25 | 99.34 | 25.94 |
| 134 | Q4K4X7_PSEF5 | survival protein SurA | 46.1 | 5.29 | 66.17 | 9.09 |
| 135 | Q1IFW8_9PSED | protein chain elongation factor (EF-Tu-A) | 44.9 | 5.39 | 85 | 14.11 |
| 136 | Q3KI97_PSEPF | carbamoyl-phosphate synthase | 42.1 | 5.41 | 97.05 | 21.76 |
| 137 | Q3K650_PSEPF | 3,4-dihydroxy-2-butanone 4-phosphate synthase | 42.4 | 5.45 | 97.8 | 22.87 |
| 138 | Q4K9U5_PSEF5 | isocitrate dehydrogenase | 44.3 | 5.52 | 99.97 | 27.75 |
| 139 | Q3K6E1_PSEPF | periplasmic ligand-binding sensor protein | 33.7 | 4.16 | 85.76 | 8.73 |
| 140 | Q4KFS1_PSEF5 | uncharacterized protein | 27.0 | 4.26 | 90.24 | 32.57 |
| 141 | Q9X4L6_PSEFL | outer membrane protein F | 36.5 | 4.57 | 90.82 | 13.08 |

| | | | | | | |
|---|---|---|---|---|---|---|
| 142 | Q3K746_PSEPF | D-alanine--D-alanine ligase | 33.1 | 4.67 | 93.49 | 14.2 |
| 143 | Q3K8U2_PSEPF | histidinol-phosphate aminotransferase 2 | 39.7 | 4.71 | 57.32 | 2.97 |
| 144 | Q3K5F2_PSEPF | phosphoglycerate kinase | 38.9 | 4.78 | 98.67 | 36.69 |
| 145 | Q4ZUZ4_PSEU2 | 3-isopropylmalate dehydrogenase | 38.9 | 4.94 | 94.04 | 22.5 |
| 146 | Q3KFP5_PSEPF | exonuclease RdgC | 35.2 | 4.82 | 88.91 | 13.4 |
| 147 | Q4K8A5_PSEF5 | phosphoribosylformylglycinamidine cyclo-ligase | 36.7 | 4.92 | 94.48 | 24.43 |
| 148 | Q4KK38_PSEF5 | ACC deaminase | 34.0 | 4.82 | 84.15 | 9.06 |
| 149 | Q4KH19_PSEF5 | xenobiotic reductase B | 37.7 | 5.11 | 96.43 | 16.33 |
| 150 | Q4K759_PSEF5 | ParA family protein | 37.6 | 5.19 | 93.12 | 15.66 |
| 151 | P80064_PSEUJ | 4-hydroxyphenylpyruvate dioxygenase | 37.7 | 5.25 | 99.65 | 31.37 |
| 152 | Q4KJY3_PSEF5 | dTDP-glucose synthase | 30.9 | 4.95 | 81.9 | 16.49 |
| 153 | Q3K9Y9_PSEPF | hypothetical protein A | 28.4 | 4.99 | 77.45 | 23.93 |
| 154 | Q3KDY8_PSEPF | NmrA-like protein | 26.2 | 5.08 | 75.2 | 13.55 |
| 155 | Q886P2_PSESM | elongation factor Ts | 27.3 | 5.16 | 99.96 | 43.9 |
| 156 | Q4ZUF6_PSEU2 | electron transfer flavoprotein, alpha subunit | 28.6 | 5.25 | 98.95 | 39.48 |
| 157 | Q9KID0_PSEAE | WbjB (similar to polysaccharide biosynthesis protein) | 36.3 | 5.35 | 67.62 | 7.85 |
| 158 | Q3KC97_PSEPF | acyl-CoA dehydrogenase | 38.2 | 5.39 | 95.43 | 18.93 |
| 159 | Q3K503_PSEPF | extracellular solute-binding protein, family1 | 40.8 | 5.52 | 93.93 | 20.46 |
| 160 | Q4KCT4_PSPF5 | nonspecific acid phosphatase | 33.6 | 5.36 | 43.02 | 5.87 |
| 161 | Q9XC61_PSEAE | polysaccharide biosynthesis protein | 36.4 | 5.42 | 59.86 | 7.56 |
| 162 | Q4K8M8_PSEF5 | phosphoserine aminotransferase | 37.4 | 5.51 | 41.82 | 2.75 |
| 163 | Q48FM8_PSE14 | phosphoserine aminotransferase | 38.8 | 5.54 | 34.27 | 2.63 |
| 164 | Q4K4E7_PSEF5 | glutathione synthetase | 32.2 | 5.44 | 89.42 | 17.67 |
| 165 | Q3K9H0_PSEPF | transaldolase | 32.0 | 5.52 | 96.25 | 15.26 |
| 166 | Q4K7R2_PSEF5 | carbamate kinase | 36.4 | 5.62 | 66.64 | 12.94 |
| 167 | Q3KEZ4_PSEPF | periplasmic binding protein/LacI transcriptional regulator | 30.4 | 5.65 | 99.19 | 31.45 |
| 168 | Q3KKE0_PSEPF | coproporphyrinogen III oxidase | 28.6 | 5.39 | 82.17 | 12.83 |
| 169 | Q3KGJ2_PSEPF | dihydrodipicolinate synthase | 28.2 | 5.51 | 97.86 | 39.04 |
| 170 | Q3KFE9_PSEPF | isocitrate lyase and phosphorylmutase | 27.7 | 5.60 | 95.24 | 20.95 |
| 171 | Q88NH2_PSEPK | dihydrodipicolinate synthase | 27.0 | 5.44 | 86.68 | 13.9 |
| 172 | Q87YS1_PSESM | enoyl-(acyl-carrier-protein) reductase | 25.4 | 5.50 | 93.18 | 28.79 |
| 173 | Q3K918_PSEPF | elongation factor P | 21.4 | 4.57 | 89.98 | 26.46 |
| 174 | Q3K918_PSEPF | elongation factor P | 21.0 | 4.72 | 99.43 | 36.51 |
| 175 | Q3KG39_PSEPF | 3-oxoacyl-(acyl-carrier-protein) synthase III | 27.5 | 4.69 | 48.36 | 13.64 |
| 176 | Q3KA81_PSEPF | outer membrane lipoprotein carrier protein LolA | 23.6 | 4.51 | 93 | 12 |
| 177 | Q4KAH1_PSEF5 | YhgI protein | 18.6 | 4.32 | 36.66 | 6.7 |
| 178 | Q4K5T2_PSEF5 | peptidyl-prolyl cis-trans isomerase | 19.2 | 4.36 | 93.87 | 32.68 |

| | | | | | | |
|---|---|---|---|---|---|---|
| 179 | Q4KIH2_PSEF5 | co-chaperone GrpE | 18.2 | 4.40 | 92.2 | 35.64 |
| 180 | Q3K7U0_PSEPF | arginine biosynthesis protein | 21.3 | 4.51 | 96.15 | 8.89 |
| 181 | Q3K535_PSEPF | ribose 5-phosphate isomerase | 21.1 | 4.65 | 91.16 | 17.86 |
| 182 | Q3KEI8_PSEPF | 3-oxoacid CoA-transferase | 20.0 | 4.58 | 94.62 | 22.17 |
| 183 | Q48PT7_PSE14 | enhancing lycopene biosynthesis protein 2 | 20.3 | 4.67 | 31 | 9 |
| 184 | Q4K5D7_PSEF5 | inorganic pyrophosphatase | 18.4 | 4.60 | 99.42 | 39.42 |
| 185 | Q3KA81_PSEPF | outer membrane lipoprotein carrier protein LolA | 17.1 | 4.69 | 90.65 | 3 |
| 186 | Q3K5U7_PSEPF | ribulose-phosphate 3-epimerase | 17.9 | 4.77 | 94.21 | 40.62 |
| 188 | Q4KJU6_PSEF5 | amino acid ABC transporter | 22.7 | 4.88 | 99.3 | 32.4 |
| 189 | Q4KJS5_PSEF5 | phosphoribosylforminino-5-aminoimidazole carboxamide ribotide isomerase | 21.3 | 4.86 | 99.09 | 29.2 |
| 190 | Q3K7J6_PSEPF | alkyl hydroperoxide reductase | 17.7 | 4.93 | 97.53 | 41 |
| 191 | Q3KA62_PSEPF | ubiquinone dehydrogenase | 21.7 | 5.11 | 73.16 | 22.77 |
| 192 | Q3KF23_PSEPF | 3-isopropylmalate dehydratase | 20.5 | 5.15 | 87.37 | 35.98 |
| 193 | Q3KH03_PSEPF | extracellular solute-binding protein, family 3 | 21.0 | 5.23 | 71.7 | 10.77 |
| 194 | Q3KGN6_PSEPF | trans-aconitate methyltransferase | 20.6 | 5.30 | 57.67 | 6.25 |
| 195 | Q3KII6_PSEPF | short-chain dehydrogenase/reductase SDR | 20.2 | 5.26 | 51 | 7.36 |
| 196 | Q3KI42_PSEPF | transcriptional regulator, Fis family | 20.6 | 5.16 | 96.13 | 24.73 |
| 197 | Q3KI42_PSEPF | transcriptional regulator, Fis family | 17.8 | 5.18 | 91.3 | 30.65 |
| 198 | Q3KKE5_PSEPF | peptide deformylase | 19.3 | 5.15 | 82.91 | 23.81 |
| 199 | Q3KI45_PSEPF | hypothetical protein | 22.4 | 5.35 | 83.22 | 12.61 |
| 200 | Q4KH87_PSEF5 | amino acid ABC transporter | 20.6 | 5.44 | 99 | 25.38 |
| 201 | Q48FA2_PSE14 | ferredoxin NADP-reductase | 21.8 | 5.55 | 97.54 | 29.73 |
| 202 | Q48FA2_PSE14 | ferredoxin NADP-reductase | 22.9 | 5.59 | 98.79 | 28.96 |
| 203 | Q3KI78_PSEPF | nicotinate-nucleotide pyrophosphorylase | 23.5 | 5.62 | 95.87 | 25.18 |
| 204 | Q4KGP5_PSEF5 | phosphoribosylaminoimidazole-succinocarboxamide synthase | 21.2 | 5.63 | 91.13 | 14.35 |
| 205 | Q3KA81_PSEPF | outer membrane lipoprotein carrier LolA | 20.1 | 5.60 | 90.65 | 26.21 |
| 206 | Q3K806_PSEPF | 2-dehydro-3-deoxyphosphogluconate aldolase | 19.0 | 5.70 | 90.47 | 24.43 |
| 207 | Q3KGH2_PSEPF | nitroreductase | 18.3 | 5.63 | 85.9 | 20.3 |
| 208 | Q3K9W9_PSEPF | ATP-dependent Clp protease proteolytic subunit | 17.4 | 5.58 | 60.19 | 3.32 |
| 209 | Q3KA81_PSEPF | outer membrane lipoprotein carrier protein LolA | 17.1 | 5.73 | 96.83 | 33.01 |
| 210 | Q3K438_PSEPF | ATP synthase delta chain | 16.2 | 5.57 | 92.38 | 32.58 |
| 211 | Q3K7N1_PSEPF | superoxide dismutase | 16.3 | 5.67 | 99.86 | 50.51 |
| 212 | Q3K5F5_PSESF | fructose-bisphosphate aldolase | 43.1 | 5.75 | 94.52 | 24.86 |
| 213 | Q4K9P7_PSEF5 | isovaleryl-CoA dehydrogenase | 40.5 | 5.77 | 60.43 | 6.46 |
| 214 | Q9Z9H2_PSEAE | tetradrodipicolinate N-succinyletransferase | 37.6 | 5.88 | 75.98 | 6.4 |
| 215 | Q3K513_PSEPF | extracellular solute-binding protein, family 1 | 34.9 | 5.70 | 82.04 | 10.67 |
| 216 | Q88DZ0_PSEPK | ketol-acid reductoisomerase | 36.1 | 5.77 | 70.26 | 10.36 |

| | | | | | | |
|---|---|---|---|---|---|---|
| 217 | Q3KFX2_PSEPF | thiosulphate-binding protein | 36.6 | 5.82 | 91.77 | 22.29 |
| 218 | Q3KHP0_PSEPF | extracellular solute-binding protein, family3 | 31.4 | 5.72 | 98.37 | 22.45 |
| 219 | Q3KJE1_PSEPF | proline iminopeptidase | 34.9 | 5.91 | 74.74 | 11.46 |
| 220 | Q9RNV2_PSEAE | conserved periplasmic hypothetical protein | 29.6 | 5.91 | 60.19 | 4.01 |
| 221 | Q3KFL9_PSEPF | septum site-determining protein MinD | 24.7 | 5.70 | 99.17 | 29.7 |
| 222 | Q4K8M4_PSEF5 | 3-demethylubiquinone-9 3-methyltransferase | 25.9 | 5.84 | 84.01 | 26.29 |
| 223 | Q4K4D6_PSEF5 | pyrroline-5-carboxylate reductase | 26.5 | 5.90 | 79.78 | 11.4 |
| 224 | Q885K6_PSESM | arginine/ornithine ABC transporter | 22.9 | 5.78 | 60.19 | 5.04 |
| 225 | Q3K875_PSEPF | lysine-arginine-ornithine-binding periplasmic protein | 23.0 | 5.81 | 93.87 | 21.01 |
| 226 | Q889F9_PSESM | phosphonate ABC transporter | 22.1 | 5.82 | 92.9 | 12.37 |
| 227 | Q3KHE3_PSEPF | adenylate kinase | 22.4 | 5.86 | 93.56 | 22.69 |
| 228 | Q88NR4_PSEPK | branched-chain amino acid ABC transporter | 42.3 | 5.98 | 44.09 | 3.23 |
| 229 | Q883Z4_PSESM | succinyl-CoA synthase | 41.6 | 6.03 | 98.07 | 28.35 |
| 230 | Q3KFH7_PSEPF | periplasmic substrate-binding protein | 37.5 | 6.07 | 94 | 10 |
| 231 | Q87UJ0_PSESM | putrescine ABC transporter | 35.5 | 6.04 | 93.7 | 15.62 |
| 232 | Q3K7Y0_PSEPF | ornithine carbamoyltransferase | 42.7 | 6.18 | 97.74 | 23.81 |
| 233 | Q4ZY90_PSEU2 | thiolase | 40.5 | 6.15 | 89.57 | 6.89 |
| 234 | Q3KHG5_PSEPF | extracellular solute-binding protein, family 1 | 39.8 | 6.23 | 91.91 | 12.01 |
| 235 | Q3K6W4_PSEPF | ribose-phosphate pyrophosphokinase | 32.4 | 6.02 | 99.93 | 35.81 |
| 236 | Q4KGI7_PSEF5 | cysteine synthase A | 32.3 | 6.16 | 97.58 | 22.49 |
| 237 | Q4ZTK7_PSEU2 | AP endonuclease, family1 | 33.6 | 6.27 | 74.92 | 8.15 |
| 238 | Q6QGZ9_PSEFL | DNA-binding response regulator | 27.6 | 6.02 | 93.7 | 21.54 |
| 239 | Q3K5H9_PSEPF | ABC-type glycine betaine transport system | 27.8 | 6.16 | 99.24 | 28.25 |
| 240 | Q1IF57_9PSED | dihydrodipicolinate reductase | 25.1 | 6.12 | 79.24 | 8.24 |
| 241 | Q4KEH4_PSEF5 | arginine/ornithine ABC transporter | 22.3 | 6.07 | 99 | 25 |
| 242 | Q3KJR8_PSEPF | extracellular solute-binding protein, family 3 | 21.9 | 6.11 | 47.8 | 4.51 |
| 243 | OTCC_PSEPK | ornithine carbamoyltransferase | 44.4 | 6.34 | 97.15 | 20 |
| 244 | Q3K882_PSEPF | acetylornithine and succinylornithine aminotransferase | 44.0 | 6.41 | 74.88 | 6.9 |
| 245 | Q3KG66_PSEPF | aminotransferase | 41.8 | 6.48 | 98.92 | 19.14 |
| 246 | Q3KHG5_PSEPF | extracellular solute-binding protein, family 1 | 46.6 | 6.53 | 98.65 | 27.15 |
| 247 | O68897_PSEFA | glutaminase-asparaginase | 43.8 | 6.51 | 68.35 | 11.6 |
| 248 | Q3KIW5_PSEPF | NH(3)-dependent NAD(+) synthetase | 35.3 | 6.33 | 93.69 | 14.18 |
| 249 | Q4K7T2_PSEF5 | sugar ABC transporter | 43.9 | 6.67 | 79‡ | 14‡ |
| 250 | Q3K722_PSEPF | aldo/keto reductase | 39.1 | 6.56 | 69.66 | 12.72 |
| 251 | Q3KFJ1_PSEPF | chorismate synthase | 39.9 | 6.63 | 75.14 | 17.36 |
| 252 | Q3K5W5_PSEPF | N-acetyl-gamma-glutamyl-phosphate reductase | 41.5 | 6.68 | 99.86 | 37.21 |
| 253 | O68897_PSEFA | glutaminase-asparaginase | 40.5 | 6.74 | 97.87 | 23.76 |
| 254 | Q4KDP6_PSEF5 | branched-chain amino acid aminotransferase | 38.4 | 6.76 | 69.37 | 6.78 |

| | | | | | | |
|---|---|---|---|---|---|---|
| 255 | Q3K4Y7_PSEPF | extracellular solute-binding protein, family 1 | 32.2 | 6.51 | 92.08 | 14.37 |
| 256 | Q886M7_PSESM | acetyl-CoA carboxylase, carboxyl transferase, alpha subunit | 31.8 | 6.64 | 93.69 | 13.02 |
| 257 | Q500N5_PSEU2 | response regulator receiver:LytTr DNA-binding protein | 28.9 | 6.68 | 81.49 | 14.52 |
| 258 | Q3KK45_PSEPF | acyl-CoA dehydrogenase | 26.7 | 6.66 | 82.18 | 12.98 |
| 259 | Q88NY2_PSEPK | amino acid ABC transporter, periplasmic amino acid-binding protein | 30.0 | 6.96 | 97.94 | 21.24 |
| 260 | Q883Z3_PSESM | succinyl-CoA synthase, alpha subunit | 27.2 | 6.39 | 99.83 | 26.62 |
| 261 | Q3KHB0_PSEPF | uridylate kinase | 25.3 | 6.48 | 93.89 | 42.51 |
| 262 | Q3KIV5_PSEPF | short-chain dehydrogenase/reductase SDR | 24.9 | 6.51 | 98.71 | 35.43 |
| 263 | Q9HT68_PSEAE | TonB-dependent receptor | 22.7 | 6.29 | 47.86 | 10.77 |
| 264 | Q4K873_PSEF5 | dienelactone hydrolase family protein | 23.2 | 6.35 | 73.81 | 5.81 |
| 265 | Q88LL6_PSEPK | 3-oxoacyl-(acyl-carrier-protein) reductase | 21.5 | 6.31 | 84.15 | 9.35 |
| 266 | Q3K6W3_PSEPF | general stress protein CTC | 20.8 | 6.40 | 98.62 | 16 |
| 267 | Q88PX7_PSEPK | ribosomal 5S rRNA E-loop binding protein | 21.2 | 6.46 | 92.2 | 10.14 |
| 268 | Q88RK2_PSEPK | thiol:disulfide interchange protein, DsbA family | 19.4 | 6.44 | 60.19 | 5.24 |
| 269 | Q9HYC9_PSEAE | deoxycytidine triphosphate deaminase | 17.1 | 6.36 | 47.38 | 7.45 |
| 270 | Q4KIG6_PSEF5 | transcription elongation factor GreA | 15.1 | 5.13 | 97.02 | 38.61 |
| 271 | Q3KIP3_PSEPF | acetyl-CoA biotin carboxyl carrier | 14.4 | 4.87 | 97.55 | 32.26 |
| 272 | Q3KD94_PSEPF | thiol specific antioxidant | 13.2 | 5.02 | 87.21 | 30.72 |
| 273 | Q4K5T4_PSEF5 | alkylphosphonate utilization operon protein PhnA | 13.3 | 5.18 | 99.51 | 55.75 |
| 274 | Q3KHY1_PSEPF | peptidyl-prolyl cis-trans isomerase, FKBP type | 12.1 | 4.22 | 75.92 | 11.8 |
| 275 | Q93TF4_PSEFL | protein-export protein secB | 11.5 | 4.22 | 60.19 | 5.62 |
| 276 | Q3K9K8_PSEPF | hypothetical protein | 12.1 | 4.37 | 33.06 | 5.29 |
| 277 | Q3K9F0_PSEPF | hypothetical protein | 12.4 | 4.59 | 91.54 | 17.02 |
| 278 | Q9KGW5_PSEFL | NADH dehydrogenase I subunit E | 11.4 | 4.68 | 43.88 | 7.83 |
| 279 | Q3K4T5_PSEPF | regulator of RpoD, Rsd/AlgQ | 9.4 | 4.45 | 55.94 | 6.83 |
| 280 | Q48NZ3_PSE14 | 30S ribosomal protein S6 | 9.8 | 4.83 | 92.93 | 52.48 |
| 281 | Q1I3U3_9PSED | transcriptional regulator PyrR | 10.8 | 5.10 | 39.15 | 9.88 |
| 282 | Q1ICG2_9PSED | hypothetical protein | 6.9 | 4.33 | 80.93 | 24.47 |
| 283 | Q4K525_PSEF5 | 50S ribosomal protein L7/L12 | 5.8 | 4.42 | 92.47 | 23.97 |
| 284 | Q1I5E1_9PSED | chaperone Hsp10, affects cell division | 8.4 | 5.17 | 84.89 | 48.45 |
| 285 | Q3K7A6_PSEPF | FeS cluster assembly scaffold IscU | 8.1 | 5.21 | 92.35 | 55.47 |
| 286 | Q1EPP6_9PSED | YjgF-like protein | 7.3 | 5.16 | 99.17 | 65.87 |
| 287 | Q500B2_PSEU2 | hypothetical protein | 6.8 | 4.96 | 82.22 | 35.19 |
| 288 | Q4K525_PSEF5 | 50S ribosomal protein L7/L12 | 6.6 | 5.15 | 77.8 | 23.97 |
| 289 | Q3KG78_PSEPF | hypothetical protein | 5.8 | 4.93 | 80.75 | 19.19 |
| 290 | Q3K4W0_PSEPF | thioredoxin | 5.9 | 5.03 | 95.81 | 44.04 |

| | | | | | | |
|---|---|---|---|---|---|---|
| 291 | Q3K6R3_PSEPF | transcription regulator TraR/DksA family | 11.3 | 5.39 | 62.4 | 20.41 |
| 292 | Q4KI21_PSEF5 | ribosomal subunit interface protein | 11.1 | 5.49 | 40.86 | 8.4 |
| 293 | Q4K5F3_PSEF5 | MaoC domain protein | 10.2 | 5.55 | 84.15 | 12.58 |
| 294 | Q3KG65_PSEPF | pterin-4-alpha-carbinolamine dehydratase | 9.9 | 5.51 | 60.19 | 13.56 |
| 295 | Q4ZYW8_PSEU2 | 50S ribosomal protein L9 | 9.4 | 5.61 | 75.28 | 15.54 |
| 296 | Q3K7L5_PSEPF | 10 Kda chaperonin (protein Cpn10) (groES protein) | 8.3 | 5.53 | 93.97 | 40.21 |
| 297 | Q48LZ8_PSE14 | nucleoside diphosphate kinase | 8.7 | 5.62 | 97.78 | 46.81 |
| 298 | Q4K3B0_PSEF5 | ATP synthase F1, epsilon subunit | 7.3 | 5.53 | 93.69 | 21.99 |
| 299 | Q03456_PSEAE | ferric uptake regulation protein | 7.8 | 5.61 | 93.8 | 36.57 |
| 300 | Q9HTR6_PSEAE | nitrogen regulatory protein P-II 2 | 6.4 | 5.55 | 92.13 | 34.82 |
| 301 | Q87YQ0_PSESM | peptidyl-prolyl cis-trans isomerase B | 11.9 | 6.02 | 71.15 | 6.59 |
| 302 | Q4K5G1_PSEF5 | iojap domain protein | 11.4 | 6.10 | 48.08 | 12.14 |
| 303 | Q3KG65_PSEPF | pterin-4-alpha-carbinolamine dehydratase | 9.9 | 5.79 | 99.4 | 78.81 |
| 304 | Q3KG65_PSEPF | pterin-4-alpha-carbinolamine dehydratase | 8.5 | 5.93 | 81.59 | 45.76 |
| 305 | Q48FR2_PSE14 | methionine-R-sulfoxide reductase | 7.7 | 5.80 | 93 | 24 |
| 306 | Q880N0_PSESM | acetyltransferase, GNAT family | 7.7 | 6.00 | 17 | 5 |
| 307 | Q4K4D1_PSEF5 | hypothetical protein | 7.5 | 6.18 | 54.31 | 15.97 |
| 308 | Q9AF87_9PSED | cold acclimation protein CapB | 6.0 | 5.93 | 74.41 | 20.29 |
| 309 | Q4KEW6_PSEF5 | cold shock protein capa | 5.1 | 6.05 | 79.5 | 15.38 |
| 310 | Q886P0_PSESM | ribosome recycling protein | 16.0 | 6.56 | 46.7 | 8.65 |
| 311 | Q88BA5_PSESM | xanthine phosphoribosyltransferase | 15.0 | 6.31 | 24.82 | 11.64 |
| 312 | Q889U1_PSESM | single strand DNA-binding protein | 14.1 | 6.32 | 46.84 | 16.93 |
| 313 | Q3K5D3_PSEPF | YceI protein | 14.6 | 6.92 | 84.14 | 15.38 |
| 314 | Q4ZPR6_PSEU2 | peptidyl-prolyl cis-trans isomerase, cyclophilin type | 11.7 | 6.73 | 12.33 | 8.56 |
| 315 | Q3K652_PSEPF | NusB antitermination factor | 10.9 | 6.36 | 90.84 | 23.49 |
| 316 | AZUR_PSEFC | azurin | 10.1 | 6.81 | 83.55 | 19.53 |
| 317 | Q4KFC6_PSEF5 | universal stress protein | 8.4 | 6.32 | 78.23 | 20.69 |
| 318 | AZUR_PSEFC | azurin | 8.5 | 6.71 | 80 | 24 |
| 319 | P72191_PSEFR | temperature acclimation protein A | 5.9 | 6.74 | 47.66 | 16.95 |
| 320 | Q51455_PSEAE | chemotactic responsor CheY | 5.4 | 6.40 | 33.02 | 19.35 |
| 321 | Q9HV43_PSEAE | Chaperone protein DnaK protein | 73.6 | 4.80 | 98 | 5 |
| 322 | Q48PI5_PSE14 | heat shock protein HslVU, ATPase subunit HslU | 50.1 | 6.13 | 82.26 | 7.64 |
| 323 | Q48JF9_PSE14 | UTP-glucose-1-phosphate uridylyltransferase | 24.0 | 5.41 | 72.17 | 15.41 |
| 324 | Q3K964_PSEPF | MOSC domain | 25.1 | 5.23 | 60 | 7 |
| 325 | Q3K8T5_PSEPF | HAD-superfamily hydrolase subfamily IA, variant 1 and 3 | 19.7 | 4.51 | 75.43 | 9.42 |
| 326 | Q4KB85_PSEF5 | lactoylglutathione lyase | 15.5 | 5.29 | 39 | 5 |
| 327 | Q4KGZ6_PSEF5 | ThiJ/PfpI family protein | 17.2 | 5.85 | 46.41 | 6.74 |
| 328 | Q4K3V8_PSEF5 | hypothetical protein | 6.9 | 4.38 | 95 | 14 |

| | | | | | | |
|---|---|---|---|---|---|---|
| 329 | Q4KFF9_PSEF5 | hypothetical protein | 6.1 | 4.87 | 92.97 | 23.42 |

*The protein identity, accession number, score, and percentage sequence coverage (SC) were determined from the top MSDB database match using PEAKS software.

†MW and p*I* were estimated from gel locations of proteins and compared to expected values.

‡these proteins were only identified by PMF. The scores and sequences coverage were exported by Mascot.

§Spots number 79, 80, and 187 were artifacts and have been omitted.

## References


Abeles, F.B., Morgan, P.W., Saltveit, Jr. M.E., 1992. Ethylene in plant biology. Academic Press, New York.

Aebersold, R., Mann, M., 2003. Mass spectrometry-based proteomics. Nature 422, 198-207.

Aebersold, R., 2003. Constellations in a cellular universe. Nature 422, 115-116.

Alban, A., David, S.O., Bjorkesten, L., Andersson, C., Sloge, E., Lewis, S., Currie, I., 2003. A novel experimental design for comparative two-dimensional gel analysis: Two-dimensional difference gel electrophoresis incorporating a pooled internal standard. Proteomics 3, 36-44.

Alloisio, N., Felix, S., Marechal, J., Pujic, P., Rouy, Z., Vallenet, D., Medigue, C., Normand, P., 2007. *Frankia alni* proteome under nitrogen-fixing and nitrogen-replete conditions. Physiologia Plantarum 130, 440-453.

America, A.H., Cordewener, J.H., 2008. Comparative LC-MS: a landscape of peaks and valleys. Proteomics 8, 731-749.

Anderson, N.L., Anderson, N.G., Pearson, T.W., Borchers, C.H., Paulovich, A.G., Patterson, S.D., Gillette, M., Aebersold, R., Carr, S.A., 2009. A human proteome detection and quantitation project. Molecular Cellular Proteomics 8, 883-886.

Andrianopoulos, A., Kourambas, S., Sharp, J.A., Davis, M.A., Hynes, M.J., 1998. Characterization of the *Aspergillus nidulans nmrA* gene involved in nitrogen metabolite repression. Journal of Bacteriology 180, 1973-1977.

Arsene, C.G., Ohlendorf, R., Burkitt, W., Pritchard, C., Henrion, A., O'Connor, G., Bunk,

D.M., Guttler, B., 2008. Protein quantification by isotope dilution mass spectrometry of proteolytic fragments: cleavage rate and accuracy. Analytical Chemistry 80, 4154-4160.

Babujee, L., Venkatesh, B., Yamazaki, A., Tsuyumu, S., 2007. Proteomic analysis of the carbonate insoluble outer membrane fraction of the soft-rot pathogen *Dickeya dadantii* (syn. *Erwinia chrysanthemi*) strain 3937. Journal of Proteome Research 6, 62-69.

Bacilio, M., Rodriguez, H., Moreno, M., Hernandez, J.P., Bashan, Y., 2004. Mitigation of salt stress in wheat seedlings by a *gfp*-tagged *Azospirillum lipoferum*. Biology and Fertility of Soils 40, 188-193.

Bagnarol, E., Popovici, J., Alloisio, N., Marechal, J., Pujic, P., Normand, P., Fernandez, M.P., 2007. Differential *Frankia* protein patterns induced by phenolic extracts from Myricaceae seeds. Physiologia Plantarum 130, 380-390.

Bairoch, A., Apweiler, R., 1997. The SWISS-PROT protein sequence data bank and its supplement TrEMBL. Nucleic Acids Research 25, 31-36.

Bais, H.P., Prithiviraj, B., Jha, A.K., Ausubel, F.M., Vivanco, J.M., 2005. Mediation of pathogen resistance by exudation of antimicrobials from roots. Nature 434, 217-221.

Bantscheff, M., Schirle, M., Sweetman, G., Rick, J., Kuster, B., 2007. Quantitative mass spectrometry in proteomics: a critical review. Analytical Bioanalytical Chemistry 389, 1017-1031.

Barassi, C.A., Ayrault, G., Creus, C.M., Sueldo, R.J., Sobrero, M.T., 2006. Seed inoculation with *Azospirillum* mitigates NaCl effects on lettuce. Scientia Horticulturae 109, 8-14.

Bateman, R.H., Carruthers, R., Hoyes, J.B., Jones, C., Langridge, J.I., Millar, A., Vissers, J.P.,

2002. A novel precursor ion discovery method on a hybrid quadrupole orthogonal acceleration time-of-flight (Q-TOF) mass spectrometer for studying protein phosphorylation. Journal of American Society of Mass Spectrometry 13, 792-803.

Belimov, A.A., Safronova, V.I., Sergeyeva, T.A., Egorova, T.N., Matveyeva, V.A., Tsyganov, V.E., Borisov, A.Y., Tikhonovich, I.A., Kluge, C., Preisfeld, A., Dietz, K.J., Stepanok, V.V., 2001. Characterization of plant growth promoting rhizobacteria isolated from polluted soils and containing 1-aminocyclopropane-1-carboxylate deaminase. Canadian Journal of Microbiology 47, 642-652.

Benschop, J.J., Mohammed, S., O'Flaherty, M., Heck, A.J., Slijper, M., Menke, F.L., 2007. Quantitative phosphoproteomics of early elicitor signaling in *Arabidopsis*. Molecular Cellular Proteomics 6, 1198-1214.

Beynon, R.J., Doherty, M.K., Pratt, J.M., Gaskell, S.J., 2005. Multiplexed absolute quantification in proteomics using artificial QCAT proteins of concatenated signature peptides. Nature Methods 2, 587-589.

Bittel, C., Tabares, L.C., Armesto, M., Carrillo, N., Cortez, N., 2003. The oxidant-responsive diaphorase of *Rhodobacter capsulatus* is a ferredoxin (flavodoxin)-NADP(H) reductase. FEBS Letters 553, 408-412.

Boeckmann, B., Bairoch, A., Apweiler, R., Blatter, M.C., Estreicher, A., Gasteiger, E., Martin, M.J., Michoud, K., O'Donovan, C., Phan, I., Pilbout, S., Schneider, M., 2003. The SWISS-PROT protein knowledgebase and its supplement TrEMBL in 2003. Nucleic Acids Research 31, 365-370.

Bradford, M. 1976. A rapid and sensitive method for the quantification of microgram quantities of protein utilizing the principle of protein-dye binding. Analytical Biochemistry 72, 248-254.

Brun, V., Masselon, C., Garin, J., Dupuis, A., 2009. Isotope dilution strategies for absolute quantitative proteomics. Journal of Proteomics 72, 740-749.

Bunik, V.I., 2003a. 2-Oxo acid dehydrogenase complexes in redox regulation. European Journal of Biochemistry 270, 1036-1042.

Bunik, V.I., 2003b. 2-Oxo acid dehydrogenase complexes of multicellular organisms. European Journal of Biochemistry 270, 1035.

Burd, G.I., Dixon, D.G., Glick, B.R., 2000. Plant growth-promoting bacteria that decrease heavy metal toxicity in plants. Canadian Journal of Microbiology 46, 237-245.

Caldelari, I., Mann, S., Crooks, C., Palmer, T., 2006. The Tat pathway of the plant pathogen *Pseudomonas syringae* is required for optimal virulence. Molecular Plant-Microbe Interactions 19, 200-212.

Cecconi, D., Orzetti, S., Vandelle, E., Rinalducci, S., Zolla, L., Delledonne, M., 2009. Protein nitration during defense response in *Arabidopsis thaliana*. Electrophoresis 30, 2460-2468.

Chelius, D., Bondarenko, P.V., 2002. Quantitative profiling of proteins in complex mixtures using liquid chromatography and mass spectrometry. Journal of Proteome Research 1, 317-323.

Chen, D.Z., Patel, D.V., Hackbarth, C.J., Wang, W., Dreyer, G., Young, D.C., Margolis, P.S., Wu, C., Ni, Z.J., Trias, J., White, R.J., Yuan, Z., 2000. Actinonin, a naturally occurring antibacterial agent, is a potent deformylase inhibitor. Biochemistry 39, 1256-1262.

Cheng, Z., Park, E., Glick, B.R., 2007. 1-Aminocyclopropane-1-carboxylate deaminase from *Pseudomonas putida* UW4 facilitates the growth of canola in the presence of salt. Canadian Journal of Microbiology 53, 912-918.

Cheng, Z., Duncker, B.P., McConkey, B.J., Glick, B.R., 2008. Transcriptional regulation of ACC deaminase expression in *Pseudomonas putida* UW4. Canadian Journal of Microbiology 54, 128-136.

Cheng, Z., Duan, J., Hao, Y., McConkey, B.J., Glick, B.R., 2009a. Identification of bacterial proteins mediating the interactions between *Pseudomonas putida* UW4 and *Brassica napus* (Canola). Molecular Plant-Microbe Interactions 22, 686-694.

Cheng, Z., Wei, C.Y.-Y., Sung, W.W.L., Glick, B.R., McConkey, B.J., 2009b. Proteomic analysis of the response of the plant growth-promoting bacterium *Pseudomonas putida* UW4 to nickel stress. Proteome Science 7, 18.

Cheng, Z., Woody, O.Z., Song, J., Glick, B.R., McConkey, B.J., 2009c. Proteome reference map for the plant growth-promoting bacterium *Pseudomonas putida* UW4. Proteomics 9, 4271-4274.

Coaker, G.L., Willard, B., Kinter, M., Stockinger, E.J., Francis, D.M., 2004. Proteomic analysis of resistance mediated by Rcm 2.0 and Rcm 5.1, two loci controlling resistance to bacterial canker of tomato. Molecular Plant-Microbe Interactions 17, 1019-1028.

Corthals, G.L., Wasinger, V.C., Hochstrasser, D.F., Sanchez, J., 2000. The dynamic range of protein expression: A challenge for proteomic research. Electrophoresis 21, 1104-1115.

Corzett, T.H., Fodor, I.K., Choi, M.W., Walsworth, V.L., Chromy, B.A., Turteltaub, K.W., McCutchen-Maloney, S.L., 2006. Statistical analysis of the experimental variation in the

proteomic characterization of human plasma by two-dimensional difference gel electrophoresis. Journal of Proteome Research 5, 2611-2619.

Cowan, S.W., Garavito, R.M., Jansonius, J.N., Jenkins, J.A., Karlsson, R., Konig, N., Pai, E.F., Pauptit, R.A., Rizkallah, P.J., Rosenbusch, J.P., Rummel, G., Schirmer, T., 1995. The structure of OmpF porin in a tetragonal crystal form. Structure 3, 1041-1050.

Cravatt, B.F., Simon, G.M., Yates 3rd, J.R., 2007. The biological impact of mass-spectrometry-based proteomics. Nature 450, 991-1000.

Culotta, V.C., 2000. Superoxide dismutase, oxidative stress, and cell metabolism. Current Topics in Cellular Regulation 36, 117-132.

Culotta, V.C., Yang, M., O'Halloran, T.V., 2006. Activation of superoxide dismutases: putting the metal to the pedal. Biochimica et Biophysica Acta 1763, 747-758.

Dancik, V., Addona, T.A., Clauser, K.R., Vath, J.E., Pevzner, P.A., 1999. De novo peptide sequencing via tandem mass spectrometry. Journal of Computational Biology 6, 327-342.

de Hoog, C.L., Mann, M., 2004. Proteomics. Annual Review of Genomics and Human Genetics 5, 267-293.

de Weert, S., Vermeiren, H., Mulders, I.H., Kuiper, I., Hendrickx, N., Bloemberg, G.V., Vanderleyden, J., De Mot, R., Lugtenberg, B.J., 2002. Flagella-driven chemotaxis towards exudate components is an important trait for tomato root colonization by *Pseudomonas fluorescens*. Molecular Plant Microbe Interactions 15, 1173-1180.

Dekkers, L.C., van der Bij, A.J., Mulders, I.H., Phoelich, C.C., Wentwoord, R.A., Glandorf, D.C., Wijffelman, C.A., and Lugtenberg, B.J., 1998. Role of the O-antigen of lipopolysaccharide, and possible roles of growth rate and of NADH:ubiquinone

oxidoreductase (nuo) in competitive tomato root-tip colonization by *Pseudomonas fluorescens* WCS365. Molecular Plant-Microbe Interactions 11, 763-771.

DeSouza, L., Diehl, G., Rodrigues, M.J., Guo, J., Romaschin, A.D., Colgan, T.J., Siu, K.W., 2005. Search for cancer markers from endometrial tissues using differentially labeled tags iTRAQ and cICAT with multidimensional liquid chromatography and tandem mass spectrometry. Journal of Proteome Research 4, 377-386.

Ding, X., Richter, T., Chen, M., Fujii, H., Seo, Y. S., Xie, M., Zheng, X., Kanrar, S., Stevenson, R.A., Dardick, C., Li, Y., Jiang, H., Zhang, Y., Yu, F., Bartley, L.E., Chern, M., Bart, R., Chen, X., Zhu, L., Farmerie, W.G., Gribskov, M., Zhu, J.K., Fromm, M.E., Ronald, P.C., Song, W.Y. 2009. A rice kinase-protein interaction map. Plant Physiology 149, 1478-1492.

Djordjevic, M.A., 2004. *Sinorhizobium meliloti* metabolism in the root nodule: a proteomic perspective. Proteomics 4, 1859-1872.

Djordjevic, M.A., Chen, H.C., Natera, S., Van Noorden, G., Menzel, C., Taylor, S., Renard, C., Geiger, O., Weiller, G. F., 2003. A global analysis of protein expression profiles in *Sinorhizobium meliloti*: discovery of new genes for nodule occupancy and stress adaptation. Molecular Plant Microbe Interactions 16, 508-524.

Domon, B., Aebersold, R., 2006. Mass spectrometry and protein analysis. Science 312, 212-217.

Dong, M.Q., Venable, J.D., Au, N., Xu, T., Park, S.K., Cociorva, D., Johnson, J.R., Dillin, A., Yates 3rd, J.R., 2007. Quantitative mass spectrometry identifies insulin signaling targets in *C. elegans*. Science 317, 660-663.

Duche, O., Tremoulet, F., Glaser, P., Labadie, J., 2002. Salt stress proteins induced in *Listeria monocytogenes*. Applied and Environmental Microbiology 68, 1491-1498.

Dupuis, A., Hennekinne, J.A., Garin, J., Brun, V., 2008. Protein Standard Absolute Quantification (PSAQ) for improved investigation of staphylococcal food poisoning outbreaks. Proteomics 8, 4633-4636.

Ekman, M., Tollback, P., Klint, J., Bergman, B., 2006. Protein expression profiles in an endosymbiotic cyanobacterium revealed by a proteomic approach. Molecular Plant Microbe Interactions 19, 1251-1261.

Eltayeb, A.E., Kawano, N., Badawi, G.H., Kaminaka, H., Sanekata, T., Shibahara, T., Inanaga, S., Tanaka, K., 2007. Overexpression of monodehydroascorbate reductase in transgenic tobacco confers enhanced tolerance to ozone, salt and polyethylene glycol stresses. Planta 225, 1255-1264.

Eng, J.K., McCormack, A.L., Yates 3rd, J.R., 1994. An approach to correlate tandem mass spectral data of peptides with amino acid sequences in a protein database. Journal of the American Society for Mass Spectrometry 5, 976-989.

Etzler, M.E., 1985. Plant lectins: molecular and biological aspects. Annuual Review of Plant Physiology 36:209-234.

Farwell, A.J., Vesely, S., Nero, V., Rodriguez, H., McCormack, K., Shah, S., Dixon, D.G., Glick, B.R., 2007. Tolerance of transgenic canola plants (*Brassica napus*) amended with plant growth-promoting bacteria to flooding stress at a metal-contaminated field site. Environmental Pollution 147, 540-545.

Fenyo, D., Qin, J., Chait, B.T., 1998. Protein identification using mass spectrometric

information. Electrophoresis 19, 998-1005.

Figueira, E.M., Lima, A.I., Pereira, S.I., 2005. Cadmium tolerance plasticity in *Rhizobium leguminosarum* bv. *viciae*: glutathione as a detoxifying agent. Canadian Journal of Microbiology 51, 7-14.

Frommer, W.B., Ludewig, U., Rentsch, D., 1999. Taking transgenic plants with a pinch of salt. Science 285, 1222-1223.

Gamalero, E., Berta, G., Massa, N., Glick, B. R., Lingua, G., 2008. Synergistic interactions between the ACC deaminase-producing bacterium *Pseudomonas putida* UW4 and the AM fungus *Gigaspora rosea* positively affect cucumber plant growth. FEMS Microbiology Ecology 64, 459-467.

Gao, M., D'Haeze, W., De Rycke, R., Wolucka, B., Holsters, M., 2001. Knockout of an azorhizobial dTDP-L-rhamnose synthase affects lipopolysaccharide and extracellular polysaccharide production and disables symbiosis with *Sesbania rostrata*. Molecular Plant-Microbe Interactions 14, 857-866.

Gardan, R., Duche, O., Leroy-Setrin, S., Labadie, J., 2003. Role of *ctc* from *Listeria monocytogenes* in osmotolerance. Applied and Environmental Microbiology 69, 154-161.

Gasteiger, E., Gattiker, A., Hoogland, C., Ivanyi, I., Appel, R.D., Bairoch, A., 2003. ExPASy: The proteomics server for in-depth protein knowledge and analysis. Nucleic Acids Research 31, 3784-3788.

Gerber, S.A., Rush, J., Stemman, O., Kirschner, M.W., Gygi, S.P., 2003. Absolute quantification of proteins and phosphoproteins from cell lysates by tandem MS. Proceedings in National Academy of Science USA 100, 6940-6945.

Gerber, I.B., Laukens, K., De Vijlder, T., Witters, E., Dubery, I.A., 2008. Proteomic profiling of cellular targets of lipopolysaccharide-induced signalling in *Nicotiana tabacum* BY-2 cells. Biochimica et Biophysica Acta 1784, 1750-1762.

Gillette, M.A., Mani, D.R., Carr, S.A., 2005. Place of pattern in proteomic biomarker discovery. Journal of Proteome Research 4, 1143-1154.

Gingras, A.C., Gstaiger, M., Raught, B., Aebersold, R., 2007. Analysis of protein complexes using mass spectrometry. Nature Review Molecular Cellular Biology 8, 645-654.

Glick, B.R., 1995. The enhancement of plant growth by free-living bacteria. Canadian Journal of Microbiology 41, 109-117.

Glick, B.R., 2005. Modulation of plant ethylene levels by the bacterial enzyme ACC deaminase. FEMS Microbiology Letters 251, 1-7.

Glick, B.R., 2010. Using soil bacteria to facilitate phytoremediation. Biotechnology Advances in press.

Glick, B.R., Karaturovic, D., Newell, P., 1995. A novel procedure for rapid isolation of plant growth-promoting rhizobacteria. Canadian Journal of Microbiology 41, 533-536.

Glick, B.R., Liu, C., Ghosh, S., Dumbroff, E.B., 1997. Early development of canola seedlings in the presence of the plant growth-promoting rhizobacterium *Pseudomonas putida* GR12-2. Soil Biology and Biochemistry 29, 1233-1239.

Glick, B.R., Penrose, D.M., Li, J., 1998. A model for the lowering of plant ethylene concentrations by plant growth-promoting bacteria. Journal of Theoretical Biology 190, 63-68.

Glick, B.R., Cheng, Z., Czarny, J., Duan, J., 2007a. Promotion of plant growth by ACC

deaminase-producing soil bacteria. European Journal of Plant Pathology 119, 329-339.

Glick, B.R., Todorovic, B., Czarny, J., Cheng, Z., Duan, J., McConkey, B., 2007b. Promotion of plant growth by bacterial ACC deaminase. Critical Review in Plant Sciences 26, 227 - 242.

Görg, A., Postel, W., Günther, S., 1988. Two-dimensional electrophoresis. The current state of two-dimensional electrophoresis with immobilized pH gradients. Electrophoresis 9, 531-546.

Görg, A., Boguth, G., Obermaier, C., Posch, A., Weiss, W., 1995. Two-dimensional polyacrylamide gel electrophoresis with immobilized pH gradients in the first dimension (IPG-Dalt): The state of the art and the controversy of vertical versus horizontal systems. Electrophoresis 16, 1079-1086.

Görg, A., Obermaier, C., Boguth, G., Csordas, A., Diaz, J.-J., Madjar, J.-J., 1997. Very alkaline immobilized pH gradients for two-dimensional electrophoresis of ribosomal and nuclear proteins. Electrophoresis 18, 328-337.

Görg, A., Boguth, G., Obermeier, C., Weiss, W., 1998. Two-dimensional electrophoresis of proteins in an immobilized pH 4-12 gradient. Electrophoresis 19, 1516-1519.

Görg, A., Obermaier, C., Boguth, G., Weiss, W., 1999. Recent developments in two-dimensional gel electrophoresis with immobilized pH gradients: Wide pH gradients up to pH 12, longer separation distances and simplified procedures. Electrophoresis 20, 712-717.

Görg, A., Obermaier, C., Boguth, G., Harder, A., Scheibe, B., Wildgruber, R., Weiss, W., 2000. The current state of two-dimensional electrophoresis with immobilized pH gradients.

Electrophoresis 21, 1037-1053.

Görg, A., Drews, O., Lück, C., Weiland, F., Weiss, W., 2009. 2-DE with IPGs. Electrophoresis 30, S122-S132.

Gourion, B., Rossignol, M., Vorholt, J.A., 2006. A proteomic study of *Methylobacterium extorquens* reveals a response regulator essential for epiphytic growth. Proceedings in National Academy of Science USA 103, 13186-13191.

Grichko, V.P., Glick, B.R., 2000. Identification of DNA sequences that regulate the expression of the *Enterobacter cloacae* UW4 1-aminocyclopropane-1-carboxylic acid deaminase gene. Canadian Journal of Microbiology 46, 1159-1165.

Grichko, V.P., Glick, B.R., 2001. Amelioration of flooding stress by ACC deaminase-containing plant growth-promoting bacteria. Plant Physiology and Biochemistry 39, 11-17.

Grison, R., Grezes-Besset, B., Schneider, M., Lucante, N., Olsen, L., Leguay, J.J., Toppan, A., 1996. Field tolerance to fungal pathogens of *Brassica napus* constitutively expressing a chimeric chitinase gene. Nature Biotechnology 14, 643-646.

Gstaiger, M., Aebersold, R., 2009. Applying mass spectrometry-based proteomics to genetics, genomics and network biology. Nature Review Genetics 10, 617-627.

Guerrera, I.C., Kleiner, O., 2005. Application of mass spectrometry in proteomics. Bioscience Reports 25, 71-93.

Gurska, J., Wang, W., Gerhardt, K.E., Khalid, A.M., Isherwood, D.M., Huang, X.-D., Glick, B.R., Greenberg, B.M., 2009. Field test of a multi-process phytoremediation system at a petroleum sludge contaminated land farm. Environmental Science & Technology 43, 4472-4479.

Gygi, S.P., Aebersold, R., 2000. Mass spectrometry and proteomics. Current Opinion in Chemical Biology 4, 489-494.

Gygi, S.P., Rist, B., Gerber, S.A., Turecek, F., Gelb, M.H., Aebersold, R., 1999. Quantitative analysis of complex protein mixtures using isotope-coded affinity tags. Nature Biotechnology 17, 994-999.

Hamdia, M., Shaddad, M.A.K., Doaa, M.M., 2004. Mechanisms of salt tolerance and interactive effects of *Azospirillum brasilense* inoculation on maize cultivars grown under salt stress conditions. Plant Growth and Regulation 44, 165-174.

Hammad, Y., Marechal, J., Cournoyer, B., Normand, P., Domenach, A.M., 2001. Modification of the protein expression pattern induced in the nitrogen-fixing actinomycete *Frankia* sp. strain ACN14a-tsr by root exudates of its symbiotic host *Alnus glutinosa* and cloning of the *sodF* gene. Canadian Journal of Microbiology 47, 541-547.

Han, X., Aslanian, A., Yates 3rd, J.R., 2008. Mass spectrometry for proteomics. Current Opinion in Chemical Biology 12, 483-490.

Hanahan, D., 1983. Studies on transformation of *Escherichia coli* with plasmids. Journal of Molecular Biology 166, 557-580.

Hao, Y., Charles, T.C. Glick, B.R., 2007. ACC deaminase from plant growth promoting bacteria affects crown gall development. Canadian Journal of Microbiology 53, 1291-1299.

Havlis, J., Shevchenko, A., 2004. Absolute quantification of proteins in solutions and in polyacrylamide gels by mass spectrometry. Analytical Chemistry 76, 3029-3036.

Hoa, L.T.P., Nomura, M., Kajiwara, H., Day, D.A., Tajima, S., 2004a. Proteomic analysis on symbiotic differentiation of mitochondria in soybean nodules. Plant Cell Physiology 45,

300-308.

Hoa, L.T.P., Nomura, M., Tajima, S., 2004b. Characterization of bacteroid proteins in soybean nodules formed with *Bradyrhizobium japonicum* USDA110. Microbes and Environments 19, 71-75.

Holguin, G., Glick, B.R., 2001. Expression of the ACC deaminase gene from *Enterobacter cloacae* UW4 in *Azospirillum brasilense*. Microbial Ecology 41, 281-288.

Hontzeas, N., Richardson, A.O., Belimov, A., Safronova, V., Abu-Omar, M.M., Glick, B.R., 2005. Evidence for horizontal transfer of 1-aminocyclopropane-1-carboxylate deaminase genes. Applied and Environmental Microbiology 71, 7556-7558.

Hoogland, C., Mostaguir, K., Appel, R.D., Lisacek, F., 2008. The World-2DPAGE Constellation to promote and publish gel-based proteomics data through the ExPASy server. Journal of Proteomics 71, 245-248.

Hopfgartner, G., Varesio, E., Tschappat, V., Grivet, C., Bourgogne, E., Leuthold, L.A., 2004. Triple quadrupole linear ion trap mass spectrometer for the analysis of small molecules and macromolecules. Journal of Mass Spectrometry 39, 845-855.

Hoving, S., Gerrits, B., Voshol, H., Müller, D., Roberts, R.C., van Oostrum, J., 2002. Preparative two-dimensional gel electrophoresis at alkaline pH using narrow range immobilized pH gradients. Proteomics 2, 127-134.

Hu, P., Brodie, E.L., Suzuki, Y., McAdams, H.H., Andersen, G.L., 2005. Whole-genome transcriptional analysis of heavy metal stresses in *Caulobacter crescentus*. Journal of Bacteriology 187, 8437-8449.

Huang, X.D., El-Alawi, Y., Penrose, D.M., Glick, B.R., Greenberg, B.M., 2004. A multi-process phytoremediation system for removal of polycyclic aromatic hydrocarbons from contaminated soils. Environmental Pollution 130, 465-476.

Hughes, V., Smith, S., Garcia-Sanchez, A., Sales, J., Stevenson, K., 2007. Proteomic comparison of *Mycobacterium avium* subspecies *paratuberculosis* grown *in vitro* and isolated from clinical cases of ovine paratuberculosis. Microbiology 153, 196-205.

Hunt, D.F., Shabanowitz, J., Yates 3rd, J.R., Zhu, N.Z., Russell, D.H., Castro, M.E., 1987. Tandem quadrupole fourier-transform mass spectrometry of oligopeptides and small proteins. Proceedings of the National Academy of Sciences of the United States of America 84, 620-623.

Ishihama, Y., Oda, Y., Tabata, T., Sato, T., Nagasu, T., Rappsilber, J., Mann, M., 2005. Exponentially modified protein abundance index (emPAI) for estimation of absolute protein amount in proteomics by the number of sequenced peptides per protein. Molecular Cellular Proteomics 4, 1265-1272.

Jensen, O.N., 2004. Modification-specific proteomics: characterization of post-translational modifications by mass spectrometry. Current Opinion in Chemical Biology 8, 33-41.

Jensen, O.N., 2006. Interpreting the protein language using proteomics. Nature Review Molecular Cellular Biology 7, 391-403.

Johnson, K.L., Muddiman, D.C., 2004. A method for calculating $^{16}O/^{18}O$ peptide ion ratios for the relative quantification of proteomes. Journal of American Society of Mass Spectrometry 15, 437-445.

Jones, A.M., Thomas, V., Truman, B., Lilley, K., Mansfield, J., Grant, M., 2004. Specific

changes in the *Arabidopsis* proteome in response to bacterial challenge: differentiating basal and *R*-gene mediated resistance. Phytochemistry 65, 1805-1816.

Jones, A.M., Bennett, M.H., Mansfield, J.W., Grant, M., 2006a. Analysis of the defence phosphoproteome of *Arabidopsis thaliana* using differential mass tagging. Proteomics 6, 4155-4165.

Jones, A.M., Thomas, V., Bennett, M.H., Mansfield, J., Grant, M., 2006b. Modifications to the *Arabidopsis* defense proteome occur prior to significant transcriptional change in response to inoculation with *Pseudomonas syringae*. Plant Physiology 142, 1603-1620.

Jones, J.D., Dangl, J.L., 2006. The plant immune system. Nature 444, 323-329.

Jorrín-Novoa, J.V., Maldonadoa, A.M., Echevarría-Zomeñoa, S., Valledorb, L., Castillejoa, M.A., Curtoa, M., Valeroa, J., Sghaiera, B., Donosoa, G., Redondoa, I., 2009. Plant proteomics update (2007–2008): Second-generation proteomic techniques, an appropriate experimental design, and data analysis to fulfill MIAPE standards, increase plant proteome coverage and expand biological knowledge. Journal of Proteomics 72, 285-314.

Kamilova, F., Kravchenko, L.V., Shaposhnikov, A.I., Azarova, T., Makarova, N., Lugtenberg, B., 2006. Organic acids, sugars, and L-tryptophane in exudates of vegetables growing on stonewool and their effects on activities of rhizosphere bacteria. Molecular Plant Microbe Interactions 19, 250-256.

Karas, M., Hillenkamp, F., 1988. Laser desorption ionization of proteins with molecular masses exceeding 10,000 daltons. Analytical Chemistry 60, 2299-2301.

Karp, N.A., Kreil, D.P., Lilley, K.S., 2004. Determining a significant change in protein expression with DeCyder during a pairwise comparison using two-dimensional difference

gel electrophoresis. Proteomics 4, 1421-1432.

Karp, N.A., Griffin, J.L., Lilley, K.S., 2005. Application of partial least squares discriminant analysis to two-dimensional difference gel studies in expression proteomics. Proteomics 5, 81-90.

Karp, N.A., McCormick, P.S., Russell, M.R., Lilley, K.S., 2007. Experimental and statistical considerations to avoid false conclusions in proteomics studies using differential in-gel electrophoresis. Molecular and Cellular Proteomics 6, 1354-1364.

Kazemi-Pour, N., Condemine, G., Hugouvieux-Cotte-Pattat, N., 2004. The secretome of the plant pathogenic bacterium *Erwinia chrysanthemi*. Proteomics 4, 3177-3186.

Kim, J.Y., Park, S.J., Jang, B., Jung, C.H., Ahn, S.J., Goh, C.H., Cho, K., Han, O., Kang, H., 2007. Functional characterization of a glycine-rich RNA-binding protein 2 in *Arabidopsis thaliana* under abiotic stress conditions. Plant Journal 50, 439-451.

Kirkpatrick, D.S., Gerber, S.A., Gygi, S.P., 2005. The absolute quantification strategy: a general procedure for the quantification of proteins and post-translational modifications. Methods 35, 265-273.

Kiss, E., Huguet, T., Poinsot, V., Batut, J., 2004. The *typA* gene is required for stress adaptation as well as for symbiosis of *Sinorhizobium meliloti* 1021 with certain *Medicago truncatula* lines. Molecular Plant-Microbe Interactions 17, 235-244.

Klose, J., 1975. Protein mapping by combined isoelectric focusing and electrophoresis of mouse tissues. A novel approach to testing for induced point mutation in mammals. Humangenetik 26, 231-243.

Klose, J., Kobalz, U., 1995. Two-dimensional electrophoresis of proteins: An updated protocol and implications for a functional analysis of the genome. Electrophoresis 16, 1034-1059.

Kolkman, A., Dirksen, E.H., Slijper, M., Heck, A.J., 2005. Double standards in quantitative proteomics: direct comparative assessment of difference in gel electrophoresis and metabolic stable isotope labeling. Molecular Cellular Proteomics 4, 255-266.

Krijgsveld, J., Ketting, R.F., Mahmoudi, T., Johansen, J., Artal-Sanz, M., Verrijzer, C.P., Plasterk, R.H., Heck, A.J., 2003. Metabolic labeling of *C. elegans* and *D. melanogaster* for quantitative proteomics. Nature Biotechnology 21, 927-931.

Kuhn, E., Wu, J., Karl, J., Liao, H., Zolg, W., Guild, B., 2004. Quantification of C-reactive protein in the serum of patients with rheumatoid arthritis using multiple reaction monitoring mass spectrometry and $^{13}$C-labeled peptide standards. Proteomics 4, 1175-1186.

Kvint, K., Nachin, L., Diez, A., Nystrom, T., 2003. The bacterial universal stress protein: function and regulation. Current Opinion in Microbiology 6, 140-145.

Larrainzar, E., Wienkoop, S., Weckwerth, W., Ladrera, R., Arrese-Igor, C., Gonzalez, E.M., 2007. *Medicago truncatula* root nodule proteome analysis reveals differential plant and bacteroid responses to drought stress. Plant Physiology 144, 1495-1507.

Larrainzar, E., Wienkoop, S., Scherling, C., Kempa, S., Ladrera, R., Arrese-Igor, C., Weckwerth, W., Gonzalez, E.M., 2009. Carbon metabolism and bacteroid functioning are involved in the regulation of nitrogen fixation in *Medicago truncatula* under drought and recovery. Molecular Plant Microbe Interactions 22, 1565-1576.

Lauzier, A., Simao-Beaunoir, A.M., Bourassa, S., Poirier, G.G., Talbot, B., Beaulieu, C., 2008. Effect of potato suberin on *Streptomyces scabies* proteome. Molecular Plant Pathology 9,

753-762.

Lee, Y., Pena-Llopis, S., Kang, Y.S., Shin, H.D., Demple, B., Madsen, E.L., Jeon, C.O., Park, W., 2006. Expression analysis of the *fpr* (ferredoxin-$NADP^+$ reductase) gene in *Pseudomonas putida* KT2440. Biochemical and Biophysical Research Communications 339, 1246-1254.

Leeds, J.A., Dean, C.R., 2006. Peptide deformylase as an antibacterial target: a critical assessment. Current Opinion in Pharmacology 6, 445-452.

Lenman, M., Sorensson, C., Andreasson, E., 2008. Enrichment of phosphoproteins and phosphopeptide derivatization identify universal stress proteins in elicitor-treated *Arabidopsis*. Molecular Plant Microbe Interactions 21, 1275-1284.

Li, J., Glick, B.R., 2001. Transcriptional regulation of the *Enterobacter cloacae* UW4 1-aminocyclopropane-1-carboxylate (ACC) deaminase gene (*acdS*). Canadian Journal of Microbiology 47, 359-367.

Li, J., Ovakim, D.H., Charles, T.C., Glick, B.R., 2000. An ACC deaminase minus mutant of *Enterobacter cloacae* UW4 no longer promotes root elongation. Current Microbiology 41, 101-105.

Liska, A.J., Shevchenko, A., Pick, U., Katz, A., 2004. Enhanced photosynthesis and redox energy production contribute to salinity tolerance in *Dunaliella* as revealed by homology-based proteomics. Plant Physiology 136, 2806-2817.

Lugtenberg, B.J., Kravchenko, L.V., Simons, M., 1999. Tomato seed and root exudate sugars: composition, utilization by *Pseudomonas* biocontrol strains and role in rhizosphere colonization. Environmental Microbiology 1, 439-446.

Lund, S.T., Stall, R.E., Klee, H.J., 1998. Ethylene regulates the susceptible response to pathogen infection in tomato. Plant Cell 10, 371-382.

Lynn, S., Yu, G.L., Yan, K., 1999. Vicinal-thiol-containing molecules enhance but mono-thiol-containing molecules reduce nickel-induced DNA strand breaks. Toxicology and Applied Pharmacology 160, 198-205.

Ma, B., Zhang, K., Hendrie, C., Liang, C., Li, M., Doherty-Kirby, A., Lajoie, G. 2003. PEAKS: powerful software for peptide de novo sequencing by tandem mass spectrometry. Rapid Communications in Mass Spectrometry 17, 2337-2342.

Mahmood, T., Jan, A., Kakishima, M., Komatsu, S., 2006. Proteomic analysis of bacterial-blight defense-responsive proteins in rice leaf blades. Proteomics 6, 6053-6065.

Mallick, P., Schirle, M., Chen, S.S., Flory, M.R., Lee, H., Martin, D., Ranish, J., Raught, B., Schmitt, R., Werner, T., Kuster, B., Aebersold, R., 2007. Computational prediction of proteotypic peptides for quantitative proteomics. Nature Biotechnology 25, 125-131.

Mann, M., Pandey, A., 2001. Use of mass spectrometry-derived data to annotate nucleotide and protein sequence databases. Trends in Biochemical Sciences 26, 54-61.

Mann, M., Jensen, O.N., 2003. Proteomic analysis of post-translational modifications. Nature Biotechnology 21, 255-261.

Mann, M., Hendrickson, R.C., Pandey, A., 2001. Analysis of proteins and proteomes by mass spectrometry. Annual Review of Biochemistry 70, 437-473.

Marchler-Bauer, A., Anderson, J.B., Derbyshire, M.K., DeWeese-Scott, C., Gonzales, N.R., Gwadz, M., Hao, L., He, S., Hurwitz, D.I., Jackson, J.D., Ke, Z., Krylov, D., Lanczycki, C.J., Liebert, C.A., Liu, C., Lu, F., Lu, S., Marchler, G.H., Mullokandov, M., Song, J.S.,

Thanki, N., Yamashita, R.A., Yin, J.J., Zhang, D., Bryant, S.H., 2007. CDD: a conserved domain database for interactive domain family analysis. Nucleic Acids Research 35, D237-D240.

Mark, G.L., Dow, J.M., Kiely, P.D., Higgins, H., Haynes, J., Baysse, C., Abbas, A., Foley, T., Franks, A., Morrissey, J., and O'Gara, F., 2005. Transcriptome profiling of bacterial responses to root exudates identifies genes involved in microbe-plant interactions. Proceedings of the National Academy of Sciences USA 102, 17454-17459.

Marouga, R., David, S., Hawkins, E., 2005. The development of the DIGE system: 2D fluorescence difference gel analysis technology. Analytical and Bioanalytical Chemistry 382, 669-678.

Mathesius, U., Mulders, S., Gao, M., Teplitski, M., Caetano-Anolles, G., Rolfe, B.G., Bauer, W.D., 2003. Extensive and specific responses of a eukaryote to bacterial quorum-sensing signals. Proceedings of National Academy of Science USA 100, 1444-1449.

Mattoo, A.K., Suttle, J.C., 1991. The Plant Hormone Ethylene. CRC Press Boca Raton, FL.

Mattinen, L., Nissinen, R., Riipi, T., Kalkkinen, N., Pirhonen, M., 2007. Host-extract induced changes in the secretome of the plant pathogenic bacterium *Pectobacterium atrosepticum*. Proteomics 7, 3527-3537.

Mayak, S., Tirosh, T., Glick, B.R., 2004a. Plant growth-promoting bacteria confer resistance in tomato plants to salt stress. Plant Physiology and Biochemistry 42, 565-572.

Mayak, S., Tirosh, T., Glick, B.R., 2004b. Plant growth-promoting bacteria that confer resistance to water stress in tomatoes and peppers. Plant Science 166, 525-530.

Mead, J.A., Bianco, L., Bessant, C., 2009. Recent developments in public proteomic MS

repositories and pipelines. Proteomics 9, 861-881.

Metzker, M.L., 2010. Sequencing technologies – the next generation. Nature Reviews Genetics 11, 31-46.

Miche, L., Battistoni, F., Gemmer, S., Belghazi, M., Reinhold-Hurek, B., 2006. Upregulation of jasmonate-inducible defense proteins and differential colonization of roots of *Oryza sativa* cultivars with the endophyte *Azoarcus* sp. Molecular Plant Microbe Interactions 19, 502-511.

Minden, J.S., Dowd, S.R., Meyer, H.E., Stühler K., 2009. Difference gel electrophoresis. Electrophoresis 30, S156-S161.

Miyagi, M., Rao, K.C., 2007. Proteolytic $^{18}$O-labeling strategies for quantitative proteomics. Mass Spectrometry Review 26, 121-136.

Moran, R., Porath, D., 1980. Chlorophyll determination in intact tissues using *N*,*N*-dimethylformamide. Plant Physiology 65, 478-479.

Moreno, J.I., Martin, R., Castresana, C., 2005. *Arabidopsis* SHMT1, a serine hydroxymethyltransferase that functions in the photorespiratory pathway influences resistance to biotic and abiotic stress. Plant Journal 41, 451-463.

Morris, A.C., Djordjevic, M.A., 2006. The *Rhizobium leguminosarum* biovar *trifolii* ANU794 induces novel developmental responses on the subterranean clover cultivar Woogenellup. Molecular Plant Microbe Interactions 19, 471-479.

Mulrooney, S.B., Hausinger, R.P., 2003. Nickel uptake and utilization by microorganisms. FEMS Microbiology Reviews 27, 239-261.

Munns, R., Tester, M., 2008. Mechanisms of salinity tolerance. Annual Review of Plant

Biology 59, 651-681.

Nadeem, S.M., Zahir, Z.A., Naveed, M., Arshad, M., 2007. Preliminary investigations on inducing salt tolerance in maize through inoculation with rhizobacteria containing ACC deaminase activity. Canadian Journal of Microbiology 53, 1141-1149.

Naher, U.A., Radziah, O., Halimi, M.S., Shamsuddin, Z.H., Mohd Razi, I., 2008. Effect of inoculation on root exudates carbon sugar and amino acids production of different rice varieties. Research Journal of Microbiology 3, 580-587.

Nakamura, T., Dohmae, N., Takio, K., 2004. Characterization of a digested protein complex with quantitative aspects: an approach based on accurate mass chromatographic analysis with Fourier transformion cyclotron resonance mass spectrometry. Proteomics 4, 2558-2566.

Natera, S.H., Guerreiro, N., Djordjevic, M.A., 2000. Proteome analysis of differentially displayed proteins as a tool for the investigation of symbiosis. Molecular Plant Microbe Interactions 13, 995-1009.

Nies, D.H., 2003. Efflux-mediated heavy metal resistance in prokaryotes. FEMS Microbiology Reviews 27, 313-339.

Niggeweg, R., Kocher, T., Gentzel, M., Buscaino, A., Taipale, M., Akhtar, A., Wilm, M., 2006. A general precursor ion-like scanning mode on quadrupole-TOF instruments compatible with chromatographic separation. Proteomics 6, 41-53.

Nixon, B.T., Ronson, C.W., Ausubel, F.M., 1986. Two-component regulatory systems responsive to environmental stimuli share strongly conserved domains with the nitrogen assimilation regulatory genes *ntrB* and *ntrC*. Proceedings of the National Academy of

Sciences of the United States of America 83, 7850-7854.

Nouwens, A.S., Cordwell, S.J., Larsen, M.R., Molloy, M.P., Gillings, M., Willcox, M.D.P., Walsh, B.J., 2000. Complementing genomics with proteomics: The membrane subproteome of *Pseudomonas aeruginosa* PAO1. Electrophoresis 21, 3797-3809.

Nuhse, T.S., Bottrill, A.R., Jones, A.M., Peck, S.C., 2007. Quantitative phosphoproteomic analysis of plasma membrane proteins reveals regulatory mechanisms of plant innate immune responses. Plant Journal 51, 931-940.

Oda, Y., Huang, K., Cross, F.R., Cowburn, D., Chait, B.T., 1999. Accurate quantitation of protein expression and site-specific phosphorylation. Proceedings in National Academy of Science USA 96, 6591-6596.

O'Farrell, P.H., 1975. High resolution two dimensional electrophoresis of proteins. Journal of Biological Chemistry 250, 4007-4021.

O'Farrell, P.Z., Goodman, H.M., O'Farrell, P.H., 1977. High resolution two-dimensional electrophoresis of basic as well as acidic proteins. Cell 12, 1133-1141.

Ohshima, M., Itoh, H., Matsuoka, M., Murakami, T., Ohashi, Y., 1990. Analysis of stress-induced or salicylic acid-induced expression of the pathogenesis-related 1a protein gene in transgenic tobacco. Plant Cell 2, 95-106.

Old, W.M., Meyer-Arendt, K., Aveline-Wolf, L., Pierce, K.G., Mendoza, A., Sevinsky, J.R., Resing, K.A., Ahn, N.G., 2005. Comparison of label-free methods for quantifying human proteins by shotgun proteomics. Molecular Cellular Proteomics 4, 1487-1502.

Ong, S.E., Mann, M., 2005. Mass spectrometry-based proteomics turns quantitative. Nature Chemical Biology 1, 252-262.

Ong, S.E., Blagoev, B., Kratchmarova, I., Kristensen, D.B., Steen, H., Pandey, A., Mann, M., 2002. Stable isotope labeling by amino acids in cell culture, SILAC, as a simple and accurate approach to expression proteomics. Molecular Cellular Proteomics 1, 376-386.

Ow, S.Y., Cardona, T., Taton, A., Magnuson, A., Lindblad, P., Stensjo, K., Wright, P.C., 2008. Quantitative shotgun proteomics of enriched heterocysts from *Nostoc* sp. PCC 7120 using 8-plex isobaric peptide tags. Journal of Proteome Research 7, 1615-1628.

Ow, S.Y., Noirel, J., Cardona, T., Taton, A., Lindblad, P., Stensjo, K., Wright, P.C., 2009. Quantitative overview of $N_2$ fixation in *Nostoc punctiforme* ATCC 29133 through cellular enrichments and iTRAQ shotgun proteomics. Journal of Proteome Research 8, 187-198.

Padliya, N.D., Cooper, B., 2006. Mass spectrometry-based proteomics for the detection of plant pathogens. Proteomics 6, 4069-4075.

Pallas, J.E., Kays, S.J., 1982. Inhibition of photosynthesis by ethylene-a stomatal effect. Plant Physiology 70, 598-601.

Palmblad, M., Bindschedler, L.V., Cramer, R., 2007. Quantitative proteomics using uniform $^{15}N$-labeling, MASCOT, and the trans-proteomic pipeline. Proteomics 7, 3462-3469.

Pan, S., Aebersold, R., Chen, R., Rush, J., Goodlett, D.R., McIntosh, M.W., Zhang, J., Brentnall, T.A., 2009. Mass spectrometry based targeted protein quantification: methods and applications. Journal of Proteome Research 8:787-797.

Pandey, A., Mann, M., 2000. Proteomics to study genes and genomes. Nature 405, 837-846.

Pang, C., Wang, B., 2008. Oxidative stress and salt tolerance in plants. Progress in Botany 69, 231-245.

Panter, S., Thomson, R., de Bruxelles, G., Laver, D., Trevaskis, B., Udvardi, M., 2000.

Identification with proteomics of novel proteins associated with the peribacteroid membrane of soybean root nodules. Molecular Plant Microbe Interactions 13, 325-333.

Patten, C.L., Glick, B.R., 2002. Role of *Pseudomonas putida* indoleacetic acid in development of the host plant root system. Applied and Environmental Microbiology 68, 3795-3801.

Patton, W.F., Schulenberg, B., Steinberg, T.H., 2002. Two-dimensional gel electrophoresis; better than a poke in the ICAT? Current Opinion in Biotechnology 13, 321-328.

Peden, K.W., 1983. Revised sequence of the tetracycline-resistance gene of pBR322. Gene 22, 277-280.

Penrose, D.M., Glick, B.R., 2001. Levels of ACC and related compounds in exudate and extracts of canola seeds treated with ACC deaminase-containing plant growth-promoting bacteria. Canadian Journal of Microbiology 47, 368-372.

Penrose, D.M., Glick, B.R., 2003. Methods for isolating and characterizing ACC deaminase-containing plant growth-promoting rhizobacteria. Physiologia Plantarum 118, 10-15.

Perkins, D.N., Pappin, D.J., Creasy, D.M., Cottrell, J.S., 1999. Probability-based protein identification by searching sequence databases using mass spectrometry data. Electrophoresis 20, 3551-3567.

Popescu, S.C., Popescu, G.V., Bachan, S., Zhang, Z., Seay, M., Gerstein, M., Snyder, M., Dinesh-Kumar, S.P., 2007. Differential binding of calmodulin-related proteins to their targets revealed through high-density *Arabidopsis* protein microarrays. Proceedings of National Academy of Science USA 104, 4730-4735.

Popescu, S.C., Popescu, G.V., Bachan, S., Zhang, Z., Gerstein, M., Snyder, M., Dinesh-Kumar, S.P., 2009. MAPK target networks in *Arabidopsis thaliana* revealed using functional

protein microarrays. Genes and Developments 23, 80-92.

Prayitno, J., Imin, N., Rolfe, B.G., Mathesius, U., 2006. Identification of ethylene-mediated protein changes during nodulation in *Medicago truncatula* using proteome analysis. Journal of Proteome Research 5, 3084-3095.

Rabie, G.H., Almadini, A.M., 2005. Role of bioinoculants in development of salt-tolerance of *Vicia faba* plants under salinity stress. African Journal of Biotechnology 4, 210-222.

Ramos-Fernandez, A., Lopez-Ferrer, D., Vazquez, J., 2007. Improved method for differential expression proteomics using trypsin-catalyzed $^{18}O$ labeling with a correction for labeling efficiency. Molecular Cellular Proteomics 6, 1274-1286.

Rao KC, Carruth RT, Miyagi M. 2005. Proteolytic $^{18}O$ labeling by peptidyl-Lys metalloendopeptidase for comparative proteomics. Journal of Proteome Research 4, 507-514.

Reed, M.L., Glick, B.R., 2004. Applications of free living plant growth-promoting rhizobacteria. Antonie Van Leeuwenhoek 86, 1-25.

Reed, M.L., Glick, B.R., 2005. Growth of canola (*Brassica napus*) in the presence of plant growth-promoting bacteria and either copper or polycyclic aromatic hydrocarbons. Canadian Journal of Microbiology 51, 1061-1069.

Reynolds, K.J., Yao, X., Fenselau, C., 2002. Proteolytic $^{18}O$ labeling for comparative proteomics: evaluation of endoprotease Glu-C as the catalytic agent. Journal of Proteome Research 1, 27-33.

Ritsema, T., Joore, J., van Workum, W., Pieterse, C.M., 2007. Kinome profiling of *Arabidopsis* using arrays of kinase consensus substrates. Plant Methods 3, 3.

Rodriguez, H., Vessely, S., Shah, S., Glick, B.R., 2008. Effect of a nickel-tolerant ACC deaminase-producing *Pseudomonas* strain on growth of nontransformed and transgenic canola plants. Current Microbiology 57, 170-174.

Rohila, J.S., Chen, M., Chen, S., Chen, J., Cerny, R., Dardick, C., Canlas, P., Xu, X., Gribskov, M., Kanrar, S., Zhu, J.K., Ronald, P., Fromm, M.E., 2006. Protein-protein interactions of tandem affinity purification-tagged protein kinases in rice. Plant Journal 46, 1-13.

Rohila, J.S., Chen, M., Chen, S., Chen, J., Cerny, R.L., Dardick, C., Canlas, P., Fujii, H., Gribskov, M., Kanrar, S., Knoflicek, L., Stevenson, B., Xie, M., Xu, X., Zheng, X., Zhu, J.K., Ronald, P., Fromm, M.E., 2009. Protein-protein interactions of tandem affinity purified protein kinases from rice. PLoS One 4, e6685.

Rolhion, N., Carvalho, F.A., Darfeuille-Michaud, A., 2007. OmpC and the sigma(E) regulatory pathway are involved in adhesion and invasion of the Crohn's disease-associated *Escherichia coli* strain LF82. Molecular Microbiology 63, 1684-1700.

Romeis, T., 2001. Protein kinases in the plant defence response. Current Opinion in Plant Biology 4, 407-414.

Rose, K., Simona, M.G., Offord, R.E., Prior, C.P., Otto, B., Thatcher, D.R., 1983. A new mass-spectrometric C-terminal sequencing technique finds a similarity between gamma-interferon and alpha 2-interferon and identifies a proteolytically clipped gamma-interferon that retains full antiviral activity. Biochemistry Journal 215, 273-277.

Rosen, R., Matthysse, A.G., Becher, D., Biran, D., Yura, T., Hecker, M., Ron, E.Z., 2003. Proteome analysis of plant-induced proteins of *Agrobacterium tumefaciens*. FEMS Microbiology Ecology 44, 355-360.

Ross, P.L., Huang, Y.N., Marchese, J.N., Williamson, B., Parker, K., Hattan, S., Khainovski, N., Pillai, S., Dey, S., Daniels, S., Purkayastha, S., Juhasz, P., Martin, S., Bartlet-Jones, M., He, F., Jacobson, A., Pappin, D.J., 2004. Multiplexed protein quantitation in *Saccharomyces cerevisiae* using amine-reactive isobaric tagging reagents. Molecular Cellular Proteomics 3, 1154-1169.

Saravanakumar, D., Samiyappan, R., 2007. ACC deaminase from *Pseudomonas fluorescens* mediated saline resistance in groundnut (*Arachis hypogea*) plants. Journal of Applied Microbiology 102, 1283-1292.

Sarma, A.D., Emerich, D.W., 2005. Global protein expression pattern of *Bradyrhizobium japonicum* bacteroids: a prelude to functional proteomics. Proteomics 5, 4170-4184.

Sarma, A.D., Emerich, D.W., 2006. A comparative proteomic evaluation of culture grown *vs* nodule isolated *Bradyrhizobium japonicum*. Proteomics 6, 3008-3028.

Schafer, A., Tauch, A., Jager, W., Kalinowski, J., Thierbach, G., Puhler, A., 1994. Small mobilizable multi-purpose cloning vectors derived from the *Escherichia coli* plasmids pK18 and pK19: selection of defined deletions in the chromosome of *Corynebacterium glutamicum*. Gene 145, 69-73.

Schenkluhn, L., Hohnjec, N., Niehaus, K., Schmitz, U., Colditz, F., 2010. Differential gel electrophoresis (DIGE) to quantitatively monitor early symbiosis- and pathogenesis-induced changes of the *Medicago truncatula* root proteome. Journal of Proteomics 73, 753-768.

Schmidt, T., Schlegel, H.G., 1994. Combined nickel-cobalt-cadmium resistance encoded by the *ncc* locus of *Alcaligenes xylosoxidans* 31A. Journal of Bacteriology 176, 7045-7054.

Sergeeva, E., Shah, S., Glick, B.R., 2006. Growth of transgenic canola (*Brassica napus* cv. Westar) expressing a bacterial 1-aminocyclopropane-1-carboxylate (ACC) deaminase gene on high concentrations of salt. World Journal of Microbiology and Biotechnology 22, 277-282.

Silva, J.C., Denny, R., Dorschel, C.A., Gorenstein, M., Kass, I.J., Li, G.Z., McKenna, T., Nold, M.J., Richardson, K., Young, P., Geromanos, S., 2005. Quantitative proteomic analysis by accurate mass retention time pairs. Analytical Chemistry 77, 2187-2200.

Silva, J.C., Denny, R., Dorschel, C., Gorenstein, M.V., Li, G.Z., Richardson, K., Wall, D., Geromanos, S.J., 2006a. Simultaneous qualitative and quantitative analysis of the *Escherichia coli* proteome: a sweet tale. Molecular Cellular Proteomics 5, 589-607.

Silva, J.C., Gorenstein, M.V., Li, G.Z., Vissers, J.P., Geromanos, S.J., 2006b. Absolute quantification of proteins by LCMS: a virtue of parallel MS acquisition. Molecular Cellular Proteomics 5, 144-156.

Singh, P.K., Schaefer, A.L., Parsek, M.R., Moninger, T.O., Welsh, M.J., Greenberg, E.P., 2000. Quorum-sensing signals indicate that cystic fibrosis lungs are infected with bacterial biofilms. Nature 407, 762-764.

Smith, A.W., Iglewski, B.H., 1989. Transformation of *Pseudomonas aeruginosa* by electroporation. Nucleic Acids Research 17, 10509.

Stasyk, T., Huber, L.A., 2004. Zooming in: Fractionation strategies in proteomics. Proteomics 4, 3704-3716.

Stearns, J.C., Glick, B.R., 2003. Transgenic plants with altered ethylene biosynthesis or perception. Biotechnology Advances 21, 193-210.

Steen, H., Mann, M., 2004. The ABC's (and XYZ's) of peptide sequencing. Nature Reviews Molecular Cell Biology 5, 699-711.

Stensjo, K., Ow, S.Y., Barrios-Llerena, M.E., Lindblad, P., Wright, P.C., 2007. An iTRAQ-based quantitative analysis to elaborate the proteomic response of *Nostoc* sp. PCC 7120 under $N_2$ fixing conditions. Journal of Proteome Research 6, 621-635.

Strittmatter, E.F., Ferguson, P.L., Tang, K., Smith, R.D., 2003. Proteome analyses using accurate mass and elution time peptide tags with capillary LC time-of-flight mass spectrometry. Journal of American Society of Mass Spectrometry 14, 980-991.

Suty, L., Lequeu, J., Lancon, A., Etienne, P., Petitot, A.S., Blein, J.P., 2003. Preferential induction of 20S proteasome subunits during elicitation of plant defense reactions: towards the characterization of "plant defense proteasomes". International Journal of Biochemical Cellular Biology 35, 637-650.

Tanaka, K., Waki, H., Ido, Y., Akita, S., Yoshida, Y., Yoshida, T., Matsuo, T., 1988. Protein and polymer analyses up to *m*/*z* 100,000 by laser ionization time-of-flight mass spectrometry. Rapid Communications in Mass Spectrometry 2, 151-153.

Tanaka, K., Matsuyama, S.I., Tokuda, H., 2001. Deletion of *lolB*, encoding an outer membrane lipoprotein, is lethal for *Escherichia coli* and causes accumulation of lipoprotein localization intermediates in the periplasm. Journal of Bacteriology 183, 6538-6542.

Tamagnini, P., Axelsson, R., Lindberg, P., Oxelfelt, F., Wunschiers, R., Lindblad, P., 2002. Hydrogenases and hydrogen metabolism of cyanobacteria. Microbiology Molecular Biology Review 66, 1-20.

Taylor, C.F., Paton, N.W., Lilley, K.S., Binz, P.A., Julian Jr., R.K., Jones, A.R., Zhu, W.,

Apweiler, R., Aebersold, R., Deutsch, E.W., Dunn, M.J., Heck, A.J., Leitner, A., Macht, M., Mann, M., Martens, L., Neubert, T.A., Patterson, S.D., Ping, P., Seymour, S.L., Souda, P., Tsugita, A., Vandekerckhove, J., Vondriska, T.M., Whitelegge, J.P., Wilkins, M.R., Xenarios, I., Yates 3rd, J.R., Hermjakob, H., 2007. The minimum information about a proteomics experiment (MIAPE). Nature Biotechnology 25, 887-893.

Teplitski, M., Chen, H., Rajamani, S., Gao, M., Merighi, M., Sayre, R.T., Robinson, J.B., Rolfe, B.G., Bauer, W.D., 2004. *Chlamydomonas reinhardtii* secretes compounds that mimic bacterial signals and interfere with quorum sensing regulation in bacteria. Plant Physiology 134, 137-146.

Timms, J.F., Cramer, R., 2008. Difference gel electrophoresis. Proteomics 8, 4886-4897.

Turck, C.W., Falick, A.M., Kowalak, J.A., Lane, W.S., Lilley, K.S., Phinney, B.S., Weintraub, S.T., Witkowska, H.E., Yates, N.A., 2007. The association of biomolecular resource facilities proteomics research group 2006 study: relative protein quantitation. Molecular Cellular Proteomics 6, 1291-1298.

Turtoi, A., Mazzucchelli, G.D., De Pauw, E., 2010. Isotope coded protein label quantification of serum proteins--Comparison with the label-free LC-MS and validation using the MRM approach. Talanta 80, 1487-1495.

Ünlü, M., Morgan, M.E., Minden, J.S., 1997. Difference gel electrophoresis. A single gel method for detecting changes in protein extracts. Electrophoresis 18, 2071-2077.

Urfer, W., Grzegorczyk. M., Jung, K., 2006. Statistics for proteomics: a review of tools for analyzing experimental data. Proteomics 6, 48-55.

Valko, M., Morris, H., Cronin, M.T., 2005. Metals, toxicity and oxidative stress. Current Medicinal Chemistry 12, 1161-1208.

van den Bergh, G., Arckens, L., 2004. Fluorescent two-dimensional difference gel electrophoresis unveils the potential of gel-based proteomics. Current Opinion in Biotechnology 15, 38-43.

van Noorden, G.E., Kerim, T., Goffard, N., Wiblin, R., Pellerone, F.I., Rolfe, B.G., Mathesius, U., 2007. Overlap of proteome changes in *Medicago truncatula* in response to auxin and *Sinorhizobium meliloti*. Plant Physiology 144, 1115-1131.

Vissers, J.P., Langridge, J.I., Aerts, J.M., 2007. Analysis and quantification of diagnostic serum markers and protein signatures for Gaucher disease. Molecular Cellular Proteomics 6, 755-766.

Wan, J., Torres, M., Ganapathy, A., Thelen, J., DaGue, B.B., Mooney, B., Xu, D., Stacey, G., 2005. Proteomic analysis of soybean root hairs after infection by *Bradyrhizobium japonicum*. Molecular Plant Microbe Interactions 18, 458-467.

Wang, C., Knill, E., Glick, B.R., Defago, G., 2000. Effect of transferring 1-aminocyclopropane-1-carboxylic acid (ACC) deaminase genes into *Pseudomonas fluorescens* strain CHA0 and its *gacA* derivative CHA96 on their growth-promoting and disease-suppressive capacities. Canadian Journal of Microbiology 46, 898-907.

Wang, G., Alamuri, P., Maier, R.J., 2006. The diverse antioxidant systems of *Helicobacter pylori*. *Molecular Microbiology* 61, 847-860.

Wang, W., Zhou, H., Lin, H., Roy, S., Shaler, T.A., Hill, L.R., Norton, S., Kumar, P., Anderle, M., Becker, C.H., 2003. Quantification of proteins and metabolites by mass spectrometry

without isotopic labeling or spiked standards. Analytical Chemistry 75, 4818-4826.

Wang, Y., Ohara, Y., Nakayashiki, H., Tosa, Y., Mayama, S., 2005. Microarray analysis of the gene expression profile induced by the endophytic plant growth-promoting rhizobacteria, *Pseudomonas fluorescens* FPT9601-T5 in *Arabidopsis*. Molecular Plant-Microbe Interactions 18, 385-396.

Washburn MP, Wolters D, Yates JR, 3rd. 2001. Large-scale analysis of the yeast proteome by multidimensional protein identification technology. Nat Biotechnol 19(3):242-247.

Webb, A.K., Matthews, R.C., Burnie, J.P., 2002. Identification of an immunodominant drug efflux pump in *Burkholderia cepacia*. Journal of Antimicrobial Chemotherapy 49, 619-624.

West, S.E., Schweizer, H.P., Dall, C., Sample, A.K., Runyen-Janecky, L.J., 1994. Construction of improved *Escherichia-Pseudomonas* shuttle vectors derived from pUC18/19 and sequence of the region required for their replication in *Pseudomonas aeruginosa*. Gene 148, 81-86.

Wheeler, D.L., Barrett, T., Benson, D.A., Bryant, S.H., Canese, K., Chetvernin, V., Church, D.M., DiCuccio, M., Edgar, R., Federhen, S., Geer, L.Y., Kapustin, Y., Khovayko, O., Landsman, D., Lipman, D.J., Madden, T.L., Maglott, D.R., Ostell, J., Miller, V., Pruitt, K.D., Schuler, G.D., Sequeira, E., Sherry, S.T., Sirotkin, K., Souvorov, A., Starchenko, G., Tatusov, R.L., Tatusova, T.A., Wagner, L., Yaschenko, E., 2007. Database resources of the National Center for Biotechnology Information. Nucleic Acids Research 35, D5-D12.

Whitehouse, C.M., Dreyer, R.N., Yamashita, M., Fenn, J.B., 1985. Electrospray interface for liquid chromatographs and mass spectrometers. Analytical Chemistry 57, 675-679.

Whiteman, S.A., Serazetdinova, L., Jones, A.M., Sanders, D., Rathjen, J., Peck, S.C.,

Maathuis, F.J., 2008. Identification of novel proteins and phosphorylation sites in a tonoplast enriched membrane fraction of *Arabidopsis thaliana*. Proteomics 8, 3536-3547.

Wiener, M.C., Sachs, J.R., Deyanova, E.G., Yates, N.A., 2004. Differential mass spectrometry: a label-free LC-MS method for finding significant differences in complex peptide and protein mixtures. Analytical Chemistry 76, 6085-6096.

Winzer, T., Bairl, A., Linder, M., Linder, D., Werner, D., Muller, P., 1999. A novel 53-kDa nodulin of the symbiosome membrane of soybean nodules, controlled by *Bradyrhizobium japonicum*. Molecular Plant Microbe Interactions 12, 218-226.

Wolters, D.A., Washburn, M.P., Yates 3rd, J.R., 2001. An automated multidimensional protein identification technology for shotgun proteomics. Analytical Chemistry 73, 5683-5690.

Wu, C.C., MacCoss, M.J., Howell, K.E., Matthews, D.E., Yates 3rd, J.R., 2004. Metabolic labeling of mammalian organisms with stable isotopes for quantitative proteomic analysis. Analytical Chemistry 76, 4951-4959.

Wu, W.W., Wang, G., Baek, S.J., Shen, R.F., 2006. Comparative study of three proteomic quantitative methods, DIGE, cICAT, and iTRAQ, using 2D gel- or LC-MALDI TOF/TOF. Journal of Proteome Research 5, 651-658.

Xing, T., Quellet, T., Miki, B.L., 2004. Towards genomic and proteomic studies of protein phosphorylation in plant-pathogen interactions. Trends in Plant Science 7, 224-230.

Yan, S., Tang, Z., Su, W., Sun, W., 2005. Proteomic analysis of salt stress-responsive proteins in rice root. Proteomics 5, 235-244.

Yao, X., Freas, A., Ramirez, J., Demirev, P.A., Fenselau, C., 2001. Proteolytic $^{18}O$ labeling for comparative proteomics: model studies with two serotypes of adenovirus. Analytical

Chemistry 73, 2836-2842.

Yates 3rd, J.R., Ruse, C.I., Nakorchevsky, A., 2009. Proteomics by mass spectrometry: approaches, advances, and applications. Annual Review of Biomedical Engineering 11, 49-79.

Yorgey, P., Rahme, L.G., Tan, M.W., Ausubel, F.M., 2001. The roles of *mucD* and alginate in the virulence of *Pseudomonas aeruginosa* in plants, nematodes and mice. Molecular Microbiology 41, 1063-1076.

Zhang, H.X., Blumwald, E., 2001. Transgenic salt-tolerant tomato plants accumulate salt in foliage but not in fruit. Nature Biotechnology 19, 765-768.

Zhang, W., Chait, B.T., 2000. ProFound – An expert system for protein identification using mass spectrometry peptide mapping information. Analytical Chemistry 72, 2482-2489.

Zhang, H.X., Hodson, J.N., Williams, J.P., Blumwald, E., 2001. Engineering salt-tolerant *Brassica* plants: characterization of yield and seed oil quality in transgenic plants with increased vacuolar sodium accumulation. Proceedings of the National Academy of Science USA 98, 12832-12836.

Zhang, R., Sioma, C.S., Wang, S., Regnier, F.E., 2001b. Fractionation of isotopically labeled peptides in quantitative proteomics. Analytical Chemistry 73, 5142-5149.

Zhang, X., Takano, T., Liu, S., 2006a. Identification of a mitochondrial ATP synthase small subunit gene (RMtATP6) expressed in response to salts and osmotic stresses in rice (*Oryza sativa* L.). Journal of Experimental Botany 57, 193-200.

Zhang, B., VerBerkmoes, N.C., Langston, M.A., Uberbacher, E., Hettich, R.L., Samatova, N.F., 2006b. Detecting differential and correlated protein expression in label-free shotgun

proteomics. Journal of Proteome Research 5, 2909-2918.

Zhang, X., Liu, S., Takano, T., 2008. Overexpression of a mitochondrial ATP synthase small subunit gene (AtMtATP6) confers tolerance to several abiotic stresses in *Saccharomyces cerevisiae* and *Arabidopsis thaliana*. Biotechnology Lettets 30, 1289-1294.

Zheng, Q., Song, J., Doncaster, K., Rowland, E., Byers, D.M., 2007. Qualitative and quantitative evaluation of protein extraction protocols for apple and strawberry fruit suitable for two-dimensional electrophoresis and mass spectrometry analysis. Journal of Agricultural and Food Chemistry 55, 1663-1673.

Zhu, W., Smith, J.W., Huang, C.M., 2010. Mass spectrometry-based label-free quantitative proteomics. Journal of Biomedical Biotechnology 2010, 840518.

Zimmer, J.S., Monroe, M.E., Qian, W.J., Smith, R.D., 2006. Advances in proteomics data analysis and display using an accurate mass and time tag approach. Mass Spectrometry Review 25, 450-482.

Zybailov, B., Coleman, M.K., Florens, L., Washburn, M.P., 2005. Correlation of relative abundance ratios derived from peptide ion chromatograms and spectrum counting for quantitative proteomic analysis using stable isotope labeling. Analytical Chemistry 77, 6218-6224.